# THE TRIFECTA: A NOVEL COMBINATORIAL THERAPY SPARES IMMUNE CELLS WHILE INDUCING IMMUNOGENIC CELL DEATH IN HUMAN MAMMARY ADENOCARCINOMA AND MOUSE MAMMARY CARCINOMA

by

Youssef Motii

A Dissertation Submitted to the Faculty of

The Charles E. Schmidt College of Science

In Partial Fulfillment of the Requirements for the Degree of

Doctor of Philosophy

Florida Atlantic University

Boca Raton, FL

December 2020

**THE TRIFECTA: A NOVEL COMBINATORIAL THERAPY SPARES IMMUNE CELLS WHILE INDUCING IMMUNOGENIC CELL DEATH IN HUMAN MAMMARY ADENOCARCINOMA AND MOUSE MAMMARY CARCINOMA**

by

Youssef Motii

This dissertation was prepared under the direction of the candidate's dissertation advisor, Dr. James X. Hartmann, Department of Biological Sciences, and has been approved by all members of the supervisory committee. It was submitted to the faculty of the Charles E. Schmidt College of Science and was accepted in partial fulfillment of the requirements for the degree of Doctor of Philosophy.

SUPERVISORY COMMITTEE:

James X. Hartmann (Nov 19, 2020 09:24 EST)

James X. Hartmann, Ph.D.
Dissertation Advisor

Vijaya Iragavarapu (Nov 19, 2020 11:17 EST)

Vijaya Iragavarapu-Charyulu, Ph.D.

David Binninger (Nov 20, 2020 10:52 EST)

David Binninger, Ph.D.

Patricia Keating (Nov 23, 2020 12:55 EST)

Patricia Keating, Ph.D.

Sarah Milton (Nov 23, 2020 12:56 EST)

Sarah Milton, Ph.D.
Chair, Department of Biological Sciences

Teresa Wilcox

Teresa Wilcox, Ph.D.
Interim Dean, Charles E. Schmidt College of Science

Robert W. Stackman Jr., Ph.D.
Dean, Graduate College

November 24, 2020

Date

**ACKNOWLEDGEMENTS**

To refer to Dr. James X. Hartmann as an advisor would be an understatement, if not an insult. In our 5 years together, he has reaffirmed my passion for research and taught me the significance of these contributions to society. Despite his profound knowledge and years of experience, he humbles himself as a student, ready and excited to hear about new mechanisms and pathways that were previously undiscovered. In life, to take you must give; and Dr. Hartmann's kindheartedness and expertise is the gift that keeps on giving. I cannot put into words the impact he has had on both my personal and professional life, and I only hope through my hard work in this dissertation that I have made him proud.

Dr. Keating, you are as sweet as you are brilliant. You inspire me to always think outside the box, and plan experiments as if I were a journal reviewer. There was no such thing as too much data, and you emphasized the importance of reproducible work day in and day out. This dissertation, along with many other accomplishments in my personal life would not have been possible without you.

Dr. Vijay, every day I grow more fascinated by you for your commitment to meaningful research and original work. It felt like yesterday I was recording your lectures in Tumor Immunology, and now I will be lecturing you on my dissertation project during my defense. Your expertise has been invaluable to this project and it would not have been possible without you. I hope that I have made you proud, and that you now see all along I

have been trying to follow in your footsteps. You are an esteemed researcher, and an even more admirable human being. Thank you.

Dr. Binninger, you have been a crucial committee member to this project but also indirectly assumed the role of a "guidance counselor." You helped me cope with the rigor and challenges of my doctoral studies, something that seemed like an insurmountable obstacle starting out. Your positivity and support is the reason I have made it through, and I cannot thank you enough.

To the Hartmann lab and Biology department: Dr. Padilla, Dr. Shibata, Rashean, Sharon, Dr. Caplan, Dr. Cavallo, Dr. Milton, and Sharon Ellis; thank you for your unwavering support.

To the late Geri Mayer, not a day goes by where I do not think of you. I wanted to keep my dissertation defense a surprise, and now I will never get to share this milestone in my life with you. You would have been so happy; so proud. In your memory, I will continue to put my best effort forth in everything that I do. I will always be a student of knowledge, but also a mentor to those around me… something you encouraged us to do every day of our lives. I would give anything in the world to have you here for just a second; to see your smile, to hear your laugh, to share this feat with you. I hope that you rest in peace, knowing good and well that all the lives you have touched will continue to strive for greatness in your memory.

## ABSTRACT

| | |
|---|---|
| Author: | Youssef Motii |
| Title: | The trifecta: a novel combinatorial therapy spares immune cells while inducing immunogenic cell death in human mammary adenocarcinoma and mouse mammary carcinoma |
| Institution: | Florida Atlantic University |
| Dissertation Advisor: | Dr. James X. Hartmann |
| Degree: | Doctor of Philosophy |
| Year: | 2020 |

According to U.S. Breast Cancer Statistics, about 1 in 8 U.S. women will develop invasive breast cancer during their lifetime. Chemotherapeutics that are used on patients currently often lead to tumor resistance, bone marrow suppression and cachexia. This study evaluated a novel combination of three non-mutagenic compounds for their effectiveness against mammary tumor cells, toxicity towards immune cells, ability to provoke the expression of immunogenic cell death (ICD) markers, and killing in 3D tumor models. Methotrexate (MTX), 2-deoxyglucose (2DG), and wogonin (WGN) were combined at doses well below their $EC_{50}$ values yet effectively killed human and mouse breast cancer cells. The combination inhibited cancer cell colony formation and induced a high degree of cell death in multiple malignant tumor cell lines. Importantly, the combination did not significantly inhibit the viability of peripheral-blood mononuclear cells (PBMCs), even when employed at 3X the concentration that killed cancer cells. In

marked contrast, low-dose doxorubicin, a common therapeutic for breast cancers, significantly decreased PBMC viability and increased the percentage of cell death. Our novel combinatorial therapy (*Trifecta*) elicited the significant expression of three ICD hallmarks: calreticulin surface expression, ATP secretion, and HMGB-1 release. In all cases, *Trifecta* elicited an equal or greater degree of ICD-marker expression compared to doxorubicin, a known inducer of ICD. We show significant efficacy of *Trifecta* against human and mouse mammary 3D tumor models grown in Matrigel® ECM-complex containing culture medium, and reaffirm the marked resistance of tumorspheres towards the conventional chemotherapeutic doxorubicin. The effectiveness of *Trifecta* in an acceptable surrogate model for mouse studies bodes well for translation of our findings to the clinic. In conclusion, *Trifecta* has proven highly effective against tumor cells grown either as monolayers or tumorspheres, without significant cytotoxic effects towards proliferating immune cells. Furthermore, treatment with this combination elicits ICD, which has the potential to prime an adaptive immune response against tumor cells and prevent future relapse. The drugs chosen for our combination target metabolic pathways that cancer cells are heavily dependent upon and do not interact with or induce mutations in DNA. These properties place *Trifecta* at the forefront of developing anticancer therapies.

## DEDICATION

To Lifetime: Younes, Khalil, Adam, Omar, Mutaz, Ayman, Zack, Vmeer, Amir, and Musa: Through hard work, anything is possible; and through brotherhood, you're never alone. We made it boys… together. May your futures be bright inshaAllah.

To the Motii family and families of Antural & Fareesa Sircar, Jamal & Ohood Ali, Omar & Linda Atway, Khames & Amal Abdelqader, Yaser and Samar Abdelquder, Sam & Lameese Aghbar, Mohammad and Nayera Zihni, and Najum Choudhy; I would not be where I am today if not for you all. Thank you all for your unconditional support.

To Imayoon, I hope this milestone pardons me from all of our months apart and days where I could not give you my full attention. You have been so patient, and I never would have imagined being blessed with such a genuine supporter and kindhearted partner. Here is to the rest of our lives together, forever in love.

To Younes, albeit my younger brother, there are times where I cannot deny looking up to you. You motivate me to pursue my dreams and persevere through any obstacle. I hope that I have been a good mentor, and an even more caring older brother.

To my parents, Jamal and Kheira Motii, every second of your lives has been spent in sacrifice to progress ours. You raised respectable, admirable children; and I hope that I have made you proud. Despite all the late nights, missed calls, and days apart… you were always there. Thank you for always putting me first, no matter what. I love you.

Alhamdulilah.

**THE TRIFECTA: A NOVEL COMBINATORIAL THERAPY SPARES IMMUNE CELLS WHILE INDUCING IMMUNOGENIC CELL DEATH IN HUMAN MAMMARY ADENOCARCINOMA AND MOUSE MAMMARY CARCINOMA**

## LIST OF TABLES

## LIST OF FIGURES

# CHAPTER 1: GENERAL INTRODUCTION

## What is Cancer?

The NIH reports that two out of every five people in the United States will be diagnosed with cancer in their lifetime. Cancer is a disease of the body's own cells, which manifests as uncontrolled and unregulated cell division. In vital organs, this abnormal division may develop a solid primary tumor, which hinders normal function of the organ and in severe cases leads to organ failure. Uncontrollable growth may cause invasion of and damage to surrounding tissue through metastasis. Unregulated growth may lead to the replication of mutant DNA, which is not repaired and in turn codes for mutant proteins in translation. The underlying mechanism for this disruption in normal cell cycle functioning is a result of acquired genomic instability. The human genome is well-equipped with DNA proofreading and DNA repair mechanisms; however, no system is perfect. Random gain-of-function mutations convert proto-oncogenes into oncogenes, which in turn code for abnormal proteins or over-active proteins that promote proliferative cell division. Random loss-of-function mutations in two copies of tumor suppressor genes inhibit the normal functioning of the gene, leading to increased error in DNA replication, lack of DNA repair, and increased phosphorylation within the cell cycle driving uncontrolled growth. Random DNA mutation within the human genome is rare and readily corrected for, however environmental factors and epigenetic mechanisms may accelerate the effects of these mutations.

Mutagens have become ever more present in the environment; commonly found in foods, UV light from the sun, and tobacco smoke[1]. The size and structure of these compounds or radioactive molecules allow them to readily interact with DNA stored in the nucleus of cells, directly interfering with the nucleotide sequence and consequently resulting in somatic mutation[2]. These acquired mutations eventually lead to abnormal cell cycle functioning. Epigenetic modifications such as histone acetylation or deacetylation and DNA methylation may lower or completely turn off the expression of certain genes. Abnormal gene expression of critical genes involved in cell cycling contribute to the onset of genomic instability fostering uncontrolled DNA replication and cell proliferation. Furthermore, recent studies have found chronic inflammation contributes to the development of cancer[3]. A plethora of growth factors, DNA damage-promoting agents, and activated stroma are hallmarks of the chronic inflammatory state that promotes cancer development and tumor progression[4]. Inevitably, the site at which these mutations occur and the genes they target within the body play a large role in disease prognosis.

## Breast Cancer

Despite numerous technological and therapeutic advances, breast cancer remains one of the leading causes of mortality in females[5]. Abnormal cell division in breast tissue may occur within ductal or glandular tissue, developing a mass of cells that interferes with normal organ function and has the capability to metastasize and invade surrounding tissue[6]. Whereas a direct cause for breast cancer has yet to be identified, researchers attribute the development of this disease to a combination of genetic, physiological, and environmental factors working in concert[7].

From a genomic standpoint, previous studies have identified the importance of breast cancer gene 1 (BRCA-1) and breast cancer gene 2 (BRCA-2), as well as human epidermal growth factor receptor 2 (HER2/neu) in disease development[8]. BRCA1 and BRCA2 are inherited genes, meaning that each individual has two copies of the gene, one inherited from their father and one inherited from their mother. This confers a heterozygote advantage, where even if one copy of the gene is mutated, the other continues to function normally. BRCA1 is characterized as a tumor suppressor gene with functions in DNA double-strand break repair and DNA mismatch repair[9]. BRCA 2 has similar functions in maintaining genomic stability. A loss-of-function mutation in both copies of either of these genes has been shown to significantly increase the risk of breast cancer in an individual, as the lack of DNA damage repair contributes to further mutations that accumulate and trigger unregulated cell division. HER2 belongs to a family of epidermal growth factor receptors with important roles in signal transduction pathways responsible for cell proliferation. Amplification of this gene as a result of mutation converts the proto-oncogene to an oncogene, leading to uncontrolled cell division and evasion of apoptosis. The overexpression of this gene occurs in approximately 30% of breast cancers, and allows breast cancer cells to sustain proliferative growth signals[10].

Endocrine disruption has been found in numerous studies to contribute to breast cancer development. This phenomenon is characterized by periods of hormonal instability, for example an increase in estrogen and progesterone levels in early-menstruating females or menopausal hormone therapy[11]. These hormones trigger the release of breast and ovarian cell growth factors, that if sustained for long periods of

time, such as in early-menstruating females or late menopausal females, will increase the incidence of this disease[12]. Certain breast cancer cells, as they arise from self-cells, possess estrogen receptors that bind to estrogen which sustains their growth[13]. Lastly, environmental factors such as mutagens and carcinogens found in foods and tobacco smoke accelerate the rate at which mutations accumulate, increasing the risk of genomic instability and inevitably abnormal cell growth as a result.

## Hallmarks of Cancer

The persistence of cancer throughout history and its fatal effects towards the patient puzzles researchers as to why the body is not able to identify and effectively eradicate cancerous cells? However, studies have shown that it is in fact the cancer that has adapted to avoid detection by the human immune system as well as a multitude of other mechanisms that allow cancerous cells to persist. From transitioning to abnormal metabolic pathways to resisting cell death, cancer cells infringe upon cellular mechanisms to sustain growth. Driven by genomic instability, abnormal and unregulated cellular division gives rise to cells capable of sustaining chronic proliferation, evading growth suppression, enabling replicative immortality, inducing angiogenesis, metastasis, avoiding immune destruction, enabling tumor-promoting inflammation, reprogramming energy metabolism, and resisting cell death (Figure 1)[14]. Together, these characteristics and mechanisms make cancer one of the top five deadliest diseases in the world[15].

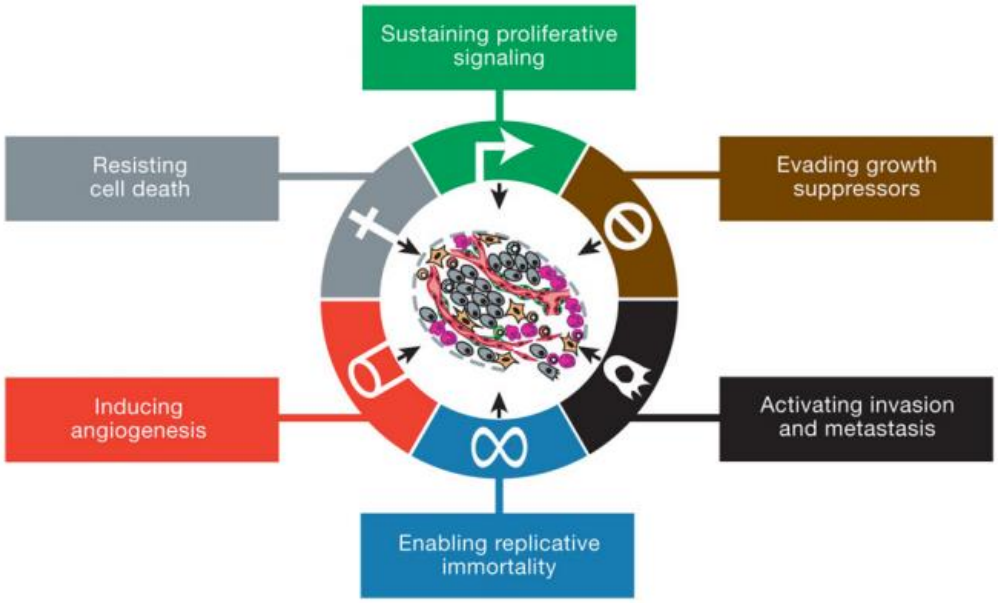


**Figure 1**. **The Hallmarks of Cancer.** The six key factors contributing to cancer cell development. Reproduced with permission from *Elsevier*©.

## Sustained Chronic Proliferation

Cell division and apoptosis is one of the most tightly regulated processes in the human body. Physiological homeostasis is preserved through negative feedback mechanisms to protect against over expression of certain mitogens and abnormal division of cells. Countless genes and proteins are involved in cellular signaling and checkpoint regulation within the cell cycle and apoptotic pathways to ensure proper tissue structure and function is maintained, as well as cell number homeostasis within the body. However, genomic instability provides the foundation for cancer cells to obstruct these mechanisms and sustain chronic proliferation.

A remarkable facet of sustained proliferative signaling in the cancer cell is autocrine function and the ability to stimulate neighboring cells to produce growth hormones via paracrine signaling (Figure 2)[16]. Cancer cells have demonstrated the ability to generate growth factor ligands, and simultaneously, react by generating receptors to

these ligands[14,17]. A study conducted by Salomon and colleagues demonstrated autocrine growth signaling via production of TGF-α in the estrogen-sensitive mammary tumor cell line MCF-7[18]. Cells were able to produce TGF-α in conditioned medium and grew in response to exogenous TGF-α[19]. Sustained proliferation has also been attributed to constitutive activation of signaling pathways in the cell cycle as a result of somatic mutation. A common example of such mutation in cancer is found in the PI3K-Akt pathway.

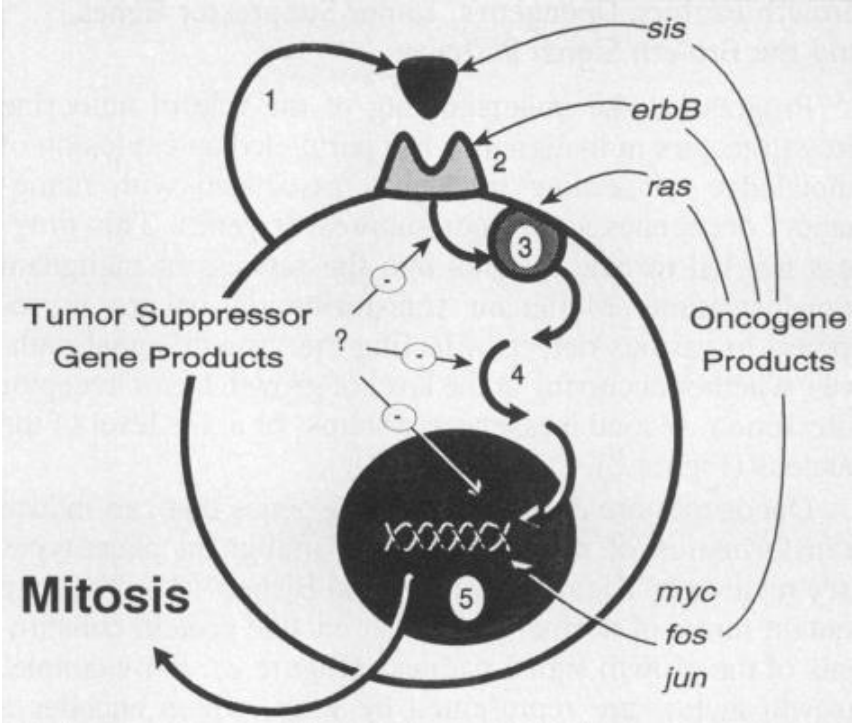


**Figure 2. Relationship between oncogene products and steps of growth signal pathway**. Growth factors (1) interact with cell surface receptors, (2) leading to the activation of second messengers (3) that relay information through the cytoplasm (4) into the nucleus (5). Oncogene products are represented at all levels of the growth signal pathway. Tumor suppressor genes may play an important regulatory role. Reproduced with permission from *Nature*©.

The PI3K-Akt pathway is a major regulatory pathway in cell proliferation and growth. In cancer, Class 1 kinases of the PI3K-Akt pathway are constitutively activated, leading to abnormal signaling and growth[20]. Furthermore, in this same pathway, cancer

cells are able to sustain chronic proliferation via inhibition of negative feedback mechanisms. Studies have shown that a loss-of-function mutation in PTEN phosphatase in cancer cells amplifies PI3K signaling, resulting in increased cell proliferation[21]. Thus, the literature provides innumerous evidence on the ability of cancer cells to sustain growth by autocrine signaling and mutation in signal transduction pathways. Additionally, cancer cells possess the ability to evade growth suppression during abnormal division, furthering tumorigenesis.

## Evading Growth Suppression

The rarity of the genome to succumb to mutation or allow for uncontrolled cell proliferation is due in part to the strength of growth suppression mechanisms which prevent abnormal division and induce apoptosis as a result of irreparable damage. As these genes directly select for the prolific properties of mutated cells, pathways to evade such signals are upregulated by cancer cells to sustain growth. The mechanism by which this occurs, however, varies from loss-of-function mutations in these tumor suppressor genes to opposing normal tissue structural complexity and cell signaling.

Key tumor suppressor genes involved in modulating cell growth, proliferation, DNA repair, and apoptosis include p53, p21, and the retinoblastoma-associated gene (RB). A shared characteristic of tumor suppressor genes is haplosufficency, the ability to function normally despite mutations in one copy of the gene[22]. This heterozygote advantage is the reasoning behind the two-hit hypothesis, which states that a loss-of-function in both copies of tumor suppressor genes is required to disrupt normal function and induce oncogenic properties. Evidence of this hypothesis is found in mice where one copy of a tumor suppressor gene is knocked out, yet normal cellular proliferation and

tissue architecture persists[23]. The p53 gene has been dubbed the "guardian of the genome" for its role in recognizing DNA damage or cellular abnormalities, halting the cell cycle for repair, and inducing apoptosis in the event of irreparable damage sustained by a cell[24]. The fundamental aspect of these functions is to ensure that normal, non-mutated cells progress through the cell cycle transiently and differentiate to effectively perform their function within the body. Similarly, the p21 gene functions to halt the cell cycle if DNA damage or abnormalities are detected via p53-dependent and independent pathways. As a cyclic-dependent kinase inhibitor, p21 expression may arrest cells at the $G_1$, S, and $G_2$ phases of the cell cycle until response to cellular stress is normalized[25]. Additionally, the RB gene functions as the gatekeeper of the cell cycle, and determines whether cells should proceed to division or if cell cycle arrest is necessary. The RB gene also has functions in maintaining cellular growth signals and inhibiting the increase of cell size in non-dividing cells[23,26]. Characterized by genomic instability, cancers arise as a result of mutation in these genes. Loss-of-function promotes uncontrolled cell growth and disrupts the balance between cell proliferation and apoptosis (Figure 3). Aside from cell cycle regulators and DNA damage modulators, tumor suppressor genes have other key functions to inhibit abnormal division; the mutations of which further promote cancerous growth.

A marker of cell division hindrance is density-dependent inhibition. Dense cell-to-cell contact stimulates the release of contact inhibitors that prohibit further cell growth[14]. This tumor suppressive function allows tissues to maintain normal structure and function, and physiological homeostasis with regards to cell number. A key example is the human NF2 gene which encodes the *merlin* protein. *Merlin* functions in contact

inhibition by isolating growth factor receptors, disrupting their ability to produce mitogenic signals and promote division[27]. Thus, loss-of-function in the NF2 gene inhibits the production of merlin, thereby enhancing the function of growth factor receptors and ultimately weakening the adhesivity of cadherin-mediated cell-to-cell attachments, allowing tumor cells to aggregate and cluster[4,27].

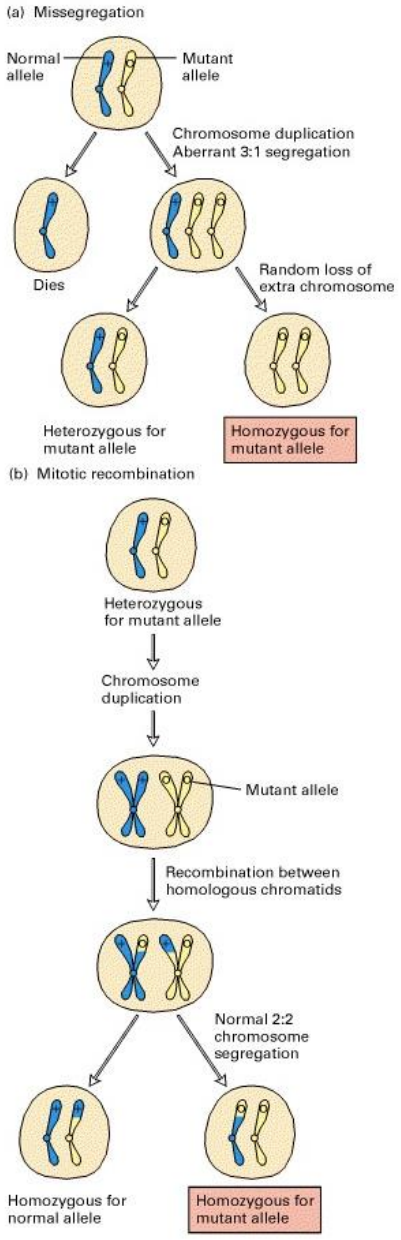


**Figure 3. Loss of heterozygosity (LOH) of tumor-suppressor genes.** A cell containing one normal and one mutant allele of a tumor-suppressor gene is generally phenotypically normal. (a) If formation of the mitotic spindle is defective, then the duplicated chromosomes bearing the normal and mutant alleles may segregate in an aberrant 3:1 ratio. A daughter cell that receives three chromosomes of a type will generally lose one; sometimes the resultant cell will contain one normal and one mutant allele, but sometimes it will be homozygous for the mutant allele. (b) Mitotic recombination between a chromosome with a wild-type and a mutant allele, followed by chromosome segregation, will frequently result in a cell that contains two copies of the mutant allele and none of the wild-type. Reproduced with permission from *W.H. Freeman*©.

## Angiogenesis

Autocrine growth signaling, mutation in tumor suppressor genes, and replicative immortality work in concert to sustain cancer cell proliferation. However, angiogenesis is the mechanism that physically sustains the cell and provides it with the nutrients and oxygen supply necessary to support its abnormal division. Under normal physiological conditions, angiogenic function is heightened during periods of embryological development to create the vasculature of the human body and wound repair[32]. Pro-angiogenic factors, such as vascular endothelial growth factor (VEGF), induce new blood vessel growth in the embryo, and maintains homeostasis in the endothelial vasculature where necessary. Inversely, anti-angiogenic factors such as thrombospodin-1 (TSP-1) function to suppress angiogenesis through negative feedback inhibition (Figure 4)[33].

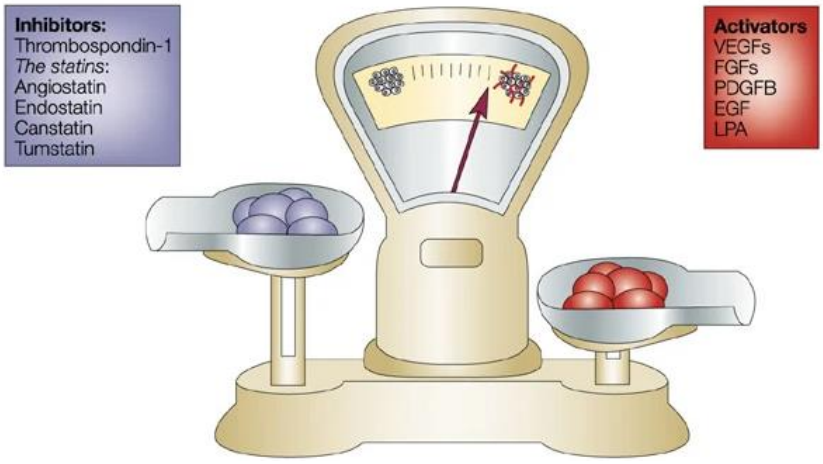


**Figure 4. The Angiogenic Balance.** Under normal physiological conditions, inhibitors of angiogenesis "outweigh" promoters of angiogenesis to prevent against abnormal tissue vascularization. Reproduced with permission from *Nature*©.

The ability of the cancer cell to disrupt the balance of these molecules and exploit angiogenesis inducers while silencing angiogenesis inhibitors increases cell viability. However, the half-life in circulation of angiogenic inhibitors is in fact longer than that of

angiogenesis inducers, and the presence of cancers has been linked to elevated levels of angiogenesis inhibitors[34]. The key to this mystery was uncovered through the discovery of endostatin, and more recently how primary tumors employ a mechanism of angiogenic inhibition to further promote their growth. Endostatin is a component of the collagen XVIII domain with antiangiogenic function[35]. The renowned work of Dr. Folkman discovered endostatin and a similar antiangiogenic factor angiostatin to be secreted from primary tumors to sequester the growth of secondary metastases[36]. The physiological "greed" of primary tumor cells is evidenced in this work, as removal of the primary tumor led to increased growth of distant metastases[37]. Furthermore, this unbalance of angiogenic inducers and inhibitors poses yet another problem: the formation of an abnormal, leaky vasculature.

To sustain growth and viability, cancer cells activate an "angiogenic switch" that functions to upregulate endogenous inducers of angiogenesis while simultaneously downregulating angiogenesis inhibitors (Figure 5)[33]. As VEGF is upregulated, matrix metalloproteases are released to degrade the extracellular matrix and facilitate endothelial cell migration[38]. This tissue injury creates an avenue for aberrant endothelial cell proliferation[39].

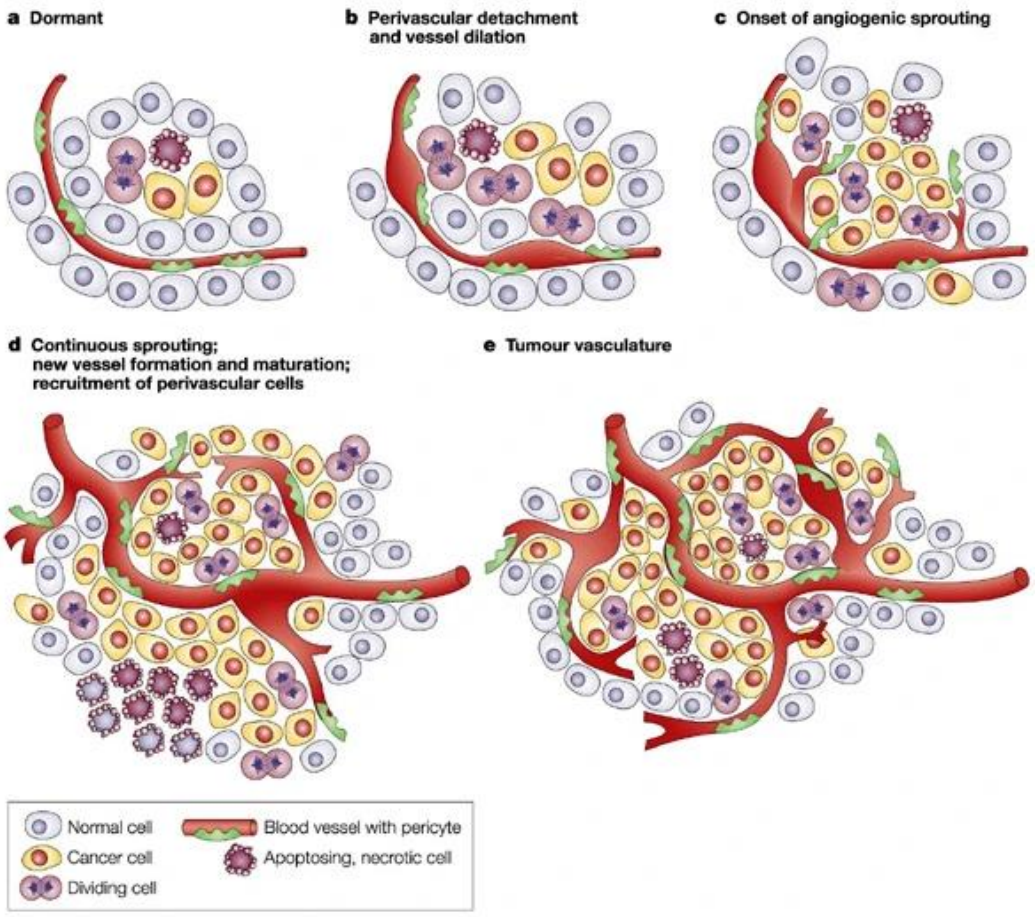


**Figure 5. The classical "angiogenic switch."** Most tumors start growing as avascular nodules (dormant) (a) until they reach a steady-state level of proliferating and apoptosing cells. The initiation of angiogenesis, or the 'angiogenic switch', has to occur to ensure exponential tumor growth. The switch begins with perivascular detachment and vessel dilation (b), followed by angiogenic sprouting (c), new vessel formation and maturation, and the recruitment of perivascular cells (d). Blood-vessel formation will continue as long as the tumor grows, and the blood vessels specifically feed hypoxic and necrotic areas of the tumor to provide it with essential nutrients and oxygen (e). Reproduced with permission from *Nature*©.

The resulting vasculature is characterized as leaky, small in diameter, and high in microvascular fluid pressure[40]. The ramifications of these malformed vessels include decreased sensitivity to macromolecular chemotherapeutic agents, hypoxic conditions harmful to tissue, and central necrosis[40–42]. Whereas the primary function of angiogenesis is to nourish tumors and remove waste, obstruction of the surrounding vasculature in the process further promotes tissue invasion and metastasis.

## Invasion and Metastasis

Tissue architecture and the vasculature of the human body is maintained in part by the basement membrane, a key component of the extracellular matrix. During carcinogenesis, primary cancer cells acquire sustenance through aberrant angiogenesis, a byproduct of which is degradation of the extracellular matrix by virtue of matrix metalloproteinase and a resulting leaky vasculature[36]. This tissue injury facilitates cancer cell migration from the site of induction to distal sites of the epithelium, and in some cases throughout the body via intravasation[43]. The mechanism of this tissue invasion and metastasis includes a multitude of steps, making the overall process inefficient, yet detrimental to patient survival.

The degradation of the extracellular membrane and ultimately the basement membrane facilitates cancer cell mechanisms of invasion. A key facet of tissue invasion is the abnormal epithelial-to-mesenchymal transition displayed by tumor cells. In embryological development, mesenchymal cells are present at functionally significant levels to aid in tissue development and influence the differentiation of cells for specific organ function[44]. An important factor in this transition is the downregulation of E-cadherin and the simultaneous upregulation of N-cadherin, dubbed "cadherin switch"[45]. In normally dividing cells, E-cadherin modulates cell-to-cell interactions and contact inhibition. The "cadherin switch" from E- to N-cadherin rearranges the cellular cytoskeleton, promoting the transition of epithelial cells to motile mesenchymal cells[45,46]. This transitionary state, and subsequent loss of E-cadherin function, is marked by frequent detachment of cells from the primary mass. Prior decomposition of the

extracellular matrix allows the transformed cancer cells to migrate into surrounding tissue and develop micrometastases (Figure 6).

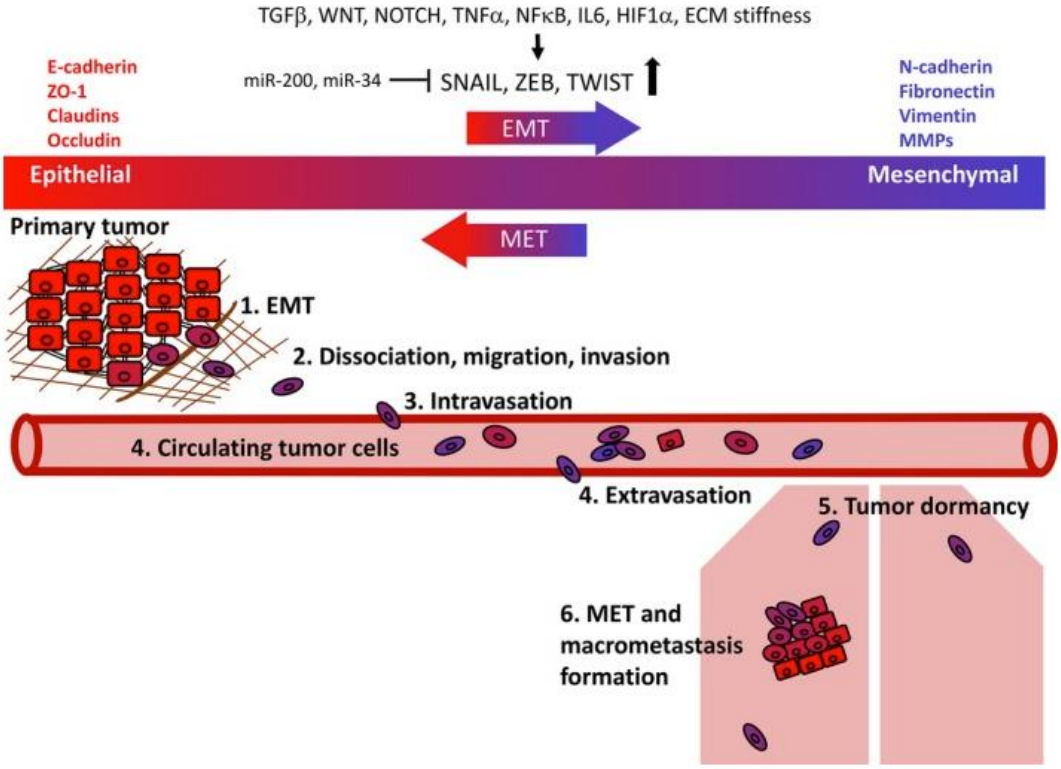


**Figure 6. Epithelial–mesenchymal transition in tumor metastasis.** Primary epithelial tumor cells undergo epithelial–mesenchymal transition (EMT) to acquire the ability to disseminate from the original site and migrate into the surrounding stroma, and intravasate into circulation. A small number of circulating tumor cells and cell clusters survive in the vasculature and eventually extravasate into distant organs such as the lung. Disseminated tumor cells could remain in dormant state for a period of time before undergoing mesenchymal–epithelial transition (MET) to proliferate and form macrometastases. Reproduced with permission from *CreativeCommons*©.

Unique to the cancer cell is the ability to travel as a cluster of cells. Studies have demonstrated the cancer cell's ability to form a cluster, highlighted by densely packed epithelial cells in the middle of mesenchymal "tips"[47]. The leading and lagging mesenchymal "tips" facilitate motility, allowing the cancer cell to transgress through surrounding tissue[48]. As these micrometastases continue invasion, some eventually encounter the blood and lymph vasculature, and proceed to enter these systems through a

process called intravasation. The cluster of tumor cells now travels through circulation with the ability to invade organs far from the primary mass, and establish distal metastases via extravasation[49]. Accounting for 90% of all cancer related deaths, metastasis imposes a large threat to patient survival[50]. Yet in the face of all these abnormalities and damage to tissue and organs, cancer cells remain undetected and as a result untargeted by the human immune system.

## Immune System Evasion

The immune system is characterized as the body's innate and adaptive line of defense against "non-self" endogenous and exogenous antigens. The innate immune system is comprised of leukocytes that are readily available to react upon infection or injury. The adaptive immune system primes a more thorough response, initiating cell-mediated attack and memory generating mechanisms that may defend against cancer recurrence in the future. More important is the immune system's function in immunosurveillance. Immunosurveillance is performed by cells of both the innate and adaptive immune system, functioning to "scan" cells and classify them as self or non-self. Self-cells do not mediate an immune response, however detection of a foreign non-self substance sounds the "immunological alarm," prompting an innate immune response in which digested antigens are presented to cells of the adaptive immune system to generate a stronger response with the added benefit of immunological memory. As a result of uncontrolled proliferation and damaged DNA repair mechanisms, cancer cells that arise from self-cells are prone to producing mutated proteins formally known as neoantigens, which subject tumor cells to immune detection. Under normal physiological conditions, cells expressing mutated proteins are phagocytosed and processed by an antigen

presenting cell, which expresses the antigen on MHC Class 1 or 2 molecules and subsequently to T cells (signal 1). If sufficient danger is sensed by the antigen presenting cells, they are prompted to up-regulate surface expression of co-stimulatory signals (signal 2) and release cytokines (signal 3) that will stimulate activation of cytotoxic T cells that may ultimately destroy the malignant cell[51]. But how do cancer cells persist? Through numerous adaptations and mechanisms, cancer cells are able to evade immune detection and targeting, beginning with the downregulation of antigen expression and in some cases induction of apoptosis in cytotoxic T lymphocytes and other tumor reactive cells.

Mutations in cancer cells generate mutant proteins which serve as suitable antigens/epitopes for immune detection[51]. Thus to avoid detection, cancer cells down-modulate antigen processing machinery, specifically targeting major histocompatibility complex 1 (MHC1) expression, which in turn downregulates cancer antigen expression[51,52]. The ability of tumor antigens to go unrecognized is further promoted by lack of co-stimulatory signals needed for antigen presentation as a result of MHC-1 downregulation. Additionally, cancer cells have been shown to escape immune targeting via expression of "don't eat me" signals (Figure 7)[53].

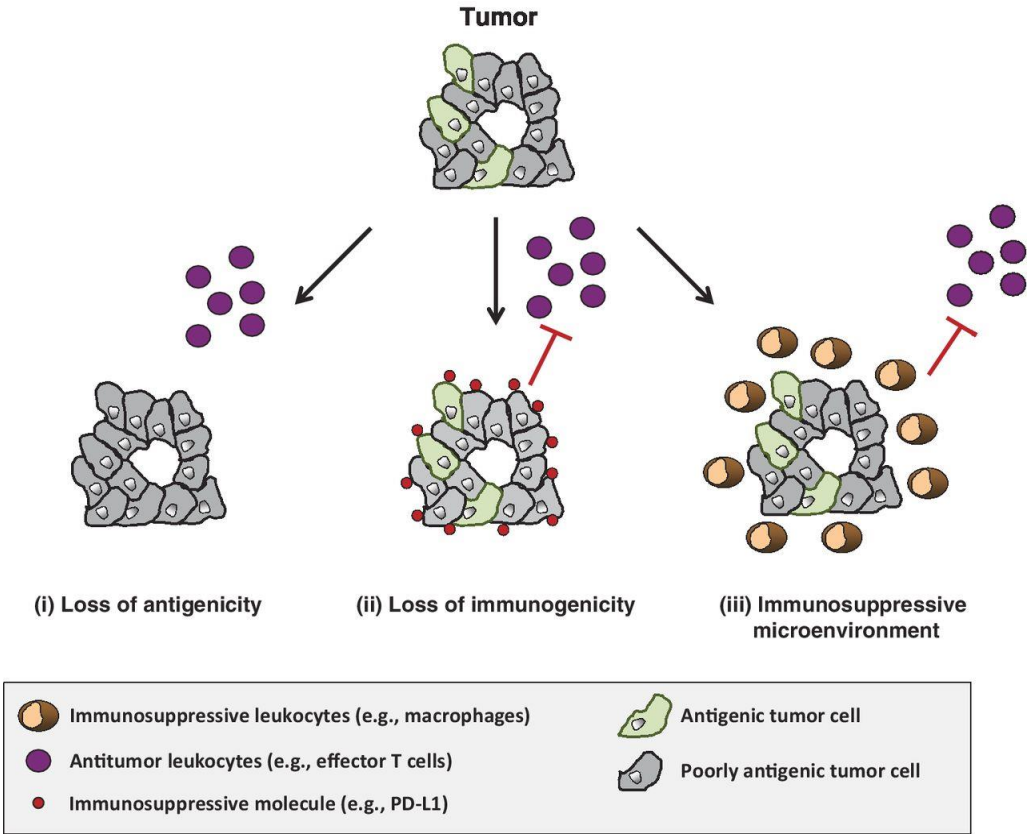


**Figure 7. Immune escape mechanisms in cancer.** Clinically apparent tumors must evolve mechanisms to evade immune elimination. During this process, nascent transformed cells may be selected for based on (i) a loss of antigenicity and/or (ii) a loss of immunogenicity. Loss of antigenicity may be achieved through the acquisition of defects in antigen processing and presentation or through the loss of immunogenic tumor antigens leading to a lack of immunogenic peptides presented in the context of a peptide–MHC complex. Although a loss of antigenicity is also associated with a loss of immunogenicity, malignant cells can gain additional immunosuppressive properties, such as expression of PD-L1 or secretion of suppressive cytokines (e.g., IL10 and TGFβ), which further reduces their immunogenicity. (iii) Tumors may also escape immune elimination by orchestrating an immunosuppressive microenvironment. Malignant transformation induced by alterations in oncogenes and tumor-suppressor genes can lead to the recruitment of an immune response that suppresses antitumor immunity. Reproduced with permission from the *American Association for Cancer Research*©.

Similar to lymphocytes and erythrocytes during splenic macrophage attack, cancer cells upregulate the surface expression of CD47, a potent inhibitor of phagocytic signals[54]. This allows cancer cells to continue dividing undisturbed by immunological sensing and attack. Cell-mediated immune responses pose a great threat to cancer cell survival. Thus, it has been shown that cancer cells constitutively express programed-death ligand 1 (PD-L1) endogenously to counter the effects of the innate immune system

and can induce PD-L1 expression exogenously to counter the attack of the adaptive immune system[55]. Functionally, PD-L1 expressed on tumor cells interacts with the PD-1 receptor found on tumor reactive cells such as cytotoxic T lymphocytes, activating signaling pathways which inhibit proliferation and cytokine release, thereby hampering cytotoxicity[56]. Lastly, as originators of self-cells, cancer cells possess the ability to secrete immunosuppressive cytokines that impede cytotoxic functioning. Primarily, studies have shown TGF-β secretions from cancer cells to inhibit cytotoxic T lymphocyte proliferation, dampening cell-mediated efficacy[57]. Furthermore, VEGF constitutively produced by cancer cells to sustain angiogenesis also functions in inhibiting maturation and differentiation of progenitors into dendritic cells, thereby downregulating antigen presentation[58]. While escape from immune detection is critical to cancer cell growth, cancer cells have also found a way to exploit the human immune system to their benefit, in the formation of the tumor immunosuppressive microenvironment.

## Immunosuppressive Tumor Microenvironment

Tumor cells have been shown to construct an immunosuppressive microenvironment (TME) via induction of hypoxia, recruitment of various immunosuppressive cells, activation of immune checkpoints, and inhibition of cytotoxic T-cell accumulation[59]. Generation of a hypoxic environment is one of the primary steps in majority of developing tumors. Hypoxia response genes are activated and in some cases overexpressed, facilitating the inundation of inflammatory cells that depend on such conditions for glycolysis[60]. Referred to as a "wound that does not heal," tumorigenesis recruits an influx of inflammatory cells[61]. While this may seem counterintuitive, as these inflammatory cells possess anti-tumor properties, the anti-inflammatory cytokines

simultaneously generated dampen their response and further promote tumor growth. T-regulatory cells ($T_{regs}$) and myeloid-derived suppressor cells (MDSCs) are the major immunosuppressive cells of the TME (Figure 8).

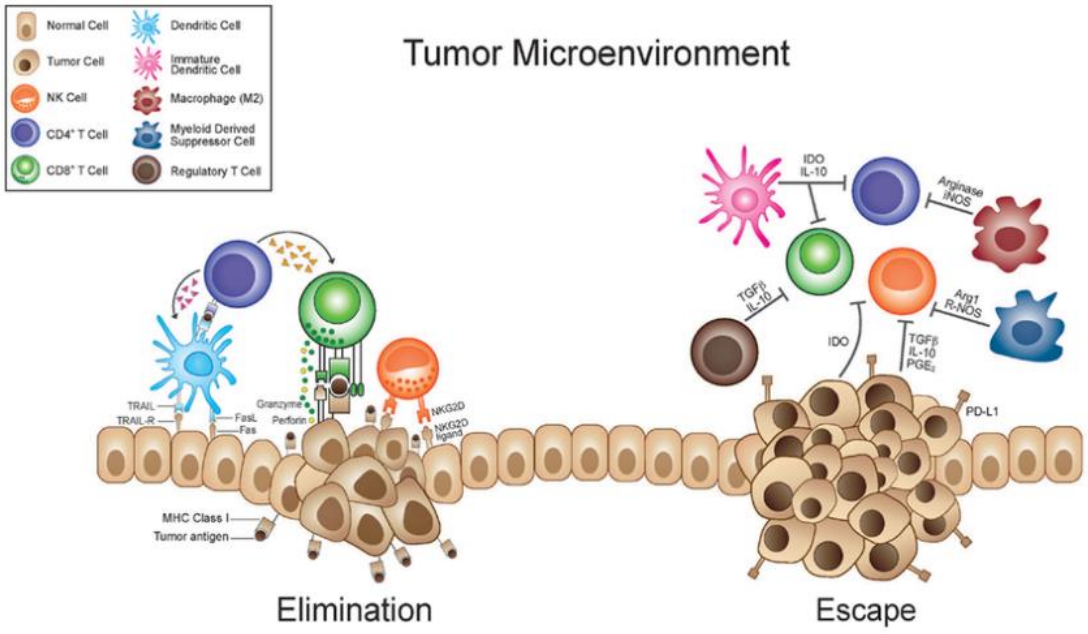


**Figure 8. Immunosuppressive Tumor Microenvironment**. Tumors recruit immunosuppressive cells, activate certain immune checkpoints, and inhibit T-cell accumulation to avoid being detected/ targeted by the immune system. Reproduced with permission from *CreativeCommons*©.

$T_{regs}$ play an enormous role in immunosuppression through maintenance of immune homeostasis, dampening inflammation, and inducing apoptosis in effector T-cells[62]. $T_{regs}$ secrete powerful immunosuppressive cytokines such as IL-10 and TGF-β which have been shown to interfere with effector T-cell function and induce anergy[62]. MDSCs display suppressive functions through similar anti-inflammatory cytokine release (TGF-B & IL-10) and increased production of ARG1 and iNos molecules that inhibit T-cell receptor function[63]. Tumor-associated macrophages (TAMs) are yet another component of the TME shown to produce TGF-β as well as VEGF, which inhibit effector cell function and dendritic cell maturation, respectively[64]. Thus, the chronic inflammatory

state of the TME promotes tumor development through paracrine growth signaling of neighboring immune cells and evasion of immune detection via immunosuppression. After induction of angiogenesis and establishment of the TME, the tumor is favored to develop and grow rapidly. A mechanism to sustain this rapid growth in tumor cells is observed in the transition to an abnormal metabolic pathway, which feeds off glucose attained from angiogenesis and surrounding hypoxic conditions to promote tumor development.

## The Warburg Effect

Normal cell energy metabolism is achieved through the process of oxidative phosphorylation, an aerobic process with an efficient energy yield. Here, glucose is taken up by cells where it is converted to pyruvate in the cytoplasm through the process of glycolysis, and further converted to ATP during the subsequent citric acid cycle and electron transport chain in the mitochondria. Glycolysis yields a net of 2 ATP, whereas the process of oxidative phosphorylation yields 36 ATP. ATP production is more favorable in oxidative phosphorylation, however, the process requires significantly more time to complete. Tumor development is characterized by rapid, uncontrolled division. Thus to sustain the speed at which these cells divide, despite decreased efficiency in ATP production, cancer cells forfeit oxidative phosphorylation and switch to glycolysis as their primary mechanism for energy metabolism. This process is known as the Warburg Effect[65].

These metabolic alterations can be partly attributed to mutations in oncogenes and tumor suppressor genes, which in turn disrupt multiple signaling pathways that affect tumor cell metabolism. Additionally, changes can occur phenotypically due to hypoxic

conditions within the tumor and up-regulation of key transcription factors. The mystery behind this mechanism is that it occurs despite the presence of oxygen and inefficiency in ATP production. However, studies have attributed this reprogramming of energy metabolism to tumor cell dependency on rapid ATP production and upregulation of glucose transport proteins[66]. Increased competition with neighboring cells and tissues drives GLUT-1 production to increase the amount of glucose taken up by the cancer cell[67]. Furthermore, hypoxic conditions of the tumor microenvironment promote the transcription of glucose transporters and glycolytic enzymes, thereby increasing the rate of glycolysis and providing a sustained stream of energy to the growing tumor cells[68]. Additionally, the implications of this rewired metabolism is highlighted in the upregulation of hypoxia inducible factors 1(HIF-1α) which have similar functions in upregulating glycolysis[69]. Fully sustained through angiogenesis and glycolysis, and immortal by nature of upregulated telomerase, cancer cells are able to persist and eventually lead to host demise by avoiding cell death.

## Avoiding Programmed Cell Death

Apoptosis is a mechanism of programmed cell death, termed "cell suicide," that induces the degradation of cells to maintain balance in cell division, eliminate cells suffering from irreparable DNA damage or mutation, and to get rid of structures once their function is no longer necessary, such as the case in embryological development. In contrast to necrosis, cell death via swelling or bursts caused by injury, the process of apoptosis is orderly; in that it does not release danger signals, the cell is reduced in size and DNA cleaved into fragments, and neighboring cells quietly phagocytose and digest the resulting apoptotic blebs (Table 1)[70].

| Apoptosis | Necrosis |
|---|---|
| Single cells or small clusters of cells | Often contiguous cells |
| Cell shrinkage and convolution | Cell swelling |
| Pyknosis and karyorrhexis | Karyolysis, pyknosis, and karyorrhexis |
| Intact cell membrane | Disrupted cell membrane |
| Cytoplasm retained in apoptotic bodies | Cytoplasm released |
| No inflammation | Inflammation usually present |

**Table 1** Comparison of morphological features of apoptosis and necrosis. Reproduced with permission from Toxicologic Pathology©.

This apoptotic circuitry is controlled by upstream regulators and downstream effector signals. The apoptotic regulation of a cell can be characterized by two distinct pathways: intrinsic and extrinsic (Figure 9)[70].

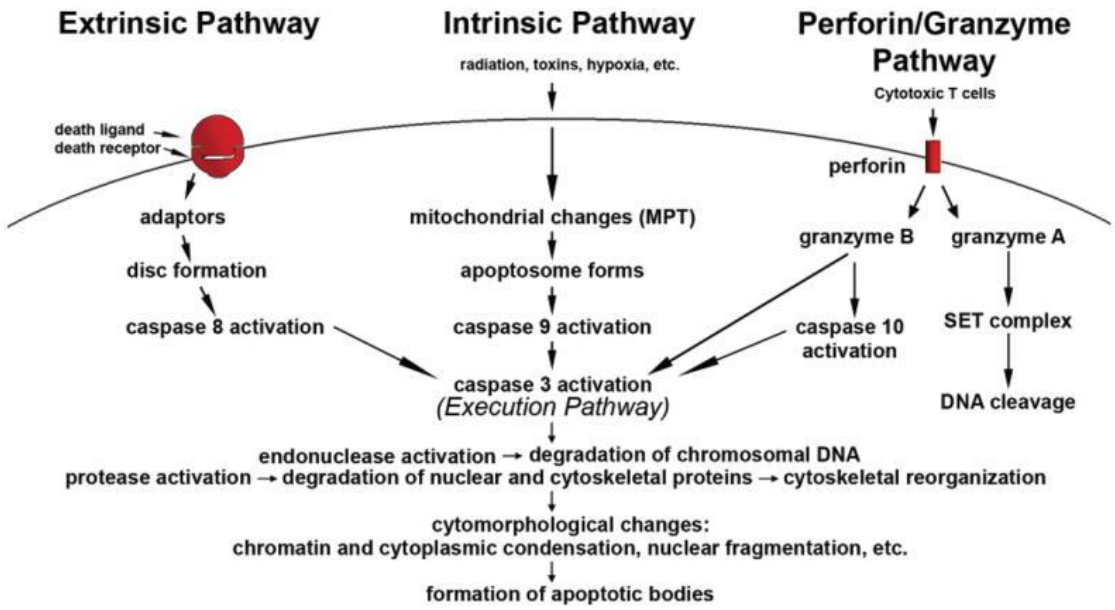


**Figure 9. The extrinsic, intrinsic, and perforin/granzyme pathways of apoptosis.** Each requires specific triggering signals to begin an energy-dependent cascade of molecular events. Each pathway activates its own initiator caspase (8, 9, 10) which in turn will activate the executioner caspase-3. However, granzyme A works in a caspase-independent fashion. The execution pathway results in characteristic cytomorphological features including cell shrinkage, chromatin condensation, formation of cytoplasmic blebs and apoptotic bodies and finally phagocytosis of the apoptotic bodies by adjacent parenchymal cells, neoplastic cells or macrophages. Reproduced with permission from *Toxicologic Pathology*©.

Cytotoxic stimuli induce intracellular signaling which triggers the intrinsic apoptotic pathway, marked by mitochondrial outer membrane permeabilization[71]. On the other hand, the extrinsic apoptotic pathway is regulated by extracellular death receptors. Binding of a death receptor to its death receptor ligand triggers intracellular signaling that drives the apoptotic trigger which conveys the message to downstream effector components to initiate programmed cell death[72]. Extracellular death receptors are members of the tumor necrosis factor (TNF) family, which are characterized by an 80 amino acid cytoplasmic "death domain," with critical functions in death signaling[72,73]. Common extracellular death receptors include CD95, mediated by APO-1 and Fas, TNFR-1, and TNF-associated apoptosis inducing ligand receptor 1 (TRAIL-1).

The triggering of these pathways and resulting induction of downstream effector function is dependent upon cellular stress signals or detected abnormalities. Cell division induces apoptosis in existing populations to maintain balance in cell number and ultimately preserve tissue architecture. Studies have shown that as cells divide rapidly, apoptosis occurs rapidly; typically evidenced in embryological development and mitogenic studies[74]. Additionally, cellular stress, by way of DNA damage or mutation, triggers the induction of programmed cell death pathways. The p53 gene serves to detect DNA damage and halt the cell cycle to correct for said damage. In some cases, the DNA damage sustained is beyond the repairable capabilities of physiological DNA repair mechanisms. Thus p53 signaling induces downstream effector functions to initiate cell death[75]. Furthermore, cells that are alive and well maintain surface expression levels of survival signals such as insulin growth factor 1 (IGF-1) and interleukin-3 (IL-3)[76]. As a cell decreases in viability, survival signal expression is decreased resulting in cell suicide.

Detection of the above abnormalities or levels of cellular stress prompts downstream effector function, primarily characterized as the activation of caspases. Synthesized as inactivated procaspases, apoptotic triggers induce cleavage of caspases which result in the activation of a proteolytic cascade[77]. Cleavage of caspase-9 is highlighted in the intrinsic pathway, which leads to mitochondrial membrane permeabilization that facilitates the release of proapoptotic signaling-protein cytochrome C[78]. Extrinsic pathway signaling, characterized by cleavage of caspase-8, triggers the activation of further downstream effectors such as caspase-3 that ultimately result in programmed cell death[78]. Thus, apoptosis signaling is attributed to procaspase activation, which is tightly controlled by the Bcl-2 protein family[79]. Members of the Bcl-2 family are classified as inducers of apoptosis or inhibitors of apoptosis. The balance of proapoptotic and antiapoptotic proteins is important in maintaining cell homeostasis, and often exploited by cancer cells. For example, Bcl-2 is an important inhibitor of apoptosis, which functions in blocking mitochondrial cytochrome c release. Alternatively, Bak and Bax proteins of the Bcl-2 protein family function as inducers of apoptosis through activation of procaspases and stimulation of cytochrome c release[79]. Thus, to avoid programmed cell death, cancer cells infringe upon these mechanisms to exploit both intrinsic and extrinsic apoptotic pathways and ultimately sustain growth.

Defined by a state of genomic instability, frequent loss-of-function mutations in the p53 gene are seen in cancer cells which facilitates escape from cellular-stress mediated apoptosis. Although cancer cells are characterized by abnormal cell division and replication of damaged and mutated DNA, the suppression of p53 function inhibits intracellular signaling which would normally induce apoptosis in such cells[75].

Additionally, cancer cells have been shown to upregulate the expression of survival signals such as IGF-1 to evade apoptotic targeting[80]. Furthermore, cancer cells have been shown to downregulate the expression of death receptors so as to avoid death receptor ligand binding, and triggering the extrinsic pathway of apoptosis[81]. Escape via these mechanisms allow cancer cells to resist cell death and hinder the function of intrinsic and extrinsic apoptotic pathways. Lastly, it has been found that cancer cells may upregulate the translation of Bcl-2, saturating the intracellular environment with apoptosis inhibitors that prevent the activation of procaspases[82]. While the obstruction by cancer cells of all the above physiological machineries and abnormality sensors may portray cancer as invincible, each mechanism of escape provides a suitable drug target designed to have potent antitumor effects.

## Chemotherapeutic Approach to Cancer Treatment

The past century has accounted for innumerous advancements in chemotherapies and alternative antitumor treatment options (Figure 10)[83].

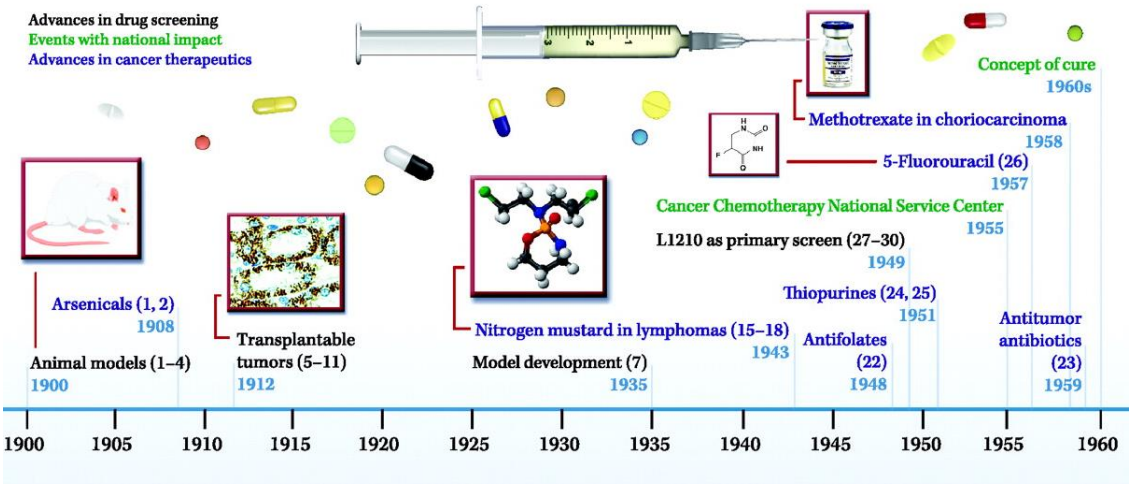

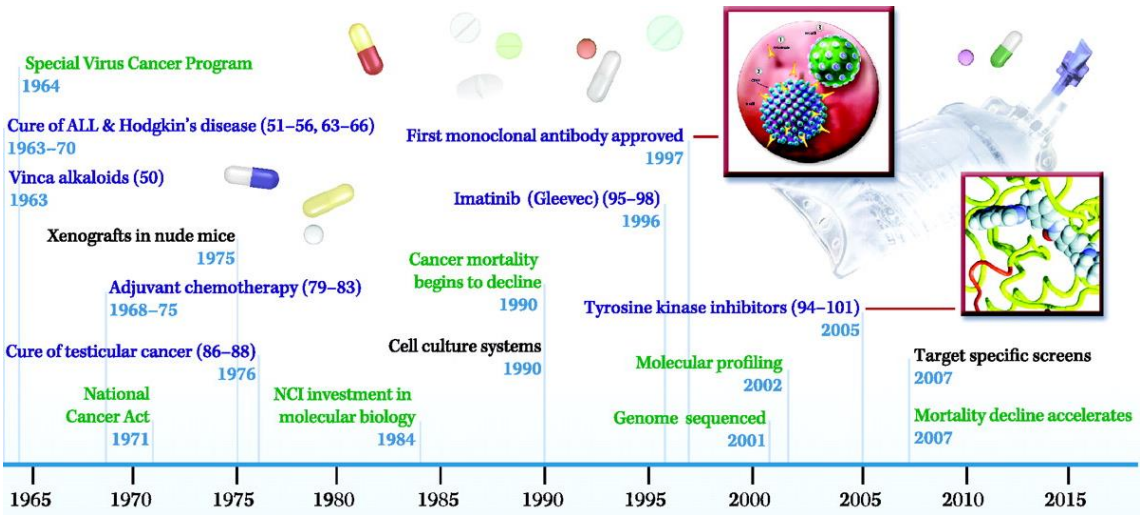


**Figure 10. Key advances in the history of cancer chemotherapy.** Reproduced with permission from the *American Association for Cancer Research*©.

Pioneer research in chemotherapy is credited to Paul Ehrlich, who investigated the use of chemicals to treat disease. His early work of utilizing arsenicals to treat syphilis became the foundation of modern chemotherapy[83]. Decades later, researchers began to explore radiation therapy, as well as combination of chemotherapy with radiation therapy and surgical removal. Currently, the majority of chemotherapies used in the treatment of early stage and late-stage advanced cancers are DNA mutagens that impact DNA replication or function in cancer cells[84]. While most are generally effective at killing cancer cells, the problem of non-specificity within this class of drugs arises. 72% of cancer patients receive chemotherapy through intravenous infusion at varying durations[85]. The non-specificity of this route of drug administration allows the chemotherapy to interact with normal cells of the human body. The significance of this interaction lies in the fact that some cells, including those contained in the bone marrow, GI tract, and epidermal skin, proliferate faster than cancer cells and therefore subject them to chemotherapeutic targeting[86]. Thus, the toxic effects of chemotherapies are endured by healthy cells and result in severe side effects manifested as cachexia. Hair loss, nausea,

and vomiting can all be attributed to the general toxicity of chemotherapeutic compounds. More importantly, the mutagenic mechanism of action of these compounds gives rise to resistant cancer cells. By targeting the cell's replicative mechanisms, clonal selection of survivors drives genome mutations which build tolerance and confer resistance to chemotherapies, rendering them ineffective[87]. Solutions frequently employed range from increasing dose, and combination of other chemotherapies to help sensitize the cancer cell to treatment; all of which further the harmful effects to normal cells in the process. Thus, recent studies have emphasized therapies with higher specificity and the ability to modulate the body's own immune system in targeting and eradicating cancer cells.

## Immunotherapeutic Approach to Cancer

Immunotherapy has become the frontier in cancer treatment over the past few decades. The human body innately possesses the mechanism to detect and destroy neoplasia via the immune system, however, cancer cells have responded with mechanisms to escape this immunological targeting. Thus, immunotherapies seek to overcome the cancer cell's pathways of immune evasion and subject them to immunological targeting. The benefits of this treatment modality are plenty, but primary focus is given to the heightened specificity to cancer cells and general non-toxicity to normally dividing cells. Immunotherapies are classified as active or passive with regards to their effect on the host's immune system[88]. Active therapies, such as cytokines, immunomodulatory monoclonal antibodies, and cancer vaccines directly induce an immune response as a result of their treatment[55]. Conversely, passive therapies including bispecific antibodies, oncolytic viruses and adjuvants, and tumor-targeting monoclonal

antibodies seek to stimulate the patient's intrinsic immune response[89]. Ultimately, these treatments facilitate the uptake of tumor neoantigens and processing by lymphocytes, which generates an adaptive cell-mediated immune response specific to cancer cells, with the added benefit of immunological memory to fend off potential tumor relapse. While immunotherapy may be perceived as the pinnacle of cancer treatment, it faces challenges with efficacy as well. As previously mentioned, a hallmark of cancer development is the establishment of the immunosuppressive tumor microenvironment. Here, the anti-tumor mechanisms of immunotherapies are counteracted by potent tumor promoting factors, thereby rendering most immunotherapies ineffective when used singly. Cancer cells are also able to adapt and confer resistance to immunotherapies through clonal selection[90]. Evidenced in proapoptotic immunotherapeutics, cancer cells have been shown to respond with upregulation of antiapoptotic factors such as Bcl-2[91]. Escalating doses drive cancer cell evolution and genetic mutation and ensuing clonal selection of these cells results in resistance to all kinds of remedies[92]. Thus, the importance of combination therapy and critical pathway targeting is necessary in developing highly effective cancer treatments.

## Glycolytic Inhibitors

The atypical shift to aerobic glycolysis from oxidative phosphorylation in cancer cells is viewed as a hallmark of tumorigenesis. Elevated rates of glycolysis lower pH and result in hypoxia, driving factors of the immunosuppressive tumor microenvironment formation. Although this mechanism confers a survival advantage to the cancer cell, it also creates a specific drug target for antitumor therapies: glycolytic inhibitors. This class of drug varies, from inhibitors of major glycolytic regulators to analogues of glucose with inhibitory function; all of which share the ultimate goal of impeding tumor glycolysis and

inducing cancer cell death. Glycolytic inhibitors have also been shown to indirectly dismantle the immunosuppressive tumor microenvironment, thereby sensitizing cancer cells to antitumor therapies[93]. One such compound, 2-deoxyglucose (2-DG), is a glucose analogue with a hydrogen substituted in place of the standard 2-hydroxyl group. This single conformational change allows 2-DG to competitively inhibit glucose-6-phosphate production at the hexokinase step of glycolysis (Figure 11)[94].

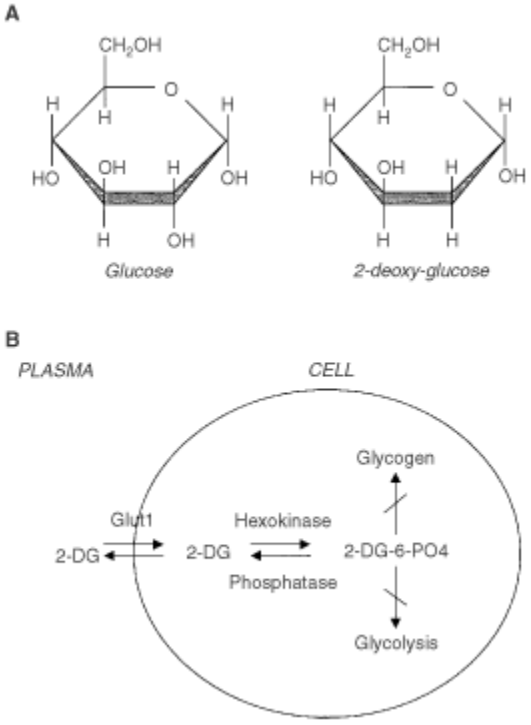


**Figure 11. (A) Structural comparison of glucose and 2-deoxy-D-glucose.** 2DG and glucose differ at the second carbon. **(B) Schematic diagram of 2-DG action.** 2DG enters the cell through the glucose transporter and is phosphorylated by hexokinase. Due to low levels of intracellular phosphatase, 2-DG-$PO_4$ is trapped in the cell. 2-DG-$PO_4$ is unable to undergo further metabolism. High intracellular levels of 2-DG-6-$PO_4$ cause allosteric and competitive inhibition of hexokinase. This results in inhibition of glucose metabolism. Reproduced with permission from *CreativeCommons*©.

This is only one of many ways 2-DG adversely affects cancer cell metabolism and growth. Additionally, 2-DG has been shown to interfere with N-glycosylation in cancer cells[95]. This interaction results in the unfolded protein response (UPR), characterized by severe endoplasmic reticulum stress within the cancer cell, eventually leading to

activation of UPR-mediated apoptotic pathways inducing programmed cell death. Furthermore, treatment with 2-DG inhibits endothelial cell-derived angiogenesis both *in vitro* and *in vivo*, accentuating its antitumor properties[96]. Although a promising mode of therapy with significant efficacy, clonal selection has allowed cancer cells to mutate and adapt to this drug target, allowing them to persist despite treatment.

## DNA Replication Inhibitors

One of the founding principles of cancer development is abnormal cell growth and uncontrolled proliferation. This disease mechanism is directly dependent upon DNA replication, despite damages to or mutation in the original sequence. Again while the dependency of cancer cells upon DNA replication facilitates neoplasia formation, targeting this cancer cell reliance in the form of DNA replication inhibitors has proven effective in mounting an antitumor response. Current chemotherapies target this mechanism, including DNA alkylating agents, anthracyclines, antimetabolites, topoisomerase inhibitors, and mitotic inhibitors. Specifically, folic acid is required for the *de novo* synthesis of the nucleoside thymidine, a key factor in DNA synthesis[97]. Folate is also crucial for the biosynthesis of purine and pyrimidine bases required for DNA synthesis[98]. This heavy reliance on folate and folic acid by cancer cells highlights the use of antifolates as an effective class of antitumor treatment. Methotrexate (MTX) is an antimetabolite of the antifolate type, and directly interferes with DNA synthesis[98]. Mechanistically, MTX competitively inhibits dihydrofolate reductase (DHFR) which decreases tetrahydrofolate (THF) levels, resulting in attenuated DNA/protein/lipid methylation, inhibition of thymidylate synthase (TS), and interference with DNA synthesis (Figure 12)[99].

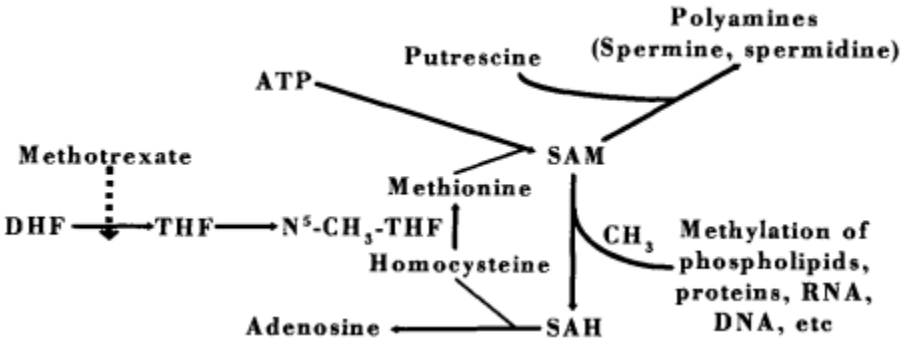


**Figure 12. Inhibition of transmethylation reactions and polyamine formation by methotrexate.** DHF= dihydrofolate; THF= tetrahydrofolate; N"-CH,-THF= N"-methyl-tetrahydrofolate; THF= tetrahydrofolate; SAM= S-adenosyl-rnethionine; SAH= S-adenosyl-hornocysteine Reproduced with permission from *John Wiley and Sons*©.

Furthermore, MTX has recently been shown to enhance DC function and in turn antigen presentation, demonstrated by increased levels of co-stimulatory markers CD80 and CD86 as well as the ability to stimulate T-cell proliferation[100]. Aside from the common cachexia associated with chemotherapies as a result of non-specificity and toxicity towards normal cells, cancer cells have demonstrated resistance to standard MTX therapy, and sustain uncontrolled proliferation.

## Overcoming Immunosuppression in the TME

As mentioned above, the formation of the immunosuppressive tumor microenvironment is detrimental to host survival, as it provides a mechanism of immune evasion and elimination by the cancer cell. T-regulatory cells ($T_{regs}$) and myeloid-derived suppressor cells (MDSCs) are the major immunosuppressive cells of the TME. The recruitment of these cells to the site of the developing tumor creates a barrier against cell-mediated and pro-inflammatory responses of the immune system by secretion of anti-inflammatory cytokines and cytotoxic T cell anergy mediated by $T_{regs}$. Without these properties, tumor cells would be susceptible to targeting by the immune system. Therefore, overcoming the immunosuppressive tumor microenvironment is a hallmark of

developing immunotherapies. Wogonin (WGN) is a recently discovered immunostimulatory flavonoid, identified to have potent anti-tumor properties (Figure 13)[101].

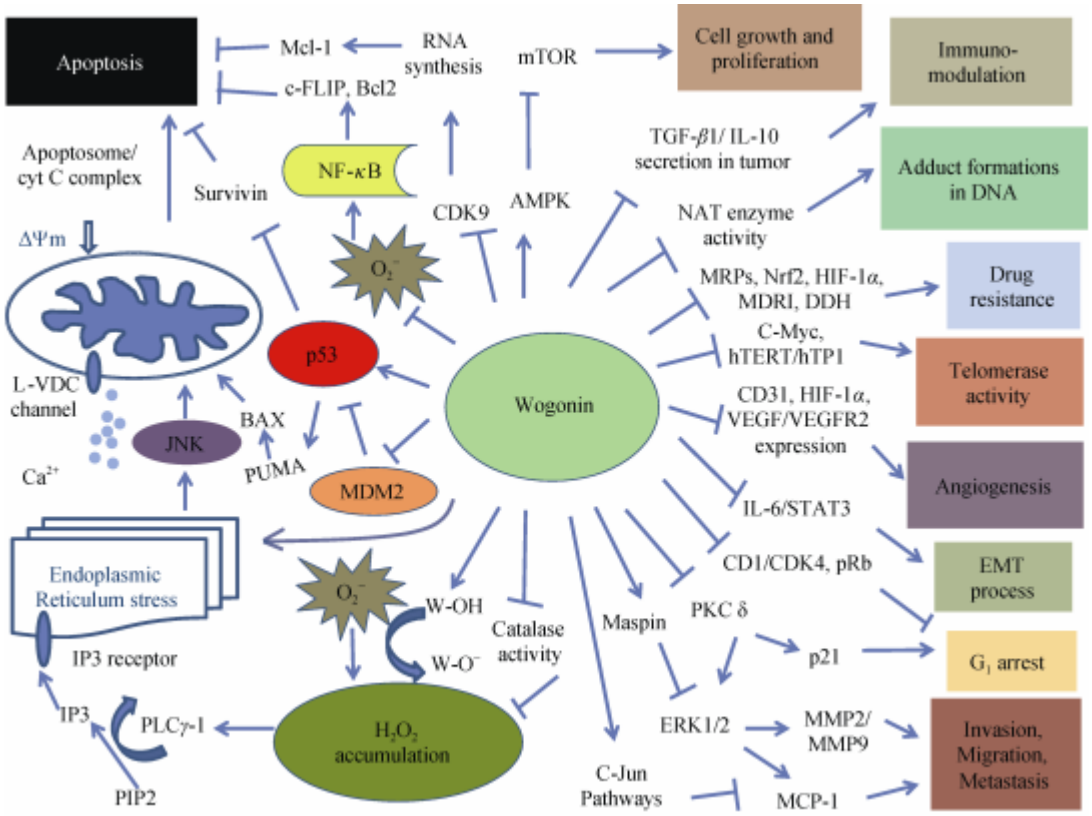


**Figure 13. Anti-cancer properties of wogonin via several signaling pathways.** Reproduced with permission from *Elsevier*©.

Concordant with these findings, WGN has been shown to inhibit angiogenesis, induce apoptosis, and synergize with IL-2 to stimulate cytotoxic T-cell function[102,103]. Remarkably, WGN has been shown to down-regulate T-regulatory cell function[103]. Modulation of this key component of the TME sensitizes the tumor to cytotoxic T-cells and other effector cells of the immune system.

## Problems with Standard Practice

While the different compounds presented above are efficacious towards cancer cells, challenges remain. In the case of 2-DG, a recent study has found hypoxia-inducible factor 1-alpha (HIF-1α) confers resistance to the glycolytic inhibitor[104]. HIF-1α is known to increase glycolytic enzymes and glucose transporters under hypoxic conditions, such as is found in the primary tumor microenvironment[66]. This upregulation counterbalances 2-DG treatment, requiring an increased dose to inhibit glycolysis, which facilitates resistance mechanisms to the compound due to the resulting increased levels of glycolytic enzymes. In the case of MTX, concordant to most standard chemotherapies, challenges are faced with multi-drug resistance (MDR) and multidrug resistance-associated proteins (MRPs). Under normal physiological conditions, ATP-binding cassette transporters (ABC transporters) hydrolyze ATP to facilitate uptake or export of substances across the cellular membrane. Members of the ABC transporter subfamily, namely multidrug resistance 1 P-glycoprotein (P-g) and MRPs, function to specifically export drugs from the intracellular matrix by way of an ATP-fueled pump[105]. To decrease intracellular drug concentrations post-treatment, cancer cells employ these MDR mechanisms, characterized by high-level expression of MDRP subfamilies in liver cells where detoxification occurs[106]. Increased concentrations of drug products have also been isolated from liver bile, suggesting anticancer drug products are exported out of cancer cells by P-g or MDRPs and subsequently transported into bile[107]. Specifically, MRP3 has been shown to confer high-level resistance to MTX in ovarian carcinoma models[108]. Additionally, studies have found MTX to be a substrate of MRPs as well as breast cancer resistance proteins (BRCPs), conferring resistance to the therapy and minimalizing its

efficacy[109]. Furthermore, by way of DHFR competitive inhibition, increased DHFR enzyme production by cancer cells to counterbalance MTX treatment promotes resistance to this therapy[110]. The takeaway from these findings is that when used singly, these compounds are subject to the full wrath of cancer cell resistance mechanisms. Therefore, it is critical that advancements in cancer treatment employ combinatorial therapy, to help overcome said mechanisms and generate a more efficacious anticancer response. Moreover, the mechanism by which these therapies induce cell death should be immunogenic, so as to prime a powerful adaptive immune response to help the patient's own immune system detect and kill cancer cells and generate immunological memory to prevent against potential relapse.

## Questions

The questions addressed by this dissertation are as follows:

1. Could the novel combination of methotrexate, 2-deoxyglucose, and wogonin at concentrations below their individual $EC_{50}$ result in anticancer effects greater than the compounds used individually? Would the proposed combinatorial therapy be non-toxic to normal cells and lymphocytes as opposed to standard chemotherapies? Would the combinatorial therapy be more effective than standard chemotherapies at inhibiting colony formation? Does the novel combinatorial therapy exhibit significant cytotoxicity to multiple malignant tumor cell lines? Does the novel combinatorial therapy exhibit significant cytotoxicity to monolayers of tumor cells as well as 3D tumorspheres?

2. What is the mechanism by which cancer cells die after treatment with the novel combinatorial therapy? Do cancer cells killed by this novel combinatorial therapy exhibit

immunogenicity via surface expression and secretion of immunogenic cell death markers?

## Hypotheses

1. A novel combination of methotrexate, 2-deoxyglucose, and wogonin would overcome the resistance mechanisms faced when each is administered singly, and combine to produce a more effective anticancer treatment that is non-toxic to rapidly dividing cells of the immune system.

2. A novel combination of methotrexate, 2-deoxyglucose, and wogonin would induce cell death with strong indications of immunogenic cell death, characterized by expression and secretion of key immunogenic cell death markers.

## Goals

The proposed study will provide valuable information on the development of a novel multi-target therapy that will kill cancer cells via glycolytic and DNA synthesis inhibition, while simultaneously generating a primed adaptive immune response and overcoming tumor immunosuppression. This novel approach to cancer immunotherapy will provide an invaluable tool for clinicians and researchers to target multiple cancer-associated pathways, with implications of powerful anticancer effects towards a variety of cancer cell lines.

## Specific Aims

1. Determine the cytotoxic effect of 2-DG, MTX, & WGN combinatorial therapy against breast cancer cells and other malignant cancer cell lines.

2. Evaluate the toxicity of 2-DG, MTX, & WGN combinatorial therapy towards rapidly proliferating cells of the immune system.

3. Gain insight into the mechanism and immunogenicity of cancer cell death post- 2-DG, MTX, & WGN combinatorial treatment.

4. Determine the cytotoxic effect of 2-DG, MTX, & WGN combinatorial therapy against 3D mammary adenocarcinoma and carcinoma tumor models.

# CHAPTER 2: A NOVEL LOW-DOSE COMBINATORIAL THERAPY IS EFFECTIVE AGAINST MALIGNANT TUMOR CELLS

## 2.1 ABSTRACT

Resistance to chemotherapy and immunotherapy by cancerous cells has been a challenge clinicians have tried to overcome for decades. The current study combined a standard chemotherapy, methotrexate, and a potent glycolytic inhibitor, 2-deoxyglucose, with an anticancer flavonoid, wogonin to overcome referenced resistance mechanisms and induce an efficacious antitumor effect. Studies were performed to determine their individual $EC_{50}$ concentrations, evaluate the pharmacochemical interaction between one another, and evaluate the efficacy of the compounds against tumor cells when used singly vs in combination. The individual $EC_{50}$ of MTX, 2-DG, and WGN were determined in the 4-T1, MCF-7, THP-1, and B-16 F10 cell lines. The concentrations of two of three compounds was held constant while altering the individual concentration of one of three compounds. Tests showed no evidence of pharmacokinetic interference or significant drug-drug interactions. Combination of the compounds showed no evidence of precipitate formation or pH fluctuation. This novel combination has proven significantly efficacious over the compounds used singly under hypoxia and normoxia, and was efficacious at concentrations 6 times below their individual $EC_{50}$ concentrations. We can conclude from these studies that treatment with our novel combinatorial therapy has potent anticancer effects *in vitro* against multiple malignant cell lines. More importantly, our studies show

the significant increase in efficacy our novel combinatorial therapy holds compared to the individual compounds administered singly.

## 2.2 INTRODUCTION

The majority of malignant tumors are characterized by 3 fundamental processes: sustained chronic proliferation, abnormal metabolism, and the construction of an immunosuppressive tumor microenvironment[111]. Mutations in tumor suppressor genes are a hallmark of genomic instability, which promotes the abnormal functioning and regulation of the cell cycle. Chronic proliferation is marked by uncontrolled DNA replication. Damages and mutations to the DNA sequence normally prompt highly regulated DNA repair mechanisms that halt cell division and induce apoptosis when necessary. In the case of cancer, cells progress through the cell cycle despite DNA damage, and exhibit an increased dependency on DNA replication[22]. The speed at which these mutated cells proliferate subsequently generates a dependency on ATP to fuel cellular processes and maintain cell viability. To account for this increased demand, cancer cells resort to aerobic glycolysis to rapidly produce ATP and sustain cell proliferation. This metabolic shift is characterized by an increase of glycolytic enzymes and glucose transporters in tumor cells, in an attempt to make this generally inefficient metabolic process more efficient for the cancer cell[66]. To protect the abnormally dividing tumor cells from immune targeting and destruction, recruitment of anti-inflammatory immune cells to the site of the tumor is observed, which contribute to the formation of the immunosuppressive tumor microenvironment. Anti-inflammatory cells constitutively secrete cytokines which promote proliferation and angiogenesis, promoting cell growth[111]. Simultaneously, these cells secrete potent anti-inflammatory cytokines that

dampen cell-mediated responses and immunosurveillance mechanisms. These characteristics, coupled with the compelling resistance mechanisms cancer cells exhibit towards therapeutic agents, pose great challenges in developing anticancer therapies.

DNA mutagens have shown great efficacy towards cancer cells but are counteracted by evermore powerful resistance mechanisms that transport these agents directly out of the cell through glycoprotein pumps. A representative compound examined in this study, methotrexate, interferes with DNA replication by inhibiting dihydrofolate reductase enzyme function, thereby inhibiting cell division[97]. Treatment of cancer cells with methotrexate increases the activity of multidrug resistance pathways, as well as increases the production of affected enzymes[108]. Used singly, cancer cells readily adapt to methotrexate cytotoxicity and confer resistance to sustain cell proliferation. Glycolytic inhibitors target a critical pathway in cancer cell metabolism yet are succumb to resistance by hypoxia inducible factor upregulation. A representative compound examined in this study, 2-deoxyglucose, is an analogue of glucose that interferes with hexokinase function in glycolysis. The inability of the cancer cell to convert 2-DG to ATP results in glycolytic inhibition and subsequent cell death. Yet the cancer cell recognizes this metabolic targeting and responds with increased levels of hypoxia inducible factor 1 (HIF-1α)[104]. This wagers an "arm's race" between the clinician and the cancer cell; as increasing the dose triggers increased enzyme levels to counteract the anticancer effects. Used singly, 2-DG is pit against the evidently more powerful resistance mechanisms of the cancer cell, rendering it ineffective and resulting in sustained cancer cell metabolism. Therefore, the heterogeneity of cancer cell populations makes it relatively impossible for a single therapeutic agent to effectively kill all cells of

the given population[112]. Thus, the development of effective combinatorial therapies against cancer is of utmost importance to the medical community.

## 2.3 BACKGROUND AND SIGNIFICANCE

Two is better than one; as is the case for combinatorial therapies against cancer. Resistance is commonly observed when a therapeutic agent is used singly, due to clonal selection of cancer cells and growth of treatment-resistant survivors. The principles of combinatorial therapy sensitize specific pathways to treatment by a second therapeutic agent, or target multiple pathways that result in a strong anticancer effect the cell is unable to overcome[113]. The significance of combinatorial therapy lies in its ability to target heterogenic cancer cell populations and be equipped with a mechanism for killing fit to eradicate all members of said population.

Challenges faced by combinatorial therapy primarily stem from the lack of knowledge of certain drug interactions when combined, and heavily rely upon data from the drugs used individually to gauge such trials. Evaluating pathway crosstalk to determine ideal combination concentrations and dynamics is costly and in some cases impossible; therefore, trial and error and a sequence of experiments is necessary to formulate an efficacious combinatorial therapy[114]. The preliminary work of combination therapy development is characterized by studying each individual component alone. Determination of cytotoxicity and $EC_{50}$ concentrations is critical in determining combined concentration values. Second, the interactions of each compound with one another must be studied to ensure no abnormal chemical reactions take place, which would alter the functioning of one or more of the compounds. Pharmacokinetic studies examine pH, precipitate formation, and evidence of chemical reactions (formation of gas,

heating, or cooling) to determine the interactions between the compounds. Furthermore, studying one compound's concentration at a time is critical in determining the optimal efficacy, and sheds more light on drug-drug interactions at varying concentrations. *In vitro* studies provide a wealth of knowledge on efficacy as well as mechanisms of cell death, all of which possess translational implications to *in vivo* practices. The ability to closely resemble *in vivo* tumor conditions and gather significant preclinical evidence make *in vitro* studies the paramount of anticancer therapy development.

Recent studies have guided our development of the novel MTX, 2-DG, and WGN combinatorial therapy. Mentioned above, cancer cells resist MTX treatment by upregulation of MDR mechanisms and 2-DG treatment by upregulation of HIF-1α. Studies conducted by *Yu et al.* show that when combined with WGN, MTX systemic exposure was increased significantly and MDRP and BCRP levels were down-regulated substantially[109]. Additionally, *Song et al.* found WGN to be a potent inhibitor of HIF-1α and VEG-F, specifically via degradation of the HIF-1α protein[115]. 2-DG targeting of glycolytic pathways, MTX targeting of DNA synthesis pathways, combined with WGN targeting of HIF-1α and MDRPs that normally confer resistance to the two compounds, respectively, signifies our reasoning behind this combinatorial therapy. Furthermore, we seek to achieve efficacy at doses well below their individual $EC_{50}$ in our combination, creating an avenue for specific and effective low-dose treatment. Our studies will also model the hypoxic conditions of the tumor by incubating *in vitro* cultures in hypoxia chambers. Normoxia studies are conducted as well, since not all developing cancers exhibit hypoxic conditions. The targeting of two critical pathways, one catabolic and one

anabolic, coupled with a therapeutic agent with its own anticancer effects as well, holds great promise for our novel development of an effective cancer therapy.

## 2.4 METHODS

### *2.4.1 Cell culturing and maintenance*

The 4-T1 (Mouse Metastatic Mammary Carcinoma) cell line was kindly donated by Dr. Vijaya Iragavarapu-Charyulu, Department of Biomedical Sciences, Florida Atlantic University. MCF-7 (Human Metastatic Mammary Adenocarcinoma) and B16-F10 (Mouse Metastatic Melanoma) cell lines were obtained from Dr. James X. Hartmann, Department of Biological Sciences, Florida Atlantic University. The THP-1 (Human Acute Monocytic Leukemia) cell line was kindly donated by Dr. Yoshimi Shibata, Department of Biomedical Sciences, Florida Atlantic University. Cells were cultured between $2\times10^5$/mL and $1\times10^6$/mL in 75 $cm^2$ Falcon cell culture flaks containing Gibco RPMI 1640-L-Glutamine medium (Life Technologies- Grand Island, NY, USA) supplemented with 10% fetal bovine serum (Life Technologies- Grand Island, NY, USA) and 100U/mL Gibco Pen Strep (Life Technologies- Grand Island, NY, USA). Cell cultures were incubated at 37 °C under 5% $CO_2$ in a humidified atmosphere.

### *2.4.2 MTS cell viability assay*

Analysis of the effects of MTX-2DG-WGN combination on cell growth was performed with an MTS kit (CellTiter 96® AQueous One Solution Cell Proliferation Assay Kit, Promega, Madison, WI, USA) according to the manufacturer's instruction. 4-T1, MCF-7, B16-F10, and THP-1 cells were seeded into 96-well plates at a density of $10\times 10^3$ cells per well with three replicates. The cells were treated as indicated (MTX, 2DG, and WGN were added initially at concentrations of 100 µM, 50 mM, and 200 µM, respectively,

followed by serial two-fold dilutions) and incubated for 48 h at 5% $CO_2$ at 37°C. After 48 h, 20 µL of CellTiter 96® AQueous One Solution MTS (5 mg/mL) (Promega- Madison, WI, USA) was added to each well and incubated at 5% $CO_2$ at 37°C for an additional 4h. Absorbance readings were taken in an Epoch microplate reader at 490 nm. Computed data was compared to untreated and normalized cells. Cells that were not administered any treatment were considered the control group. Cell viability was calculated by the following formula: Cell viability (%) = (average OD in treated group/average OD in control group) × 100%.

*2.4.3 Determination of $EC_{50}$*

The $EC_{50}$ was extrapolated from the dose-response graph. The drug concentration that caused 50% maximum effect with regards to cytotoxicity was determined by plotting triplicate data points over a concentration range and calculating values using regression analysis of GraphPad PRISM v8 program.

*2.4.4 Cell viability assay via trypan blue exclusion*

4-T1 cells ($1 \times 10^6$ cells/mL) were seeded in CellTreat 15 mL Bio-reaction Cell Culture tubes in 5 mL Gibco RPMI 1640 L-Glutamine (Life Technologies- Grand Island, NY, USA), supplemented with 10% certified heat-inactivated fetal bovine serum (FBS), treated with MTX, 2DG, and WGN drug combination. MCF-7 cells ($1 \times 10^6$ cells/mL) were seeded in CellTreat 15 mL Bio-reaction Cell Culture tubes in 5 mL Gibco RPMI 1640 L-Glutamine (Life Technologies- Grand Island, NY, USA), supplemented with 10% certified heat-inactivated fetal bovine serum (FBS), treated with MTX, 2DG, and WGN drug combination. Cells were incubated for 24 h at 5% $CO_2$ at 37°C. After 24 h, cells were centrifuged at 1200 RPM for 10 minutes. The resulting cell pellet was

resuspended in 1 mL of cell culture media. 10 µL of 0.4% trypan blue was mixed with 10 µL of cell suspension in a 96-well plate and incubated for 2 minutes at room temperature. 10 µL of the 0.4% trypan blue/cell suspension mixture was loaded onto a hemacytometer and stained vs unstained cells were counted. The percentage of viable cells was calculated using the formula: $\% \, Viability =$

$$\frac{total\ number\ of\ unstained\ cells}{total\ number\ of\ stained\ and\ unstained\ cells}\ x\ 100$$

*2.4.4 MTS cell viability assay under hypoxia*

Analysis of the effectiveness of MTX-2DG-WGN combination under hypoxia on cell growth was performed with an MTS kit (CellTiter 96® AQueous One Solution Cell Proliferation Assay Kit, Promega, Madison, WI, USA) according to the manufacturer's instruction. 4-T1 and MCF-7 were seeded into 96-well plates at a density of $10\times 10^3$ cells per well with three replicates. The cells were treated as indicated (MTX, 2DG, and WGN were added initially at concentrations of 100 µM, 50 mM, and 200 µM, respectively, followed by serial two-fold dilutions) and incubated for 48 h at 1% $O_2$ 5% $CO_2$ at 37°C. After 48 h, 20 µL of CellTiter 96® AQueous One Solution MTS (5 mg/mL) (Promega-Madison, WI, USA) was added to each well and incubated at 5% $CO_2$ at 37°C for an additional 4h. Absorbance readings were taken in an Epoch microplate reader at 490 nm. Computed data was compared to untreated and normalized cells. Cells that were not administered any treatment were considered the control group. Cell viability was calculated by the following formula: Cell viability (%) = (average OD in treated group/average OD in control group) × 100%.

*2.4.5 In vitro colony-forming assay*

Freshly isolated 4-T1 cells were seeded at a clonal density of 500 cells/well onto tissue culture-treated polystyrene 6 well flat bottom plates and cultured in growth medium Gibco RPMI 1640 L-Glutamine (Life Technologies- Grand Island, NY, USA), supplemented with 10% certified heat-inactivated fetal bovine serum (FBS). Freshly isolated MCF-7 cells were seeded at a clonal density of 500 cells/well onto tissue culture-treated polystyrene 6 well flat bottom plates and cultured in growth medium Gibco RPMI 1640 L-Glutamine (Life Technologies- Grand Island, NY, USA), supplemented with 10% certified heat-inactivated fetal bovine serum (FBS). Freshly isolated B16-F10 cells were seeded at a clonal density of 500 cells/well onto tissue culture-treated polystyrene 6 well flat bottom plates and cultured in growth medium Gibco RPMI 1640 L-Glutamine (Life Technologies- Grand Island, NY, USA), supplemented with 10% certified heat-inactivated fetal bovine serum (FBS). Careful attention was made to not disturb cells 72 hr after culture to allow adherence. A 50% media change was performed on day 3. After 72 h, media was changed and experimental wells were treated with MTX-2DG-WGN drug combination. Control wells were left untreated. Colonies were monitored microscopically to ensure they were derived from single cells. Cells were incubated for 72 h at 5% $CO_2$ at 37°C. Cultures were terminated after 72 h, and washed free of media with cold PBS. Colonies were fixed with methanol, and stained with 0.5% crystal violet tissue culture stain for counting.

*2.4.6 Statistical analysis*

GraphPad Prism v8 software was used for statistical analyses. Data is presented as mean ± s.d. t-test was used to determine statistical significance between groups for normally

distributed data. Linear regression analysis performed by the GraphPad Prism software was used to calculate $r^2$. For all tests, *$p<0.05$ was considered significant. Experiments and measurements were performed in triplicate. Graphed data depicts means of triplicates ± s.e.m. and are representative of three experiments where indicated.

## 2.5 RESULTS

### 2.5.1 Determination of MTX, 2-DG, and WGN individual $EC_{50}$ in 4-T1, MCF-7, B16-F10, and THP-1 cancer cell lines.

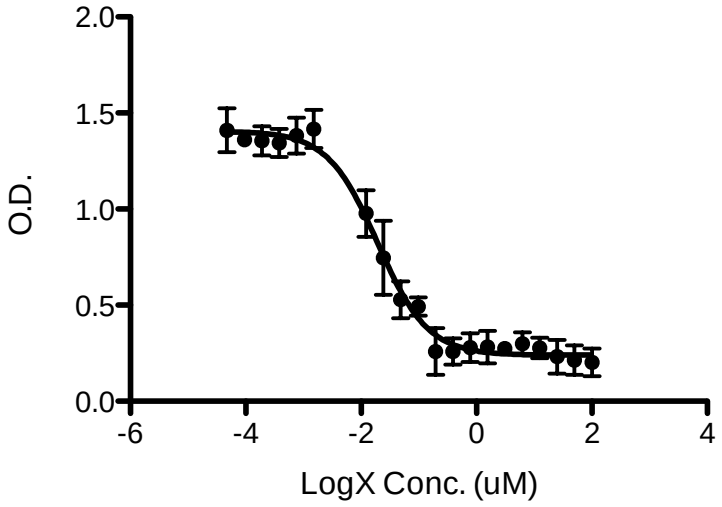


**Figure 14. The cytotoxic effects of MTX against 4-T1 cells.** 4-T1 cells were treated with 100 µM MTX followed by serial two-fold dilutions. Plotted points represent the averages of triplicate determinations ± s.e.m. in three separate experiments.

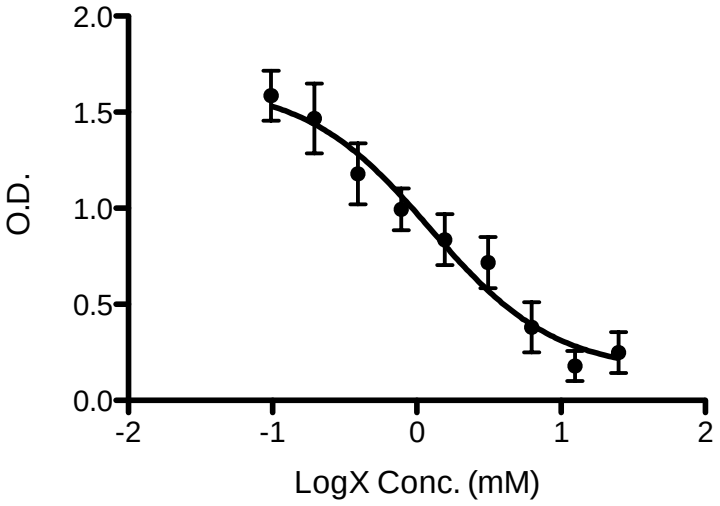


**Figure 15. The cytotoxic effects of 2DG against 4-T1 cells.** 4-T1 cells were treated with 50 mM 2-DG followed by serial two-fold dilutions. Plotted points represent the averages of triplicate determinations ± s.e.m. in three separate experiments.

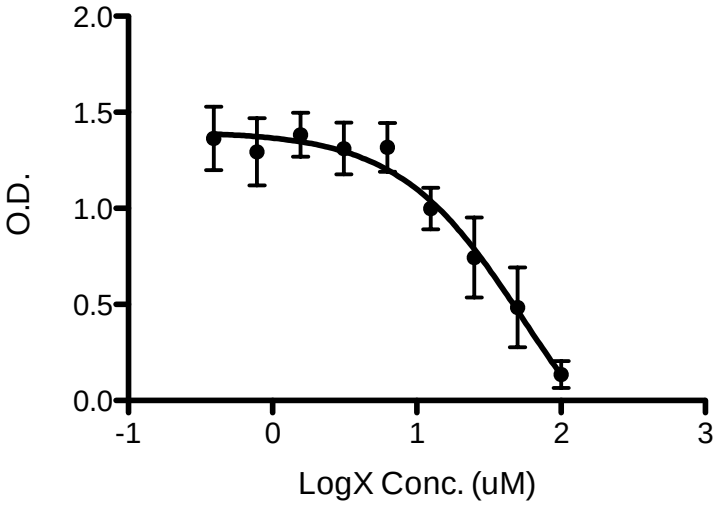


**Figure 16. The cytotoxic effects of WGN against 4-T1 cells.** 4-T1 cells were treated with 200 µM WGN followed by serial two-fold dilutions. Plotted points represent the averages of triplicate determinations ± s.e.m. in three separate experiments.

MTX was cytotoxic at concentrations ranging from 0.0048 to 100 µM in the 4-T1 cell line, with an $EC_{50}$ of 0.049 µM derived from dose-response curve. (Fig. 14, $r^2$= 0.92). 2-DG displayed cytotoxicity at concentrations ranging from 1.5 to 25 mM, with an $EC_{50}$

of 6.25 mM derived from dose-response curve (Fig. 15, $r^2$= 0.90). Finally, WGN was studied for its anti-tumor effects. WGN exhibited cytotoxicity at concentrations ranging from 12.5 to 200 µM with an $EC_{50}$ of 85 µM against the 4-T1 cells, derived from dose-response curve (Fig. 16, $r^2$= 0.87).

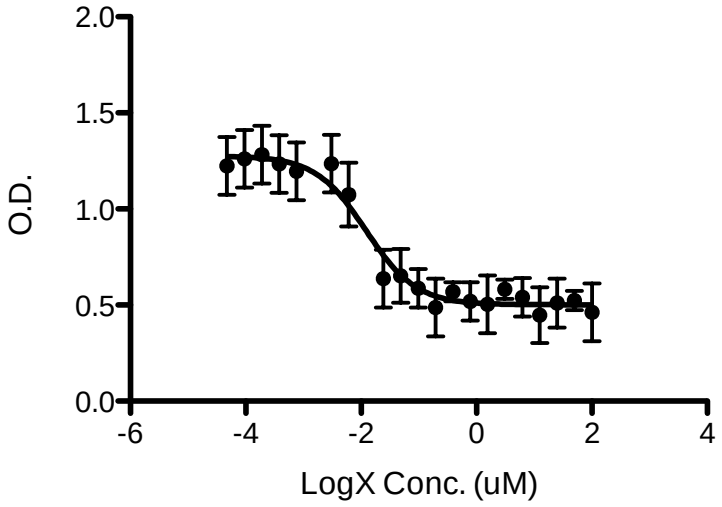


**Figure 17. The cytotoxic effects of MTX against MCF-7 cells.** MCF-7 cells were treated with 100 µM MTX followed by serial two-fold dilutions. Plotted points represent the averages of triplicate determinations ± s.e.m. in three separate experiments.

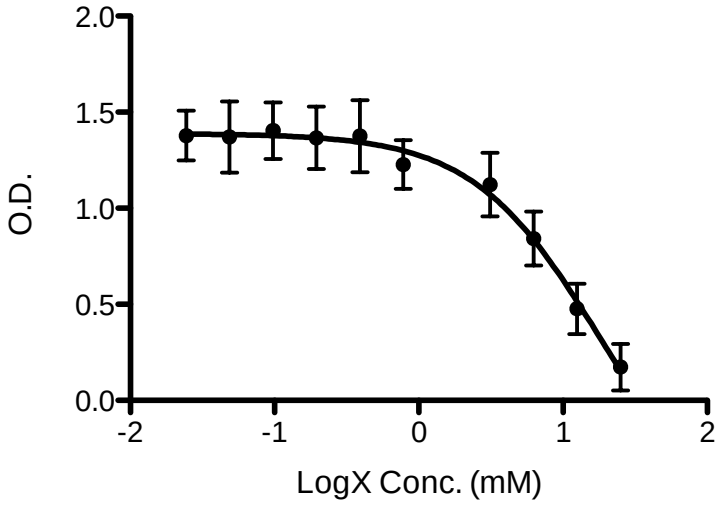


**Figure 18. The cytotoxic effects of 2-DG against MCF-7 cells.** MCF-7 cells were treated with 50 mM 2DG followed by serial two-fold dilutions. Plotted points represent the averages of triplicate determinations ± s.e.m. in three separate experiments.

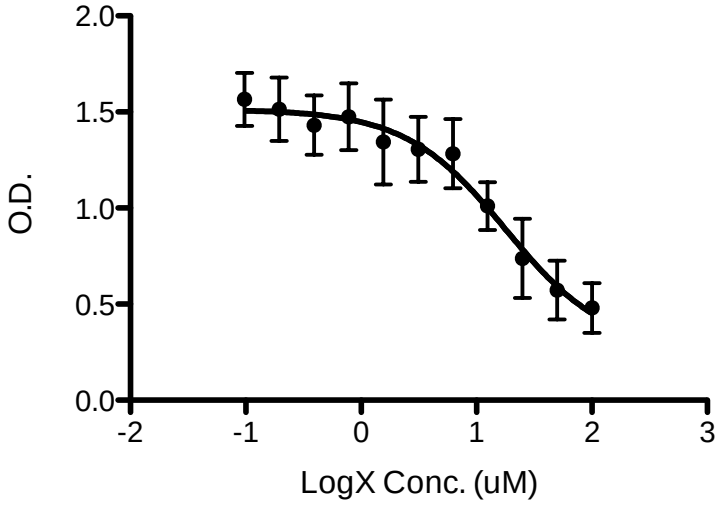


**Figure 19. The cytotoxic effects of WGN against MCF-7 cells.** MCF-7 cells were treated with 200 µM WGN followed by serial two-fold dilutions. Plotted points represent the averages of triplicate determinations ± s.e.m. in three separate experiments.

MTX was cytotoxic at concentrations ranging from 0.0006 to 100 µM in the MCF-7 cell line, with an $EC_{50}$ of 0.049 µM derived from dose-response curve. (Fig. 17, $r^2$= 0.83). 2-DG displayed cytotoxicity at concentrations ranging from 1.5 to 25 mM, with

an $EC_{50}$ of 19.65 mM derived from dose-response curve (Fig. 18, $r^2$= 0.87). WGN exhibited cytotoxicity at concentrations ranging from 12.5 to 200 µM with an $EC_{50}$ of 20.22 µM against the MCF-7 cells, derived from dose-response curve (Fig. 19, $r^2$= 0.82).

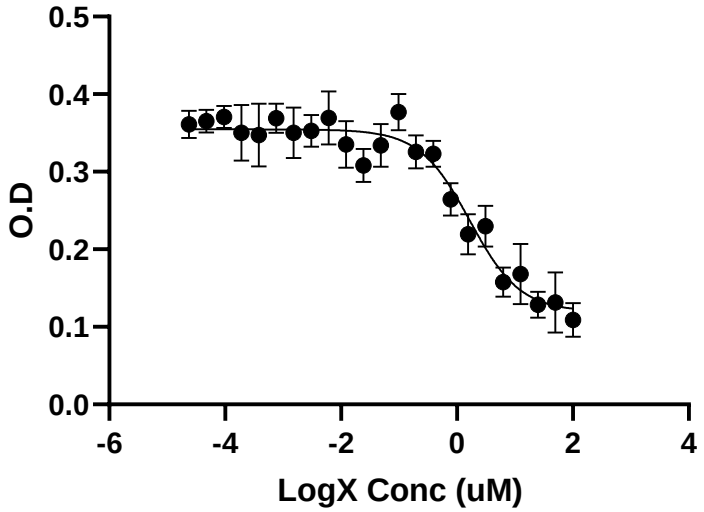


**Figure 20. The cytotoxic effects of MTX against THP-1 cells.** THP-1 cells were treated with 100 µM MTX followed by serial two-fold dilutions. Plotted points represent the averages of triplicate determinations ± s.e.m. in three separate experiments.

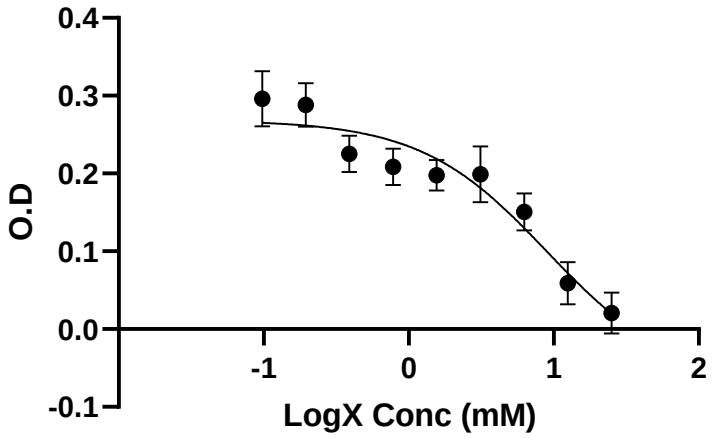


**Figure 21. The cytotoxic effects of 2DG against THP-1 cells.** THP-1 cells were treated with 50 mM 2DG followed by serial two-fold dilutions. Plotted points represent the averages of triplicate determinations ± s.e.m. in three separate experiments.

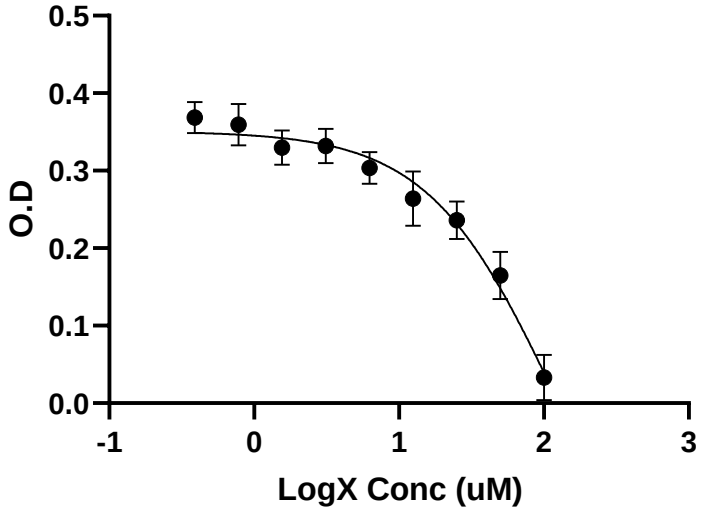


**Figure 22. The cytotoxic effects of WGN against THP-1 cells.** THP-1 cells were treated with 200 µM WGN followed by serial two-fold dilutions. Plotted points represent the averages of triplicate determinations ± s.e.m. in three separate experiments.

MTX was cytotoxic at concentrations ranging from 0.0144 to 100 µM in the THP-1 cell line, with an $EC_{50}$ of 1.82 µM derived from dose-response curve. (Fig. 20, $r^2$= 0.90). 2-DG showed cytotoxicity at concentrations ranging from 0.78 to 25 mM, with an $EC_{50}$ of 11.62 mM derived from dose-response curve (Fig. 21, $r^2$= 0.87). WGN exhibited cytotoxicity at concentrations ranging from 12.5 to 200 µM with an $EC_{50}$ of 83 µM against the THP-1 cells, derived from dose-response curve (Fig. 22, $r^2$= 0.94).

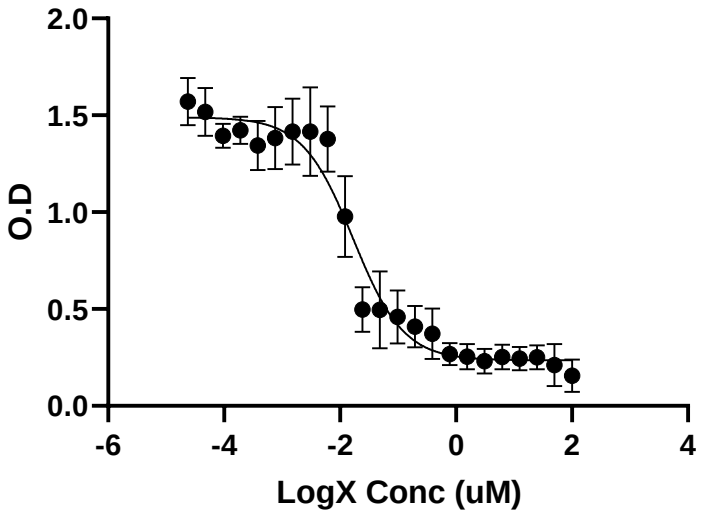


**Figure 23. The cytotoxic effects of MTX against B16-F10 cells.** B16-F10 cells were treated with 100 µM MTX followed by serial two-fold dilutions. Plotted points represent the averages of triplicate determinations ± s.e.m. in three separate experiments.

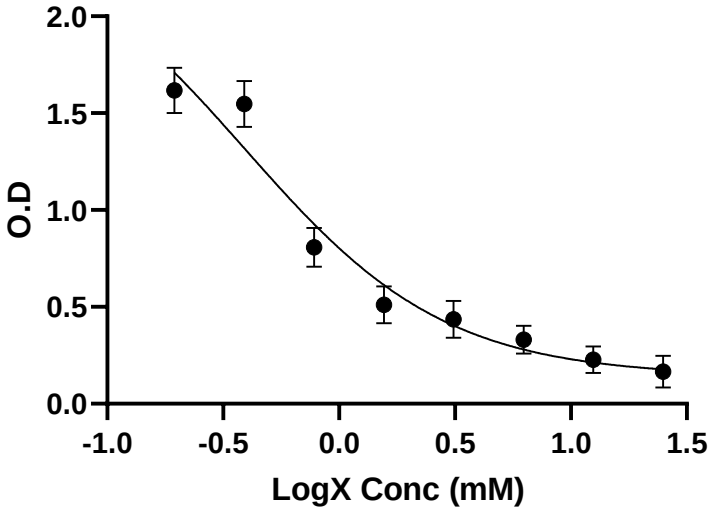


**Figure 24. The cytotoxic effects of 2DG against B16-F10 cells.** B16-F10 cells were treated with 50 mM 2DG followed by serial two-fold dilutions. Plotted points represent the averages of triplicate determinations ± s.e.m. in three separate experiments.

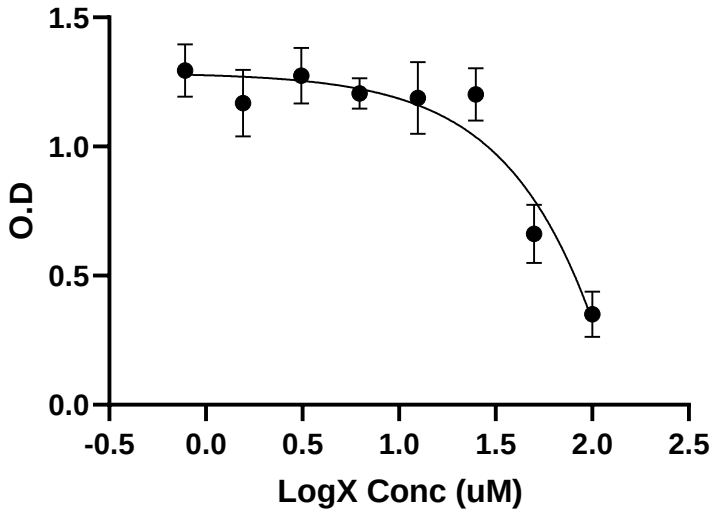


**Figure 25. The cytotoxic effects of WGN against B16-F10 cells.** B16-F10 cells were treated with 200 µM WGN followed by serial two-fold dilutions. Plotted points represent the averages of triplicate determinations ± s.e.m. in three separate experiments.

MTX was cytotoxic at concentrations ranging from 0.0003 to 100 µM in the B16-F10 cell line, with an $EC_{50}$ of 0.019 µM derived from dose-response curve. (Fig. 23, $r^2$= 0.93). 2-DG displayed cytotoxicity at concentrations ranging from 0.19 to 25 mM, with an $EC_{50}$ of 0.35 mM against the B16-F10 cells, derived from dose-response curve (Fig. 24, $r^2$= 0.94). WGN exhibited cytotoxicity at concentrations ranging from 25 to 200 µM with an $EC_{50}$ of 76 µM against the B16-F10 cells, derived from dose-response curve (Fig. 25, $r^2$= 0.86).

### 2.5.2 Evaluation of pairwise interactions show efficacious relationship between three-drug combination.

The combination of three-drugs yields four theoretic interactions: the interaction between Compound A + Compound B + Compound C, Compound A + Compound B, Compound A + Compound C, and Compound B + Compound C. To better visualize these interactions and guide our decision on the concentration of each to be used in our

combination, a drug interaction panel was performed. For each screen, the concentrations of two compounds were held constant at their $EC_{50}$ concentrations. The third compound was serially diluted twice from its initial $EC_{50}$ concentration, and not added at all in one experimental group to allow analysis of pairwise interaction between the other two compounds at their respective $EC_{50}$. Cell viability was measured using MTS cell viability assay. Cell viability is expressed as a percentage of the control (100%).

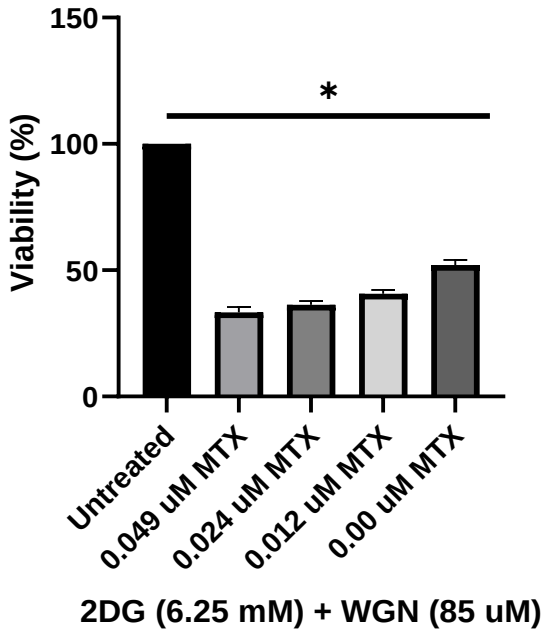


**Figure 26. The effect of varying MTX concentrations in combination with constant 2DG+ WGN concentrations against 4-T1 cells.** Cells were treated with a combination of 2DG and WGN at their $EC_{50}$ of 6.25 mM and 85 µM, respectively. MTX was added at its $EC_{50}$ of 0.049 µM to the first experimental group, followed by two serial two-fold dilutions. The last experimental group contained 2DG+WGN and no MTX. Bars represent the average of triplicate experiments ± s.e.m. Difference between each varying MTX concentration and untreated control was statistically significant (*= $p < 0.05$).

The first panel observed the pairwise interaction between 2DG and WGN, with varying concentrations of MTX (Figure 26). At 0.00 µM MTX and 2DG and WGN combined at their respective $EC_{50}$, 4-T1 cells were 51% viable relative to untreated cells. At 0.012 µM MTX and 2DG and WGN combined at their respective $EC_{50}$, 4-T1 cells

were 42% viable relative to untreated controls. At 0.024 µM MTX and 2DG and WGN combined at their respective $EC_{50}$, 4-T1 cells were 39% viable relative to untreated controls. At 0.049 µM MTX and 2DG and WGN combined at their respective $EC_{50}$, 4-T1 cells were 34% viable relative to untreated controls.

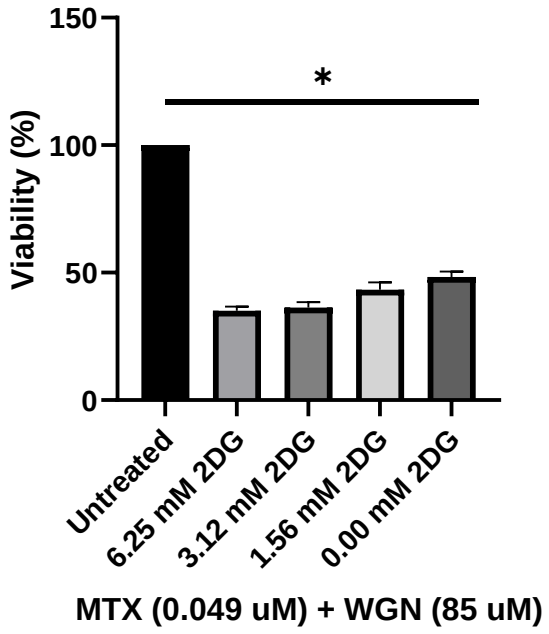


**Figure 27. The effect of varying 2DG concentrations in combination with constant MTX+ WGN concentrations against 4-T1 cells.** Cells were treated with a combination of MTX and WGN at their $EC_{50}$ of 0.049 µM and 85 µM, respectively. 2DG was added at its $EC_{50}$ of 6.25 mM to the first experimental group, followed by two serial two-fold dilutions. The last experimental group contained MTX+WGN and no 2DG. Bars represent the average of triplicate experiments ± s.e.m. Difference between each varying 2DG concentration and untreated control was statistically significant (*= $p < 0.05$).

The second panel examined the pairwise interaction between MTX and WGN, with varying concentrations of 2DG (Figure 27). At 0.00 mM 2DG and MTX and WGN combined at their respective $EC_{50}$, 4-T1 cells were 49% viable relative to untreated controls. At 1.56 mM 2DG and MTX and WGN combined at their respective $EC_{50}$, 4-T1 cells were 45% viable relative to untreated controls. At 3.12 mM 2DG and MTX and WGN combined at their respective $EC_{50}$, 4-T1 cells were 38% viable relative to untreated

controls. At 6.25 mM 2DG and MTX and WGN combined at their respective $EC_{50}$, 4-T1 cells were 34% viable relative to untreated controls.

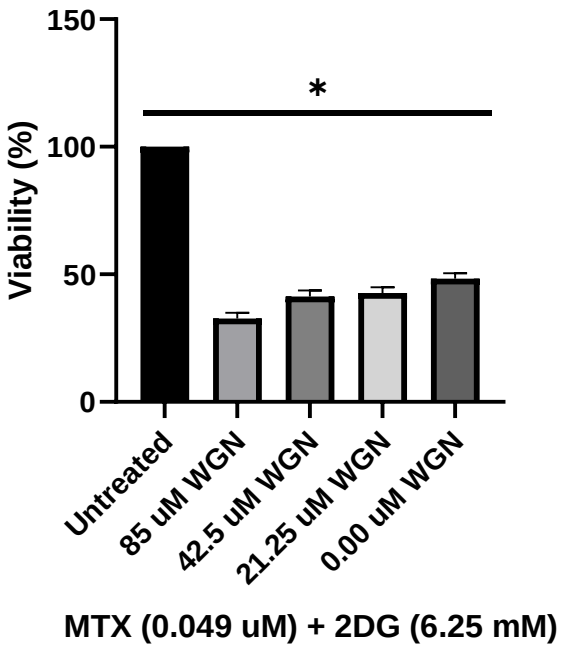


**Figure 28. The effect of varying WGN concentrations in combination with constant MTX +2DG concentrations against 4-T1 cells.** Cells were treated with a combination of MTX and 2DG at their $EC_{50}$ of 0.049 µM and 6.25 mM, respectively. WGN was added at its $EC_{50}$ of 85 µM to the first experimental group, followed by two serial two-fold dilutions. The last experimental group contained MTX+2DG and no WGN. Bars represent the average of triplicate experiments ± s.e.m. Difference between each varying WGN concentration and untreated control was statistically significant (*= $p < 0.05$).

The third panel studied the pairwise interaction between MTX and 2DG, with varying concentrations of WGN (Figure 28). At 0.00 µM WGN and MTX and 2DG combined at their respective $EC_{50}$, 4-T1 cells were 50% viable relative to untreated controls. At 21.25 µM WGN and MTX and 2DG combined at their respective $EC_{50}$, 4-T1 cells were 44% viable relative to untreated controls. At 42.5 µM WGN and MTX and 2DG combined at their respective $EC_{50}$, 4-T1 cells were 40% viable relative to untreated controls. At 85 µM WGN and MTX and 2DG combined at their respective $EC_{50}$, 4-T1 cells were 34% viable relative to untreated controls.

### 2.5.3 MTX, 2DG, and WGN combined 6 times below their $EC_{50}$ is effective against 4-T1 and MCF-7 cells whereas use singly has no effect.

Analysis of the pairwise and three-drug interactions between our compounds of study suggested the most efficacious combination to be the three compounds at their $EC_{50}$. However, in an effort to delve deeper into the effects of the combination vs the efficacy of each drug singly, a series of two-fold serial dilutions were performed on our initial combination concentrations. Cell viability was measured using MTS cell viability assay. Cell viability is expressed as a percentage of the control (100%).

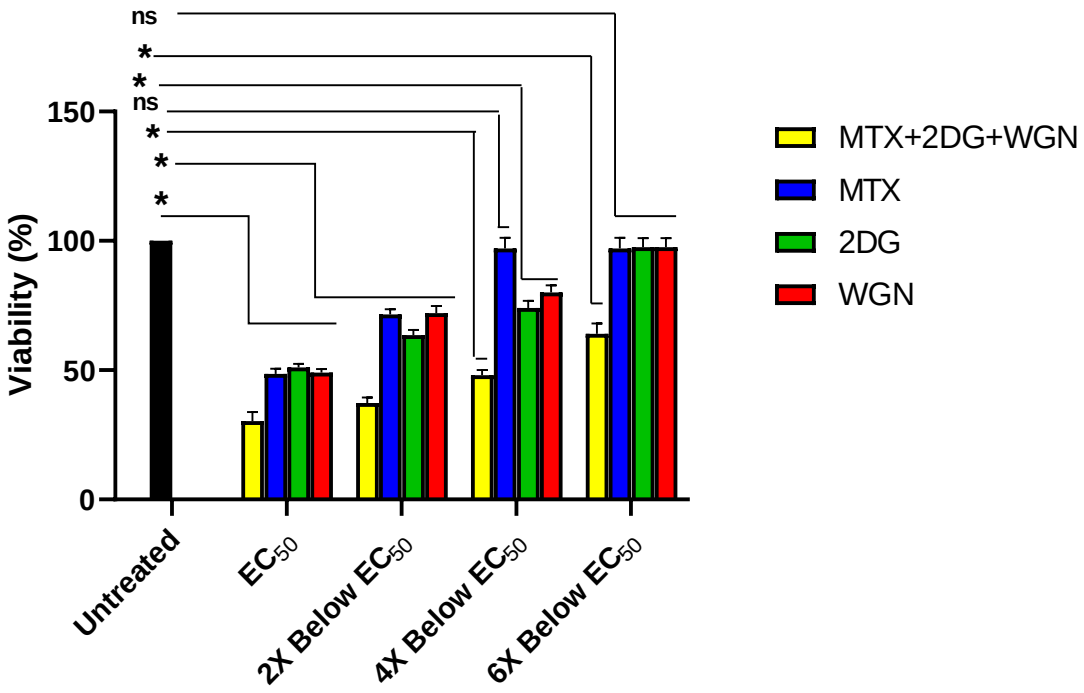


**Figure 29. A combination of three non-mutagenic drugs at combinations 6 times below their $EC_{50}$ are more effective at killing 4-T1 mouse mammary carcinoma cells compared to individual use.** MTX, 2DG and WGN were added at their respective $EC_{50}$, followed by three serial two-fold dilutions. Data representing compounds used singly is also graphed, highlighting the significance of the combination. Bars represent the average of triplicate experiments ± s.e.m. (ns= not significant, *=$p<0.05$).

In the present study, MTX, 2DG, and WGN were combined at 0.049 μM, 6.25 mM, and 85 μM respectively (Figure 29). Treated with the combination, the 4-T1 cells were reduced to 34% viability. Compared to the combination, individual treatment with MTX, 2DG, and WGN reduced 4-T1 cell viability to 50%, significantly higher ($p<0.05$). In the second experimental group, MTX, 2DG, and WGN were combined at 0.024 μM, 3.125 mM, 42.5 μM respectively; 2 times below their individual $EC_{50}$. Treatment with this combination reduced 4-T1 cell viability to 38%. Compared to the combination, individual treatment with MTX at 0.024 μM reduced 4-T1 viability to 70%, significantly higher ($p<0.05$). Compared to the combination, individual treatment with 2DG at 3.125 mM reduced 4-T1 viability to 62%, significantly higher ($p<0.05$). Compared to the combination, individual treatment with WGN at 42.5 μM reduced 4-T1 viability to 70%, significantly higher ($p<0.05$). In the third experimental group, MTX, 2DG, and WGN were combined at 0.012 μM, 1.56 mM, and 21.25 μM respectively; 4 times below their individual $EC_{50}$. Treatment with this combination reduced 4-T1 cell viability to 48%. Compared to the combination, individual treatment with MTX at 0.012 μM had no effect on 4-T1 cell viability ($p<0.05$). Compared to the combination, individual treatment with 2DG at 1.56 mM reduced 4-T1 viability to 72%, significantly higher ($p<0.05$). Compared to the combination, individual treatment with WGN at 21.25 μM reduced 4-T1 viability to 78%, significantly higher ($p<0.05$). In the fourth experimental group, MTX, 2DG, and WGN were combined at 0.006 μM, 0.78 mM, and 10.62 μM respectively; 6 times below their individual $EC_{50}$. Treatment with this combination reduced 4-T1 cell viability to 58%. Compared to the combination, MTX, 2DG, and WGN individually at

concentrations of 0.006 µM, 0.78 mM, and 10.62 µM, respectively had no effect on 4-T1 cell viability (ns, p>0.05).

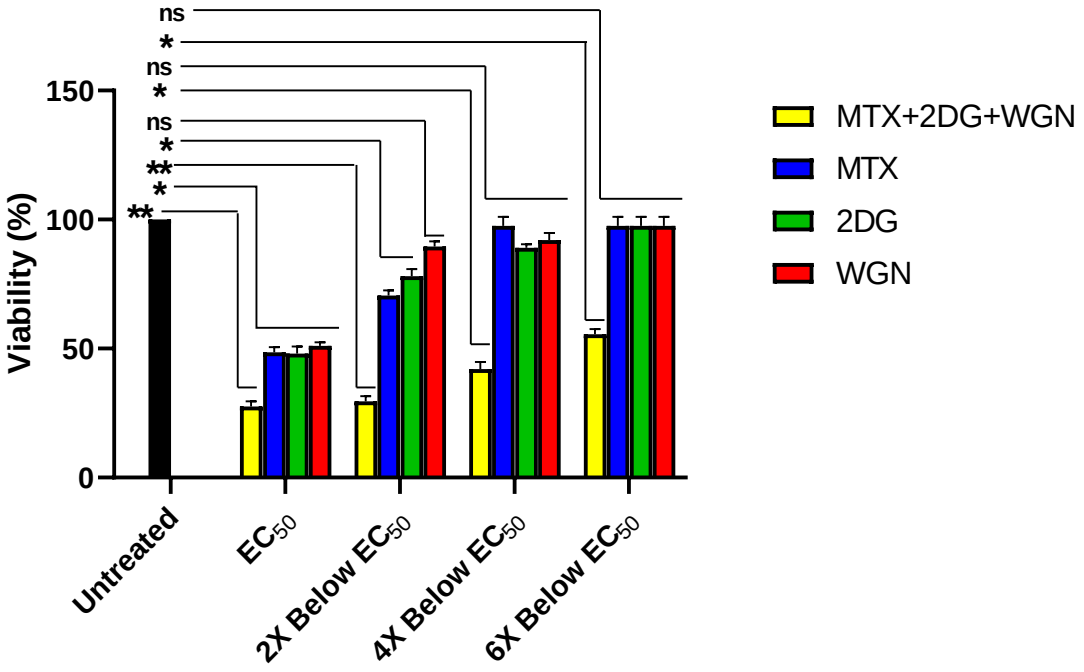


**Figure 30. A combination of three non-mutagenic drugs at combinations 6 times below their $EC_{50}$ are more effective at killing MCF-7 human mammary adenocarcinoma cells than when they are used singly.** MTX, 2DG and WGN were added at their respective $EC_{50}$, followed by three serial two-fold dilutions. Data representing compounds used singly is also graphed, highlighting the significance of the combination. Bars represent the average of triplicate experiments ± s.e.m. (ns= not significant, *=p<0.05, **=p<0.01).

In the present study, MTX, 2DG, and WGN were combined at 0.049 µM, 19.65 mM, and 20.22 µM respectively (Figure 30). Treated with the combination, the MCF-7 cells were reduced to 29% viability (p<0.05). Compared to the combination, individual treatment with MTX, 2DG, and WGN reduced MCF-7 cell viability to 50%, significantly higher (p<0.05). In the second experimental group, MTX, 2DG, and WGN were combined at 0.024 µM, 9.8 mM, 10.1 µM respectively; 2 times below their individual $EC_{50}$. Treatment with this combination reduced MCF-7 cell viability to 32% (p<0.01). Compared to the combination, individual treatment with MTX at 0.024 µM reduced

MCF-7 viability to 72% ($p<0.05$). Compared to the combination, individual treatment with 2DG at 9.8 mM reduced MCF-7 viability to 80% ($p<0.05$). Compared to the combination, individual treatment with WGN at 10.1 µM reduced MCF-7 viability to 88% ($p>0.05$). In the third experimental group, MTX, 2DG, and WGN were combined at 0.012 µM, 4.9 mM, and 5.05 µM respectively; 4 times below their individual $EC_{50}$. Treatment with this combination reduced MCF-7 cell viability to 44% ($p<0.05$). Compared to the combination, individual treatment with MTX at 0.012 µM had no effect on MCF-7 cell viability ($p>0.05$). Compared to the combination, individual treatment with 2DG at 4.9 mM reduced MCF-7 viability to 88% ($p>0.05$). Compared to the combination, individual treatment with WGN at 5.05 µM reduced MCF-7 viability to 90% ($p>0.05$). In the fourth experimental group, MTX, 2DG, and WGN were combined at 0.006 µM, 2.45 mM, and 2.5 µM respectively; 6 times below their individual $EC_{50}$. Treatment with this combination reduced MCF-7 cell viability to 57% ($p<0.05$). Compared to the combination, MTX, 2DG, and WGN individually at concentrations of 0.006 µM, 2.45 mM, and 2.5 µM, respectively had no effect on MCF-7 cell viability (ns, $p>0.05$).

### 2.5.4 MTX, 2DG, and WGN combined 4 times below their $EC_{50}$ is more effective against 4-T1 and MCF-7 mammary tumor cells under hypoxia compared to normoxia.

To model conditions present at the site of the tumor, the above study was mimicked under hypoxia. This experimental design allowed us to directly compare the efficacy of our novel combinatorial therapy in normoxia vs hypoxia. Cell viability was

measured using MTS cell viability assay. Cell viability is expressed as a percentage of the control (100%).

In the present study, MTX, 2DG, and WGN were combined at 0.049 µM, 6.25 mM, and 85 µM respectively and incubated for 48 h at 1% $O_2$ and 5% $CO_2$ (Figure 31). 48 h post-treatment, viability was recorded. Treated with the combination, 4-T1 cell viability was reduced to 19%, significantly lower compared to treatment under normoxia ($p<0.01$). Individual treatment with MTX at 0.049 µM reduced 4-T1 viability to 43%, significantly lower compared to treatment under normoxia ($p<0.01$). Individual treatment with 2DG at 6.25 mM reduced 4-T1 viability to 38%, significantly lower compared to treatment under normoxia ($p<0.01$). Individual treatment with WGN at 85 µM reduced 4-T1 viability to 49%, similar to treatment under normoxia ($p>0.05$). In the second experimental group, MTX, 2DG, and WGN were combined at 0.024 µM, 3.125 mM, 42.5 µM respectively; 2 times below their individual $EC_{50}$. Treatment with this combination reduced 4-T1 cell viability to 22%, significantly lower compared to treatment under normoxia ($p<0.05$). Individual treatment with MTX at 0.024 µM reduced 4-T1 viability to 52%, significantly lower compared to treatment under normoxia ($p<0.05$). Individual treatment with 2DG at 3.125 mM reduced 4-T1 viability to 44%, significantly lower compared to treatment under normoxia ($p<0.05$). Individual treatment with WGN at 42.5 µM reduced 4-T1 viability to 64%, little difference compared to treatment under normoxia ($p>0.05$). In the third experimental group, MTX, 2DG, and WGN were combined at 0.012 µM, 1.56 mM, and 21.25 µM respectively; 4 times below their individual $EC_{50}$. Treatment with this combination reduced 4-T1 cell viability to 32%, significantly lower compared to treatment under normoxia ($p<0.05$). Individual

treatment with MTX at 0.012 µM reduced 4-T1 viability to 68%, significantly lower compared to treatment under normoxia ($p<0.05$). Individual treatment with 2DG at 1.56 mM reduced 4-T1 viability to 63%, significantly lower compared to treatment under normoxia ($p<0.01$). Individual treatment with WGN at 21.25 µM reduced 4-T1 viability to 72%, little difference compared to treatment under normoxia ($p>0.05$).

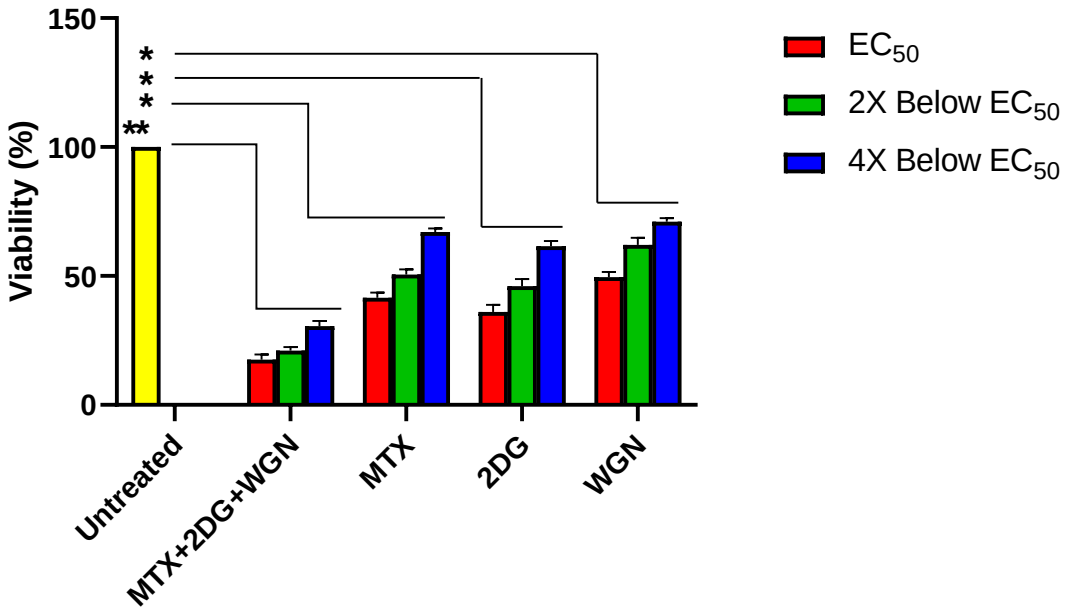


**Figure 31. A combination of three non-mutagenic drugs at combinations 4 times below their $EC_{50}$ are more effective at killing 4-T1 mouse mammary carcinoma cells compared to individual use under hypoxia.** MTX, 2DG and WGN were added at their respective $EC_{50}$, followed by two serial two-fold dilutions. Data representing compounds used singly is also graphed, highlighting the significance of the combination. Bars represent the average of triplicate experiments ± s.e.m. (*=$p<0.05$, **=$p<0.01$).

The experiment was performed similarly in MCF-7 cells. MTX, 2DG, and WGN were combined at 0.049 µM, 19.65 mM, and 20.22 µM respectively and incubated for 48 h at 1% $O_2$ and 5% $CO_2$ (Figure 32). 48 h post-treatment, viability was recorded. Treated with the combination, MCF-7 cell viability was reduced to 14%, significantly lower compared to treatment under normoxia ($p<0.01$). Individual treatment with MTX at 0.049 µM reduced MCF-7 viability to 45%, lower compared to treatment under normoxia

($p<0.05$). Individual treatment with 2DG at 19.65 mM reduced MCF-7 viability to 33%, significantly lower compared to treatment under normoxia ($p<0.01$). Individual treatment with WGN at 20.22 µM reduced MCF-7 viability to 47%, close to treatment under normoxia ($p>0.05$). In the second experimental group, MTX, 2DG, and WGN were combined at 0.024 µM, 9.8 mM, 10.1 µM respectively; 2 times below their individual $EC_{50}$. Treatment with this combination reduced MCF-7 cell viability to 24%, significantly lower compared to treatment under normoxia ($p<0.05$). Individual treatment with MTX at 0.024 µM reduced MCF-7 viability to 58%, significantly lower compared to treatment under normoxia ($p<0.05$). Individual treatment with 2DG at 9.8 mM reduced MCF-7 viability to 63%, significantly lower compared to treatment under normoxia ($p<0.05$). Individual treatment with WGN at 10.1 µM reduced MCF-7 viability to 80%, little difference compared to treatment under normoxia ($p>0.05$). In the third experimental group, MTX, 2DG, and WGN were combined at 0.012 µM, 4.9 mM, and 5.05 µM respectively; 4 times below their individual $EC_{50}$. Treatment with this combination reduced MCF-7 cell viability to 34%, significantly lower compared to treatment under normoxia ($p<0.05$). Individual treatment with MTX at 0.012 µM reduced MCF-7 viability to 74%, significantly lower compared to treatment under normoxia ($p<0.05$). Individual treatment with 2DG at 4.9 mM reduced MCF-7 viability to 77%, significantly lower compared to treatment under normoxia ($p<0.05$). Individual treatment with WGN at 5.05 µM had no observed effect on MCF-7 cell viability ($p>0.05$).

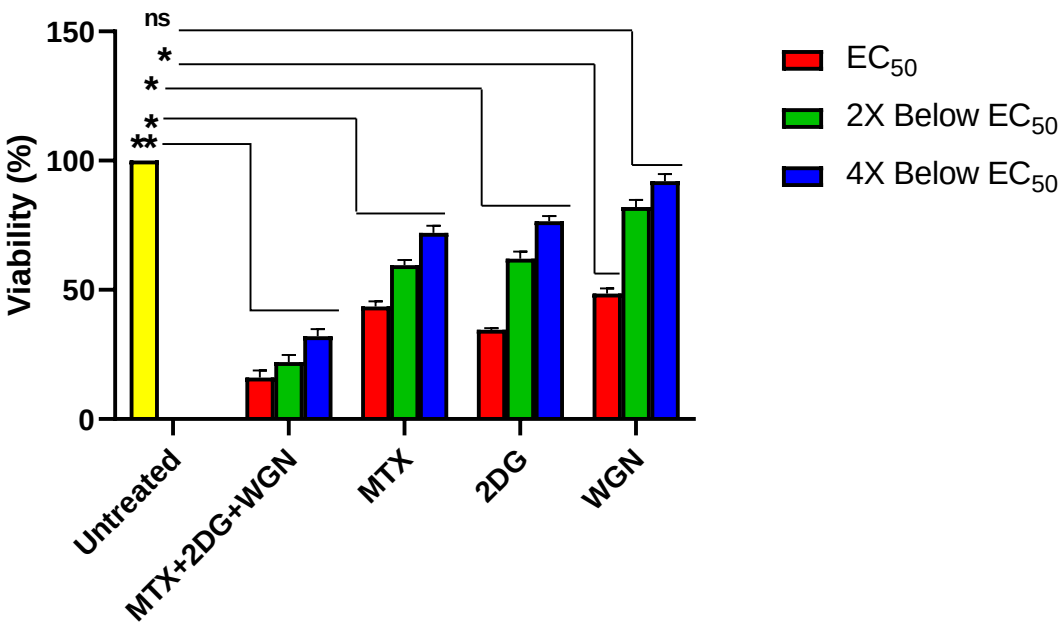


**Figure 32. A combination of three non-mutagenic drugs at combinations 4 times below their $EC_{50}$ are more effective at killing MCF-7 human mammary adenocarcinoma cells compared to individual use under hypoxia.** MTX, 2DG and WGN were added at their respective $EC_{50}$, followed by two serial two-fold dilutions. Data representing compounds used singly is also graphed, highlighting the significance of the combination. Bars represent the average of triplicate experiments ± s.e.m. (ns= not significant, *=p<0.05, **=p<0.01).

### 2.5.5 MTX, 2DG, and WGN combined 6 times below their $EC_{50}$ is effective against B16-F10 and THP-1 cancer cells.

The remarkable efficacy of our low-dose combination and the importance of the cancer survival pathways our combinatorial therapy targets led us to study the effects of our therapy against two malignant cancer cell lines: B16-F10 mouse metastatic melanoma and THP-1 human acute monocytic leukemia. Cell viability was measured using MTS cell viability assay. Cell viability is expressed as a percentage of the control (100%).

In this study, MTX, 2DG, and WGN were combined at 0.003 µM, 0.06 mM, and 12 µM, respectively; 6 times below their individual $EC_{50}$ against B16-F10 cells (Figure

33). Treatment by the combination induced a significant cytotoxic effect, reducing cell viability to 39% ($p<0.01$).

In a subsequent study, MTX, 2DG, and WGN were combined at 0.3 µM, 1.9 mM, and 13.8 µM, respectively; 6 times below their individual $EC_{50}$ against THP-1 cells (Figure 34). Treatment by the combination induced a significant cytotoxic effect, reducing cell viability to 57% ($p<0.01$).

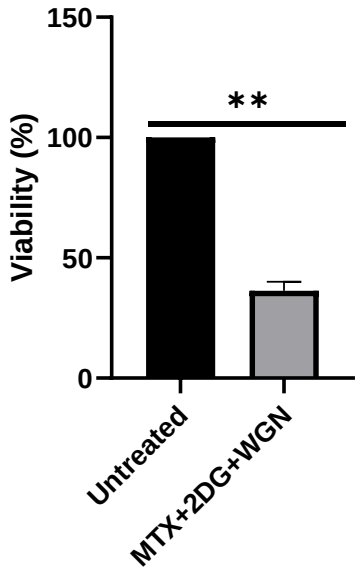


**Figure 33. A combination of three non-mutagenic drugs at combinations 6 times below their $EC_{50}$ are effective at killing B16-F10 mouse metastatic melanoma cells.** Cells were treated with 0.003 µM, 0.06 mM, and 12 µM MTX, 2DG, and WGN respectively for 48 h and analyzed via MTS cell viability assay. Bars represent the average of triplicate experiments ± s.e.m. (**=$p<0.01$).

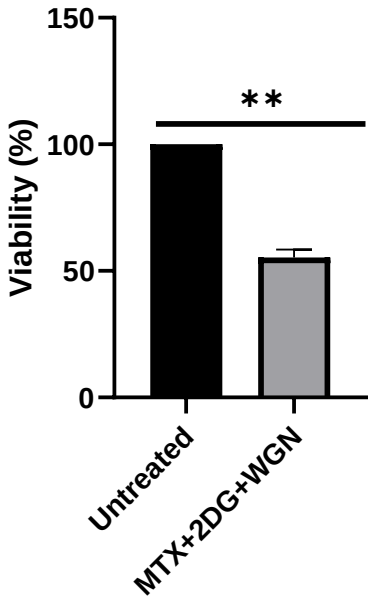


**Figure 34. A combination of three non-mutagenic drugs at combinations 6 times below their $EC_{50}$ are effective at killing THP-1 human acute monocytic leukemia cells.** Cells were treated with 0.3 µM, 1.9 mM, and 13.8 µM MTX, 2DG, and WGN respectively for 48 h and analyzed via MTS cell viability assay. Bars represent the average of triplicate experiments ± s.e.m. (*=$p<0.05$).

### 2.5.6 MTX, 2DG, and WGN combined 6 times below their $EC_{50}$ is effective at inhibiting colony formation in the 4-T1 and MCF-7 cell lines.

In the present study, *in vitro* assays were performed to evaluate the effectiveness of our novel combinatorial therapy at inhibiting colony formation. Prior to treatment, cells were observed under the microscope 72 h after culture to ensure adherence. All wells were comparable. Media was then changed, and cells were treated. Treatment with the combinatorial therapy was administered to the experimental group wells, and the plate was incubated for 72 h (Figure 35). In the 4-T1 cell line, 492 colonies were counted in the untreated control wells. In the experimental group, no colonies were formed, nor cells remained. These observations were confirmed microscopically and by absence of staining. In the MCF-7 cell line, untreated control cell colonies were determined to be too

many to count (TMTC). < ~70% confluence of the tumor tissue monolayer was achieved in the untreated cell wells. In the experimental group, no colonies were formed, nor cells remained. These observations were confirmed microscopically and by absence of staining.

(A)

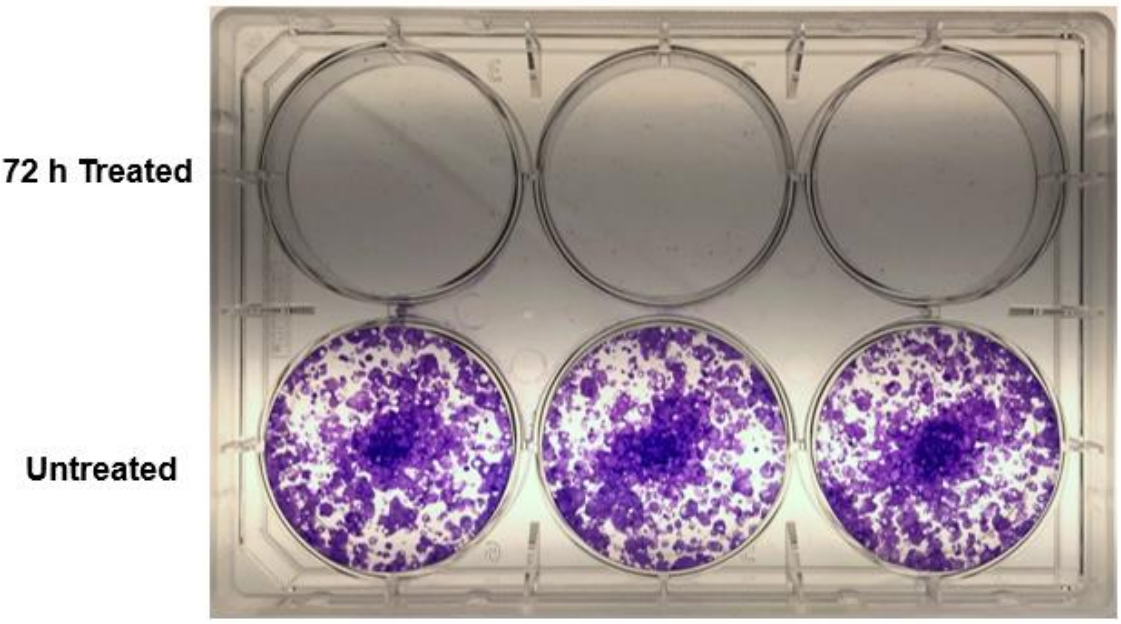

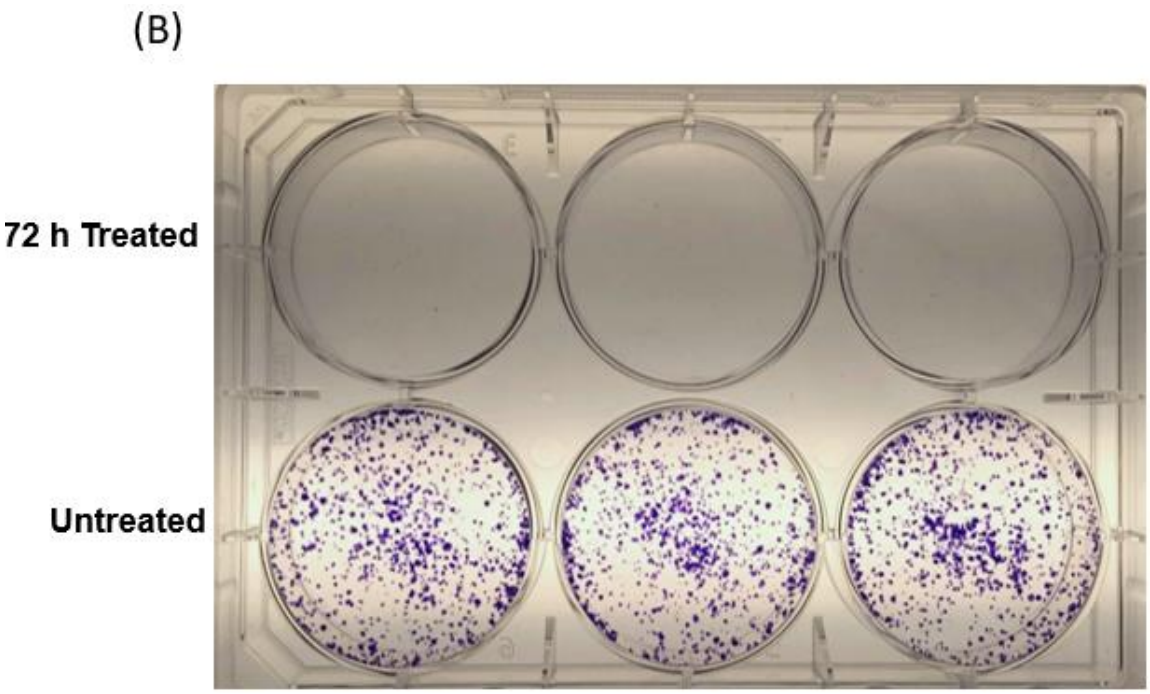


**Figure 35. A combination of three non-mutagenic drugs at combinations 6 times below their $EC_{50}$ are effective at inhibiting colony formation in human adenocarcinoma and mouse mammary carcinoma cells.** MCF-7 cells (A) and 4-T1 cells (B). All experiments involved three different populations of cells and were repeated three times. Photographs are representative of a typical experiment out of three independent ones.

## 2.6 DISCUSSION

Clinical evidence showcases the powerful resistance mechanisms cancer cells exhibit towards therapeutic agents used singly and highlights the importance of developing combinatorial therapies. Treatments used individually generally target a specific, critical cancer survival pathway, such as cell division or metabolism. The significance of these pathways drives cancer cells to adapt to said anticancer compounds, and the plethora of genetic mutations in the cancer cell genome creates a heterogenous population able to withstand and evolve resistant to these agents. Two compounds of study include methotrexate and 2-deoxyglucose, powerful anticancer agents that target critical anabolic and catabolic cancer survival pathways, respectively.

MTX competitively inhibits DHFR which decreases THF levels, resulting in attenuated DNA/protein/lipid methylation, inhibition of TS, and subsequent interference with DNA synthesis. Cancer cells are unable to proliferate without sufficient replicated DNA, thus targeting of this critical anabolic pathway forces the cancer cell to adapt or succumb to cell death. Primarily, this drug targeting fosters clonal selection of cancer cells. The heterogeneity of cancer cells supplemented by their founding genomic instability significantly increases the potential of a resistant subpopulation. This subpopulation of cells innately resistant to methotrexate treatment are referred to as "survivors," which continue to proliferate uncontrollably, forming a population of MTX-resistant cells. In a more immediate fashion, cancer cells detect the impacted levels of DHFR as a result of MTX-treatment and respond by upregulating the production of this enzyme. Enzyme kinetics teaches that increased substrate or enzyme concentration has the potential to counteract competitive inhibition and increase rate of enzyme action, decreasing $K_m$. To overcome this counterattack, a higher dose of MTX is required, with potentially toxic implications to surrounding normal tissue. A more active form of resistance machinery exhibited by cancer cells are MDR-mediated pathways. The ability of cancer cells to hijack ABC transporters and utilize these pathways and pumps decreases intracellular levels of MTX, rendering it ineffective.

Similarly, 2-deoxyglucose targets a critical catabolic cancer survival pathway. Rapid uncontrolled proliferation creates a direct dependence on ATP, which cancer cells readily adjust for by reverting to aerobic glycolysis. This transition in metabolic machinery is fostered by the hypoxic environment at the site of the tumor and marked by key glycolytic enzyme upregulation. HIF-1α modulates the production of glycolytic

enzymes and is found to be overexpressed in cancer cells[116]. The resulting increase in hexokinase and GLUT-1 levels facilitates increased glucose uptake and rapid ATP production via glycolysis. Cancer cells are unable to survive without ATP to fuel their cellular processes, thus targeting of this critical catabolic pathway forces the cancer cell to adapt or succumb to cell death. Much like MTX, uptake of 2DG elicits upregulation of HIF-1α to counteract hexokinase targeting. To overcome this counterattack, a higher dose of 2DG is required, with potentially toxic implications to surrounding lymphocytes and highly proliferative normal cells that also depend on glycolysis for clonal expansion. The significance of these findings indicates that targeting of critical cancer survival pathways warrants powerful resistance counterattacks by the cancer cell. Furthermore, the use of anticancer agents singly is readily adapted against, and generally ineffective at targeting an entire heterogenic population of cancer cells.

This study presented a novel combinatorial therapy that targets three critical cancer survival pathways: DNA synthesis, metabolism, and immune evasion. Our compounds of interest were: MTX, an antifolate; 2DG, a glycolytic inhibitor; and WGN, a flavonoid with various potent anticancer effects. To guide the development of a combinatorial therapy, emphasis was given to studying the individual efficacy of each of these compounds against multiple malignant cancer cell lines. In the 4-T1 mouse mammary carcinoma cell line, the $EC_{50}$ of MTX, 2DG, and WGN was determined to be 0.049 µM, 6.25 mM, and 85 µM respectively (Figure 14, 15, & 16). In the MCF-7 human mammary tumor cell line, the $EC_{50}$ of MTX, 2DG, and WGN was determined to be 0.049 µM, 19.66 mM, and 20.22 µM respectively (Figure 17, 18, & 19). In the THP-1 human acute monocytic leukemia cell line, the $EC_{50}$ of MTX, 2DG, and WGN was determined

to be 1.8 µM, 11.62 mM, and 83 µM respectively (Figure 20, 21, & 22). In the B16-F10 mouse metastatic melanoma cell line, the $EC_{50}$ of MTX, 2DG, and WGN was determined to be 0.019 µM, 0.35 mM, and 76 µM respectively (Figure 23, 24, & 25). The resulting individual data was used to construct a drug panel, providing valuable information on pairwise and three-drug combination interactions. The first panel examined the effect of varying MTX concentrations after treatment with 2DG and WGN at constant concentration. The difference between each varying MTX concentration was statistically significant and most efficacious at 0.049 µM ($p<0.05$) (Figure 26). The second panel examined the effect of varying 2DG concentrations after treatment with MTX and WGN at constant concentration. The difference between each varying 2DG concentration was statistically significant and most efficacious at 6.25 mM ($p<0.05$) (Figure 27). The third panel examined the effect of varying WGN concentrations after treatment with 2DG and MTX at constant concentration. The difference between each varying WGN concentration was statistically significant and most efficacious at 82.5 µM ($p<0.05$) (Figure 28).

The above drug panel data was extrapolated to arrive at a combination comprised of each compound at their respective $EC_{50}$. Furthermore, additive or synergistic effects of the combination were explored by diluting it 6 times below their respective $EC_{50}$, and compared the efficacy of this combination to the efficacy of the drugs used singly at these respective concentrations. In the 4-T1 cell line, at concentrations where MTX, 2DG, and WGN singly had no cytotoxic effect; treatment with the combination reduced viability to 60%. The cytotoxicity of the combination compared to the cytotoxicity of the individual compounds at these respective concentrations was statistically significant ($p<0.05$). In the

MCF-7 cell line, at concentrations where MTX, 2DG, and WGN singly had no cytotoxic effect; treatment with the combination reduced viability to 57%. The cytotoxicity of the combination relative to the cytotoxicity of the individual compounds at these respective concentrations was statistically significant ($p<0.05$). Evidence of cytotoxicity at such low concentrations in the combination compared to no effect individually highlights the effectiveness of our combinatorial therapy.

Furthermore, the effectiveness of this lose-dose combination was exemplified in two other malignant cancer cell lines. In B16-F10 mouse metastatic melanoma, viability was reduced to 39% ($p<0.01$) (Figure 33). In THP-1 human acute monocytic leukemia, viability was reduced to 56% ($p<0.05$) (Figure 34). The efficacy towards multiple murine and human cancer cells showcases the applicability and effectiveness of our novel combinatorial therapy.

To model conditions found at the site of the tumor, efficacy of the combination and compounds used individually were evaluated under hypoxic conditions. A parallel study comprised of the same population of cells and treatment was performed under normoxia to signify the effect of hypoxia. Compared to normoxia, cell viability under hypoxia was significantly decreased. In the 4-T1 cell line, MTX, 2DG, and WGN combined at their $EC_{50}$ decreased cytotoxicity by an additional 15% under hypoxia compared to normoxia ($p<0.05$). Combined at 2 times below their respective $EC_{50}$, viability was decreased by an additional 16% under hypoxia compared to normoxia in the 4-T1 cell line ($p<0.05$). Combined at 4 times below their respective $EC_{50}$, viability was again shown to be decreased by an additional 16% under hypoxia compared to normoxia against 4-T1 cells ($p<0.05$) (Figure 31). In the MCF-7 cell line, MTX, 2DG, and WGN

combined at their $EC_{50}$ decreased cytotoxicity by an additional 15% under hypoxia compared to normoxia ($p<0.05$). Combined at 2 times below their respective $EC_{50}$, viability was decreased an additional 8% under hypoxia compared to normoxia in the MCF-7 cell line ($p<0.05$). Combined at 4 times below their respective $EC_{50}$, viability was decreased by an additional 10% under hypoxia compared to normoxia against MCF-7 cells ($p<0.05$) (Figure 32). We attribute this increase in efficacy to the acceleration of cancer cell growth under hypoxic conditions. Hypoxic conditions are favorable to the cancer cell and leads to increased cell division and metabolism[117]. Thus, effective targeting of these pathways by our combination was evidenced by increased cytotoxicity as compared to normoxia.

Lastly, our novel combinatorial therapy was found to be effective at inhibiting colony formation, evidenced by *in vitro* colony-forming assays. Treatment of the 4-T1 cell line by the combination was 100% effective at inhibiting colony formation relative to untreated control. 492 colonies were counted in the untreated control wells, compared to 0 counted in the experimental group treated with our combinatorial therapy. In the MCF-7 cell line, treatment with the combination effectively inhibited colony formation. Untreated control well colonies were determined to be too many to count, compared to 0 counted in the experimental group treated with our combinatorial therapy. The ability of our novel low-dose drug combination to eradicate a tumor tissue monolayer and inhibit the growth of a dynamic population of tumor cells is a significant discovery in the field of oncology research. Future studies will delve into the mechanisms of the induced cell death and evaluate tumor cell death for signs of immunogenicity. Additionally, the effects of or combinatorial therapy against normally dividing and stimulated immune cells will

be studied to evaluate the toxicity against healthy human cells. Furthermore, the efficacy of our combinatorial therapy will be assessed in 3D tumorsphere models that closely mimic *in vivo* studies.

In conclusion, our novel combinatorial therapy showed significant efficacy at low doses compared to the individual compounds used singly. Efficacy was increased under hypoxia, by mimicking the favorable hypoxic tumor microenvironment. The novel combinatorial therapy completely inhibited colony formation and eradicated tumor tissue monolayers in two highly metastatic, rapidly proliferating cancer cell lines. Further research will assess the toxicity towards proliferating immune cells and provide greater insight into the mechanism and immunogenicity of elicited cell death.

# CHAPTER 3: A NOVEL LOW-DOSE COMBINATORIAL THERAPY HAS NO EFFECT ON NORMALLY DIVIDING AND PROLIFERATING HEALTHY HUMAN PERIPHREAL BLOOD MONONUCLEAR CELLS

## 3.1 ABSTRACT

The toxicity of newly discovered and currently used therapeutic agents towards normal cells of the body pose severe clinical challenges in cancer treatment. The high-toxicity and non-specificity of current chemotherapeutic agents render them clinically insignificant, as their anticancer properties are meaningless if they pose great harm to the patient. The current study evaluated the toxicity of a novel combinatorial therapy, comprised of methotrexate, 2-deoxyglucose, and wogonin, against human peripheral blood mononuclear cells (PBMC). A parallel study was performed on the same human peripheral blood mononuclear cells stimulated for growth via Phytohemagglutinin (PHA-P), a potent mitogen inducing activation and proliferation of lymphocytes. Quiescent PBMCs showed no evidence of membrane compromise or significant decrease in viability 48 h post-treatment. PHA-stimulated PBMCs showed no evidence of combinatorial therapy cytotoxic effects. A statistically insignificant decrease in cell viability was observed 48 h after high-dose 2DG treatment. We attribute the observed cytotoxic effect of 2DG towards PBMCs to be the result of glycolytic targeting and inhibition, as no cytotoxic effects were observed at similar doses of 2DG against quiescent PBMCs. Neither of the other two compounds that make up the three-drug combination showed evidence of cytotoxicity towards either population of PBMC. We

can conclude from these studies that our novel combinatorial therapy has potent anticancer effects, and no observed clinically significant toxicity towards normal healthy cells.

## 3.2 INTRODUCTION

A single Ultra High-Throughput screening machine has the potential to analyze and define the toxicity of 100,000 new chemicals a day[118]. In the world of cancer therapy research, a plethora of new anticancer agents are screened by the minute. So why are so few compounds available for clinical use? The answer lies not so much in their efficacy towards cancer cells, rather their toxicity towards normal cells. The majority of chemotherapies administered by oncologists target rapid cell division[86]. The mechanism of action of this class of drugs revolves around inducing S-phase arrest or impairment of mitosis by targeting of cell microtubules. Because cancers arise from self-cells, the mechanisms of cell division are synonymous, albeit uncontrolled and unregulated in cancer. Thus, the administration of these chemotherapeutic agents intended to kill cancer cells have indirect cytotoxic effects on surrounding normal cells. Coupled with continuously evolving resistance mechanisms, treating cancer is as challenging as ever.

It has long been shown that cancerous growths are characterized by rapid, uncontrolled proliferation. However, recent studies over the past few decades show that not all cancer cells abide by this designation, and in fact some cases found them to proliferate slower than normal healthy cells[119]. Importantly, many normal cells of the body exhibit rapid proliferation, including but not limited to: white blood cells, gastrointestinal cells, cells of the hair follicle, and bone marrow cells[120]. With many cancer chemotherapies targeting replication, clinicians have long hypothesized cancer

cells to be more susceptible to this therapeutic targeting due to their rapid proliferation. However, researchers are now understanding the detrimental effects these therapies have on the above mentioned normal cells, and consequently, physiological homeostasis. Unfortunately, cancer patients as a result of this high toxicity must battle the underlying disease of cancer, along with the detrimental effects of cachexia.

Toxicity to normal cells manifests in a number of ways, but more commonly presents as cachexia: the withering away of the cancer patient. Primarily, chemotherapeutic treatment causes nausea and diarrhea in patients. As mentioned above, cells of the gastrointestinal tract proliferate rapidly making them susceptible to chemotherapeutic agents. These GI tract complications are attributed to normal GI cell death, highlighted by the loss of these symptoms after chemotherapy termination. In some cases, however, recovery from chemotherapeutic side effects are not so immediate. Hair follicle cells proliferate rapidly as well, making them equally susceptible to chemotherapeutic agents. Even after termination of chemotherapy, hair may not regrow for another 6 months[121]. This emphasizes the long-lasting, damaging effects of this commonly used treatment modality. Similarly, the rapid proliferation of bone marrow cells subjects them to chemotherapeutic toxicity, resulting in anemia. Yet more important is the effect chemotherapy has against cells of the innate and adaptive immune system. All leukocytes and lymphocyte precursors originate in the bone marrow. Classified as highly proliferative, treatment with replication inhibitors is highly toxic to these cells. Moreover, chemotherapy has been directly linked to lowered white blood cell count[122]. The implications of this indirect toxicity place the patient at high risk for a multitude of health concerns, including immunodeficiency which leads to a significant increase in

risks of infection and communicable disease. Furthermore, studies have shown that some cases of lowered white blood cell count as a result of chemotherapy are irreversible, signifying the lasting harmful effects[122]. Side effects of chemotherapy should not be underestimated and may be considered more fatal than the cancer itself. Thus, studies evaluating the toxicity towards normal cells are critical in the drug development process.

## 3.3 BACKGROUND AND SIGNIFICANCE

Significant toxicity towards normal cells of the body often prohibit chemotherapeutic development of newly discovered anticancer therapies. Whereas a threshold for accepted toxicity exists, as per regulatory agencies, development of novel anticancer therapies should seek to induce as little toxicity as possible towards these healthy cells. Thus, the attention has shifted to targeted drugs and away from non-specific replicative inhibitors and other commonly used chemotherapeutic agents. Nonetheless, evaluation of all drug cytotoxicity towards normal cells, no matter their mechanism of action, should be mandated.

A pernicious side effect of chemotherapy is bone marrow cell suppression. Concordantly, the resulting long-lived damage to the immune system and increased risk of infection caused by chemotherapy calls for careful analysis of chemo drug effects. Thus, studying the effects of anticancer agents specifically on human peripheral blood mononuclear cells is of utmost importance. To circumvent the lasting suppression of cell and humoral immunity, a developing therapy should demonstrate little-to-no toxicity towards normal human PBMCs, as well PHA-stimulated PBMCs that approximate a model of their activation and clonal expansion.

Methotrexate, a component of our novel drug combination, is an antifolate and has long been employed as a chemotherapeutic drug in multiple cancers. Methotrexate's inhibition of dihydrofolate reductase interrupts the folic acid cycle, resulting in inhibited nucleic acid synthesis and consequently cell death[98]. Importantly, in contrast to many conventional chemotherapeutic compounds, it is not mutagenic. To elicit sufficient efficacy and overcome anticipated cancer cell resistance, MTX is often administered at high doses. High-risk patients receive 5 $g/m^2$ every 24 hours, equivalent to a serum concentration of 65 μM[123]. Normal cells have a similar dependence on folic acid to sustain division and physiological homeostasis. Accordingly, MTX is toxic to normal proliferating cells of the body at high doses. Evidence of severe toxicity as a result of MTX treatment is currently remedied by dose reduction or withdrawal from treatment[124]. In either case, efficacy of MTX is significantly decreased and the cancer persists.

2-deoxyglucose, another component of our novel drug combination, is a glycolytic inhibitor that is currently in clinical trials as a potent anticancer targeted therapy. 2DG is highly toxic towards cells that rely heavily on glycolytic metabolism, as is the case for cancer cells. Resembling glucose, 2DG is taken up by glucose transporters and competitively inhibits hexokinase function, impairing glucose metabolism[95]. This leads to decreased ATP production inevitably resulting in cell death. Additionally, as a mannose analogue, 2DG has been shown to interfere with N-glycosylation, responsible for modifying a large number of proteins[96]. 2DG targeting leads to the unfolded protein response (UPR) in the ER, resulting in increased cellular stress which leads to cell death[96]. Although highly efficacious at counteracting the Warburg effect, recent studies have found activated lymphocytes also exhibit "Warburg-like" metabolic transformations

as well[125]. To support rapid clonal expansion, lymphocytes will convert to aerobic glycolysis to sustain their increased metabolic needs. Concordant with these findings, high-dose administration of glycolytic inhibitors have been found to suppress activated lymphocyte expansion[126].

Wogonin, the final component of our novel drug combination, is a flavonoid that is currently undergoing clinical trials as a phytopharmacuetical drug. WGN has been shown to elicit multiple anticancer effects, ranging from anti-proliferation to pro-apoptosis. With regards to mitogenesis, WGN effectively inhibits protein tyrosine kinase activity, hampering cell proliferation[127]. WGN also increases the expression of *Bax*, a potent pro-apoptotic protein necessary in procaspase activation[128]. Additionally, WGN downregulates VEGF and VEGF-R1 expression, strong proangiogenic and anti-inflammatory signals[129]. Most importantly, WGN has been shown to decrease T-regulatory cell function and simultaneously synergize with IL-2 to stimulate effector T-cell function. Dubbed a "miracle extract," WGN boasts the above mentioned anticancer properties with generally no toxicity to normal cells at efficacious doses[130].

Through previous experiments and mechanistic evaluation, we anticipate little-to-no toxicity towards both normally dividing and stimulated healthy PBMCs. The literature states that MTX is administered at a serum concentration of 65 μM in high-risk patients. Our novel combinatorial therapy shows significant cytotoxicity at a mere 0.006 μM. The literature finds 2DG to have toxic effects towards activated effector lymphocytes at concentrations of 25 mM. Our novel combinatorial therapy demonstrates significant cytotoxicity at a mere 5 mM. Moreover, voluminous evidence in the literature supports the relative non-toxicity of WGN, and potent cytotoxicity towards cancer cells. The

significant efficacy of our novel combinatorial therapy paired with its anticipated non-toxicity towards healthy human immune cells may place it at the forefront of anticancer treatments.

## 3.4 METHODS

### *3.4.1 Cell culturing and maintenance*

Whole blood was obtained from the OneBlood Blood Bank (Orlando, FL). Human peripheral blood mononuclear cells were derived from whole blood using Ficoll-Paque density gradient media (Cytiva, USA) and centrifugation. Cells were cultured at $1\times10^6$/mL in 75 $cm^2$ Falcon cell culture flaks containing Gibco RPMI 1640-L-Glutamine medium (Life Technologies- Grand Island, NY, USA) supplemented with 10% fetal bovine serum (Life Technologies- Grand Island, NY, USA) and 100U/mL Gibco Pen Strep (Life Technologies- Grand Island, NY, USA). Cell cultures were incubated at 37 °C under 5% $CO_2$ in a humidified atmosphere.

### *3.4.2 PHA-P stimulation*

Whole blood-derived human peripheral blood mononuclear cells were cultured at $2\times10^6$/mL in 75 $cm^2$ Falcon cell culture flaks containing Gibco RPMI 1640-L-Glutamine medium (Life Technologies- Grand Island, NY, USA) supplemented with 10% fetal bovine serum (Life Technologies- Grand Island, NY, USA) and 100U/mL Gibco Pen Strep (Life Technologies- Grand Island, NY, USA). PHA-P was added at a final concentration of 5µg/mL. Cell cultures were incubated at 37 °C under 5% $CO_2$ in a humidified atmosphere for 24 h prior to treatment.

*3.4.3 Trypan blue exclusion cell viability assay*

Whole blood-derived human peripheral blood mononuclear cells cultured at $2\times10^6$/mL in 75 $cm^2$ Falcon cell culture flaks containing Gibco RPMI 1640-L-Glutamine medium (Life Technologies- Grand Island, NY, USA) supplemented with 10% fetal bovine serum (Life Technologies- Grand Island, NY, USA) and 100U/mL Gibco Pen Strep (Life Technologies- Grand Island, NY, USA)., were harvested by adding 10 mL of PBS to the flask and incubating on ice for 20 minutes. A P1000 micropipette was used to pipette 1000 µL of ice-cold PBS repeatedly. The harvested cells ($2x10^4$ cells/ mL) were seeded in 5 mL of complete RPMI 1640 in CellTreat 15 mL Bio-reaction Cell Culture tubes, treated with the MTX, 2DG, and WGN drug combination. Cells were incubated for 48 h at 5% $CO_2$ at 37°C. 48 h post-treatment, cells were centrifuged at 1200 RPM for 10 minutes. The resulting cell pellet was resuspended in 1 mL of complete RPMI 1640 cell culture media. 10 µL of 0.4% trypan blue was mixed with 10 µL of cell suspension in a 96-well plate well and incubated for 2 minutes at room temperature. 10 µL of the 0.4% trypan blue/cell suspension mixture was loaded onto a hemacytometer and stained vs unstained cells were counted. The percentage of viable cells was calculated using the formula:

$$\%\, Viability = \frac{total\ number\ of\ unstained\ cells}{total\ number\ of\ stained\ and\ unstained\ cells}\ x\ 100$$

*3.4.4 Flow Cytometry*

A Guava easyCyte flow cytometer with InCyte software (EMD Millipore, USA), was used to determine PBMC viability. Quiescent and PHA-stimulated PBMCs were treated with our novel combinatorial therapy for 48 h. After 48 h, cells were centrifuged and resuspended in 1X Annexin V binding buffer solution (BD Pharmingen, USA). 100 µL of

cell suspension was transferred to a 5 mL reaction tube. 5 µL of Annexin V-FITC apoptosis detection dye (BD Pharmingen, USA) was added to the reaction tube. 10 µL of 7-AAD (BD Pharmingen, USA) nucleic acid staining dye was added to the 5 mL reaction tube. Reaction tubes were gently mixed and incubated for 15 min at RT. 400 µL of 1X binding buffer was added after incubation. Samples were then read by flow cytometry and analyzed with FlowJo v9 software. Annexin V+ and 7-AAD+ populations of treated cells were compared to Annexin V+ and 7-AAD + populations of untreated cells.

*3.4.5 MTS cell viability assay under hypoxia*

Human whole blood-derived peripheral blood mononuclear cells ($1 \times 10^5$ cells/mL) were seeded in 96-well plate Analysis of the effectiveness of MTX-2DG-WGN combination under hypoxia on cell growth was performed with an MTS kit (CellTiter 96® AQueous One Solution Cell Proliferation Assay Kit, Promega, Madison, WI, USA) according to the manufacturer's instruction. Human whole blood-derived peripheral blood mononuclear cells were seeded into 96-well plates at a density of $20\times 10^3$ cells per well with three replicates. The cells were treated as indicated (MTX, 2DG, and WGN were administered individually and in combination at 5X above their $EC_{50}$, and also with two serial two-fold dilutions from their $EC_{50}$) and incubated for 48 h at 1% $O_2$ 5% $CO_2$ at 37°C. After 48 h, 20 µL of CellTiter 96® AQueous One Solution MTS (5 mg/mL) (Promega- Madison, WI, USA) was added to each well and incubated at 5% $CO_2$ at 37°C for an additional 4h. Absorbance readings were taken in an Epoch microplate reader at 490 nm. Computed data was compared to untreated and normalized cells. Cell viability was calculated by the following formula: Cell viability (%) = (average OD in treated group/average OD in control group) × 100%.

*3.4.6 Statistical analysis*

GraphPad Prism v8 software was used for statistical analyses. Data is presented as mean ± s.d. t-test was used to determine statistical significance between groups for normally distributed data. For all tests, *$p<0.05$ was considered significant. Experiments and measurements were performed in triplicate. Graphed data depicts means of triplicates ± s.e.m. and are representative of three experiments.

## 3.5 RESULTS

### 3.5.1 MTX, 2DG, and WGN combined 3 times above their $EC_{50}$ is non-toxic towards human whole blood-derived peripheral blood mononuclear cells.

In the present study, two populations of whole-blood derived human PBMCs (quiescent vs. PHA-stimulated) were treated with MTX-2DG-WGN at 3 times above their $EC_{50}$ in combination and individually, as well as at $EC_{50}$ and 2 times below. The significance of studying two populations of cells, specifically the PHA-stimulated population, is to mimic conditions observed in the bone marrow. Phytohemagglutinin (PHA-P) is a potent mitogen that induces activation and proliferation of lymphocytes. During immune activation, PBMCs resemble cancer cells in that they proliferate rapidly and have been shown to similarly undergo aerobic glycolysis to fulfill their increased metabolic needs[126]. While these properties in cancer cells make them more susceptible to drug targeting, we aim to show that this is not the case in healthy immune cells that are needed to combat neoplastic growths. After 48 h treatment under the above conditions, both populations were analyzed via trypan blue exclusion to determine cell viability and evaluate the toxicity of our combinatorial therapy against these normal cells.

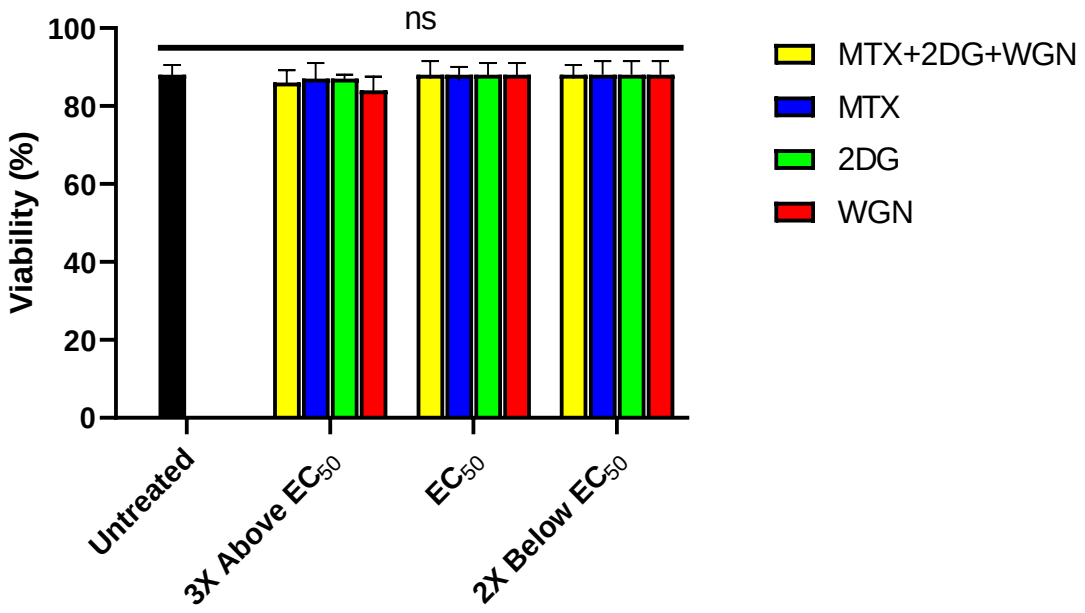


**Figure 36. MTX-2DG-WGN combined at 3 times above their individual EC50 is non-toxic towards quiescent human PBMCs.** Cells were treated for 48 h in combination or individually with MTX-2DG-WGN and analyzed via trypan blue exclusion. Bars represent the average of triplicate experiments ± s.e.m. (ns= not significant, $p>0.05$).

After 48 h, untreated control cell viability of quiescent PBMCs was determined to be 88%. In the first experimental group, quiescent human PBMCs were treated with MTX, 2DG, and WGN at 0.147 µM, 58 mM, and 60 µM, respectively, in combination and individually (Figure 36). After 48 h of treatment with the combination, quiescent PBMCs exhibited 86% viability, no significant differences compared to untreated controls ($p>0.05$). When quiescent PBMCs were treated only with MTX at 0.147 µM, or only 2DG at 58 mM, or only WGN at 60 µM for 48 h, PBMC viability was reduced to 87%, 87%, and 84% respectively, indicating that these drugs singly did not significantly alter the viability of quiescent PBMCs with respect to untreated controls ($p>0.05$). In the second experimental group, MTX, 2DG, and WGN were administered at 0.049 µM, 19.6 mM, and 20 µM, respectively, in combination and individually. Treated with the combination, PBMC viability after 48 h was comparable to that of the untreated control.

Compared to the combination, individual treatment with MTX, 2DG, or WGN at these concentrations for 48 h had no effect on PBMC viability. In the third experimental group, MTX, 2DG, and WGN were combined at 0.025 µM, 9.8 mM, and 10 µM respectively; 2 times below their individual $EC_{50}$. Treated with the combination, PBMC viability after 48 h was comparable to that of the untreated control. Compared to the combination, individual treatment with MTX, 2DG, or WGN at these concentrations for 48 h had no effect on PBMC viability ($p>0.05$).

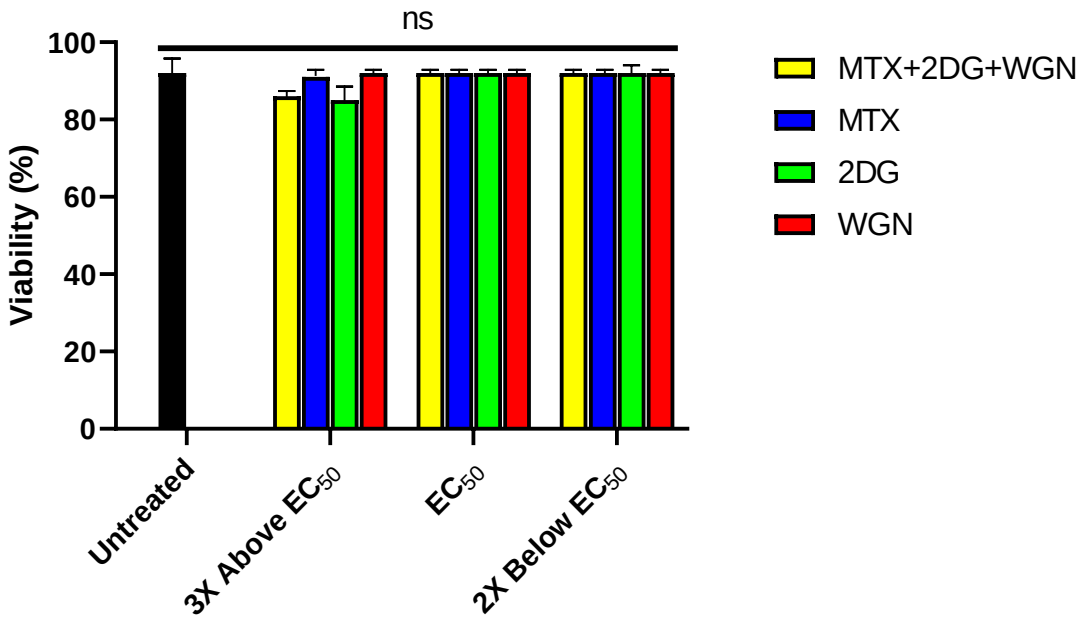


**Figure 37. MTX-2DG-WGN combined at 3 times above their individual EC50 is non-toxic towards PHA-stimulated human PBMCs.** Cells were treated for 48 h in combination or individually with MTX-2DG-WGN and analyzed via trypan blue exclusion. Bars represent the average of triplicate experiments ± s.e.m. (ns= not significant, $p>0.05$).

High-dose combination was further studied in PHA-stimulated PBMCs. After 48 h, untreated control cell viability of PHA-stimulated PBMCs was determined to be 92%. In the first experimental group, PHA-stimulated human PBMCs were treated with MTX, 2DG, and WGN at 0.147 µM, 58 mM, and 60 µM, respectively, in combination and

individually (Figure 37). Treated with the combination, PBMCs were reduced to 82% viability after 48 h. When PHA-stimulated PBMCs were treated only with MTX at 0.147 µM, or only 2DG at 58 mM, or only WGN at 60 µM for 48 h, PBMC viability was reduced to 91%, 85%, and no effect respectively, indicating that these drugs singly did not significantly alter the viability of PHA-stimulated PBMCs with respect to untreated controls ($p>0.05$). In the second experimental group, MTX, 2DG, and WGN were administered at 0.049 µM, 19.6 mM, and 20 µM, respectively, in combination and individually. Treated with the combination, PBMC viability after 48 h was comparable to that of the untreated control. Compared to the combination, individual treatment with MTX, 2DG, and WGN for 48 h had no significant effect on PBMC viability ($p>0.05$). In the third experimental group, MTX, 2DG, and WGN were combined at 0.025 µM, 9.8 mM, and 10 µM respectively; 2 times below their individual $EC_{50}$. Treated with the combination, PBMC viability after 48 h was comparable to that of the untreated control. Compared to the combination, individual treatment with MTX, 2DG and WGN for 48 h had no effect on PBMC viability ($p>0.05$).

### 3.5.2 MTX, 2DG, and WGN combined 3 times above their $EC_{50}$ is non-toxic towards human whole blood-derived peripheral blood mononuclear cells under hypoxia whereas doxorubicin induces significant cell death.

In the present study, PHA-stimulated human PBMCs were treated with MTX-2DG-WGN at 3 times above their $EC_{50}$ in combination as well as at their $EC_{50}$ and 2 times below, under hypoxia. Phytohemagglutinin (PHA-P) is a potent mitogen that induces activation and proliferation of lymphocytes. To sustain this rapid division,

lymphocytes have been shown to alter their metabolic machinery and shift to aerobic glycolysis. Furthermore, clonal expansion in immunological sites throughout the body have been found to be promoted by physiological hypoxia[131]. Thus, in this study, we seek to mimic the microenvironment during immune activation by subjecting rapidly proliferating PBMCs to hypoxic conditions. This study provides us with a better understanding of the toxicity our novel combinatorial therapy displays towards normal rapidly dividing cells of the body. Cell viability was measured using MTS cell viability assay. Cell viability is expressed as a percentage of the control (100%).

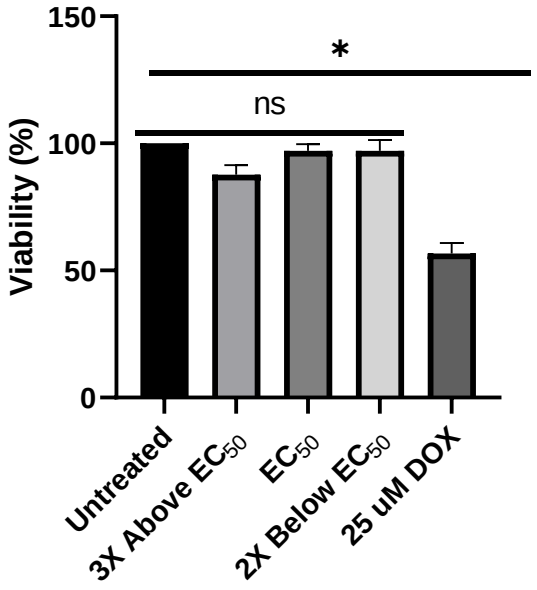


**Figure 38. MTX-2DG-WGN combined at 3 times above their individual EC50 is relatively non-toxic towards PHA-stimulated human PBMCs.** Cells were incubated under hypoxic conditions and treated for 48 h in combination with MTX-2DG-WGN or doxorubicin and analyzed via MTS cell viability. Bars represent the average of triplicate experiments ± s.e.m. (ns= not significant, $p>0.05$, **= $p<0.01$).

In the first experimental group, PHA-stimulated human PBMCs were treated with MTX, 2DG, and WGN at 0.147 µM, 58 mM, and 60 µM, respectively, in combination and incubated for 48 h at 1% $O_2$ and 5% $CO_2$ (Figure 38). Treated with the combination, PBMCs were reduced to 86% viability relative to the untreated control ($p>0.05$). In the

second experimental group, MTX, 2DG, and WGN were administered at 0.049 µM, 19.6 mM, and 20 µM, respectively, in combination for 48 h at 1% $O_2$ and 5% $CO_2$. Treated with the combination, PBMC viability was comparable to that of the control. In the third experimental group, MTX, 2DG, and WGN were combined at 0.025 µM, 9.8 mM, and 10 µM respectively; 2 times below their individual $EC_{50}$. Treated with the combination for 48 h at 1% $O_2$ and 5% $CO_2$, PBMC viability was comparable to that of the control. Low-dose doxorubicin was administered for 48 h, and reduced PBMC viability to 58% ($p<0.05$).

### 3.5.3 MTX, 2DG, and WGN combined 3 times above their $EC_{50}$ spares human whole blood-derived peripheral blood mononuclear cells whereas doxorubicin induces significant cell death.

In the present study we determined the mechanism of cell death in immune cells treated with our novel combinatorial therapy versus cells left untreated. Additionally, we studied two populations of immune cells: quiescent and slow growing and stimulated and rapidly proliferating. By activating these cells, we simultaneously mimic conditions found in the bone marrow as well as resemble the replicative profile of cancer cells. Furthermore, two experimental groups of cells were treated with 25 µM doxorubicin, an anthracycline and widely-used chemotherapy for breast cancer that targets rapidly dividing cells. Although known to have indirect toxicity towards healthy cells in the patient, the concentration used in this study is well below the suggested clinical dose[132]. This study allows us to directly compare the effects our novel combinatorial therapy and a standard chemotherapy have on healthy immune cells of the body.

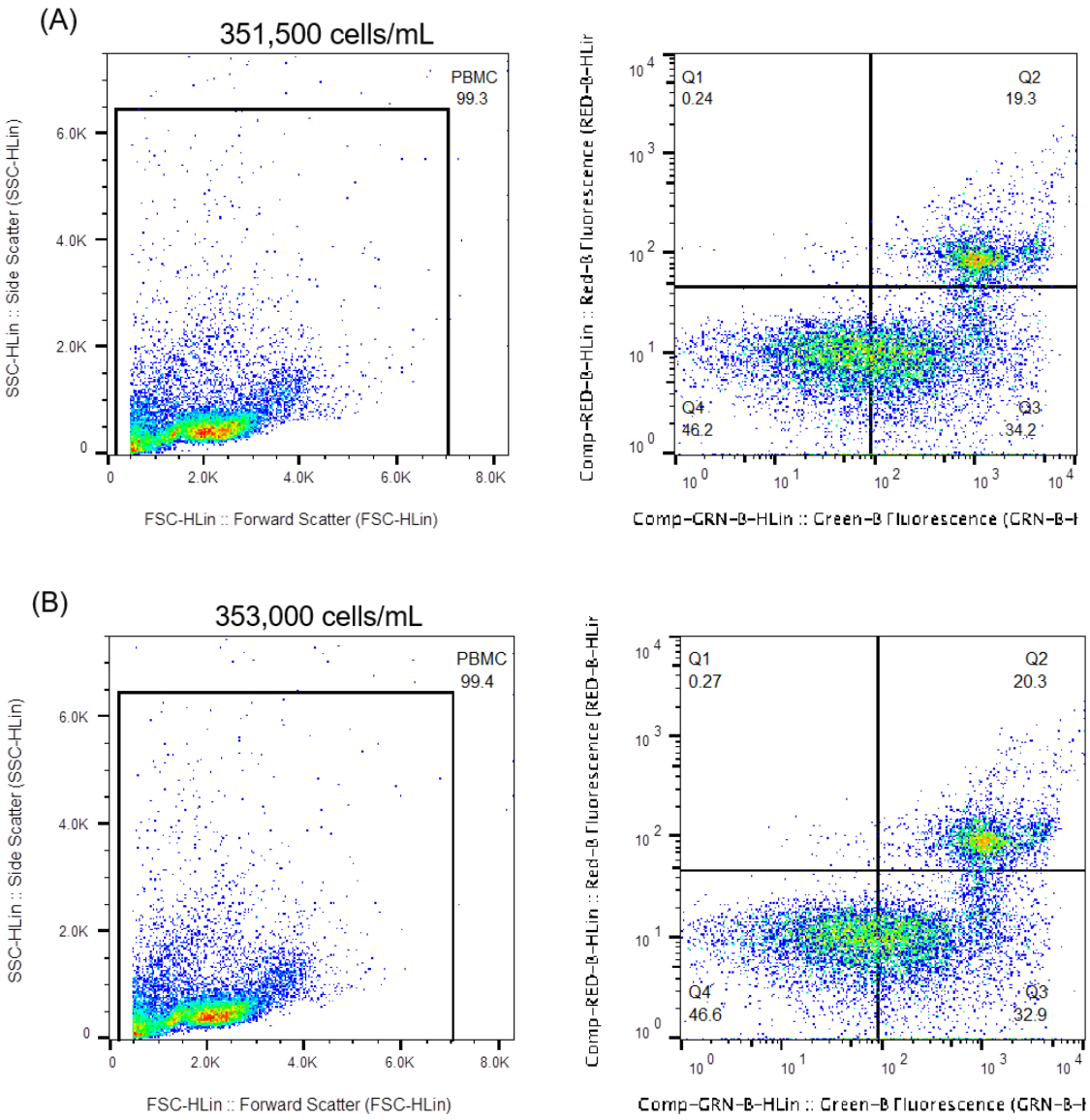
(A)
351,500 cells/mL
PBMC
99.3
SSC-HLin :: Side Scatter (SSC-HLin)
FSC-HLin :: Forward Scatter (FSC-HLin)
Q1
0.24
Q2
19.3
Q4
46.2
Q3
34.2
Comp-GRN-B-HLin :: Green-B Fluorescence (GRN-B-H
(B)
353,000 cells/mL
PBMC
99.4
SSC-HLin :: Side Scatter (SSC-HLin)
FSC-HLin :: Forward Scatter (FSC-HLin)
Q1
0.27
Q2
20.3
Q4
46.6
Q3
32.9
Comp-GRN-B-HLin :: Green-B Fluorescence (GRN-B-H

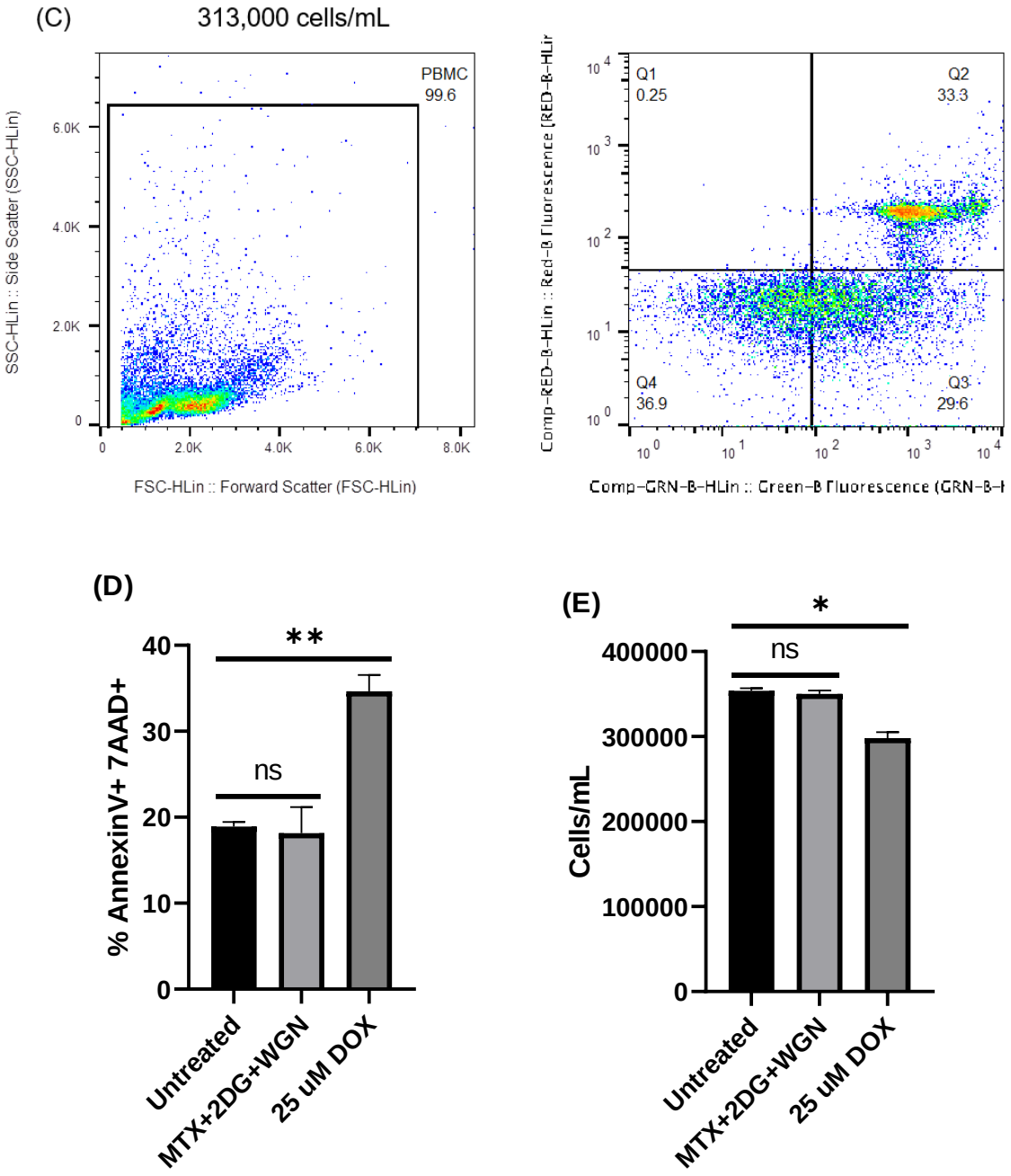


**Figure 39. Our novel combinatorial therapy spares quiescent immune cells whereas doxorubicin induces significant cell death.** Quiescent PBMC's were left untreated **(A)** treated with our novel combinatorial therapy **(B)** or treated with 25 µM doxorubicin **(C)** for 48 h and dot plots of AnnexinV and 7AAD staining were obtained from flow cytometry. The lower right quadrant (Annexin V+/7AAD-) reflects cells at varying stages of apoptosis, while the upper right quadrant (Annexin V+/7AAD+) indicates cells that are dead. The percentage of cell death was significant in the doxorubicin treatment group with respect to untreated control **(D)**. Cell number was significantly reduced by doxorubicin treatment with respect to untreated control **(E)**. Cell counts were determined via trypan blue exclusion. Dot plots are representative of a typical experiment out of two independent ones. Bars represent the average of duplicate experiments ± s.e.m. (ns= not significant, $p>0.05$, *= $p<0.05$, **=$p<0.01$).

After 48 h, untreated quiescent PBMCs were 19.3% AnnexinV+7AAD+ (Figure 39). After 48 h, quiescent PBMCs treated with our combinatorial therapy were 20.3% AnnexinV+7AAD+. No significant difference was observed between these two groups of cells (ns, $p>0.05$). However, after 48 h, quiescent PBMCs treated with 25 µM doxorubicin were 33.3% AnnexinV+7AAD+. Although cells were not rapidly dividing, low-dose doxorubicin treatment caused increased cell death with respect to untreated control ($p<0.01$).

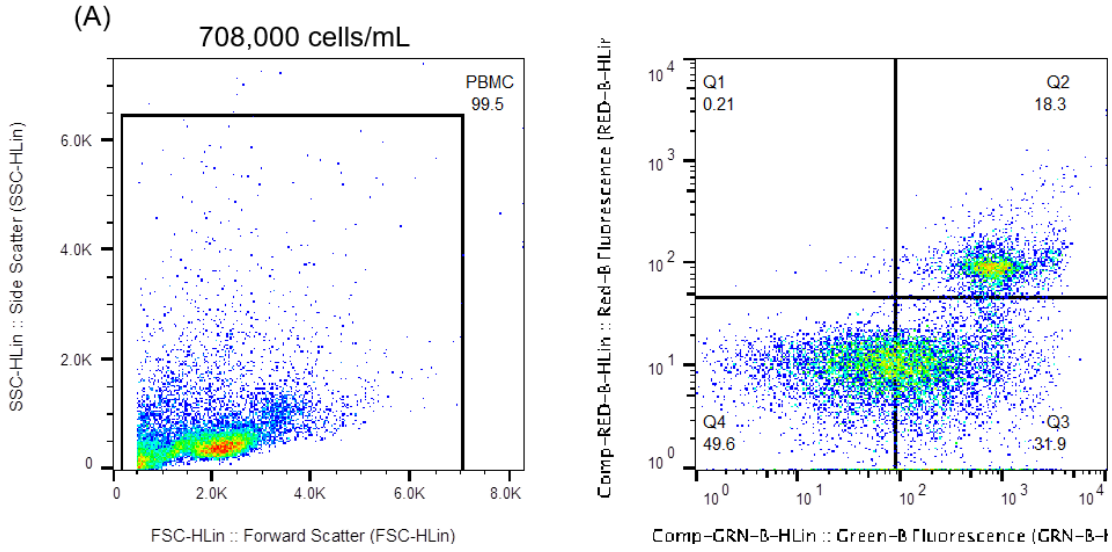

(B)

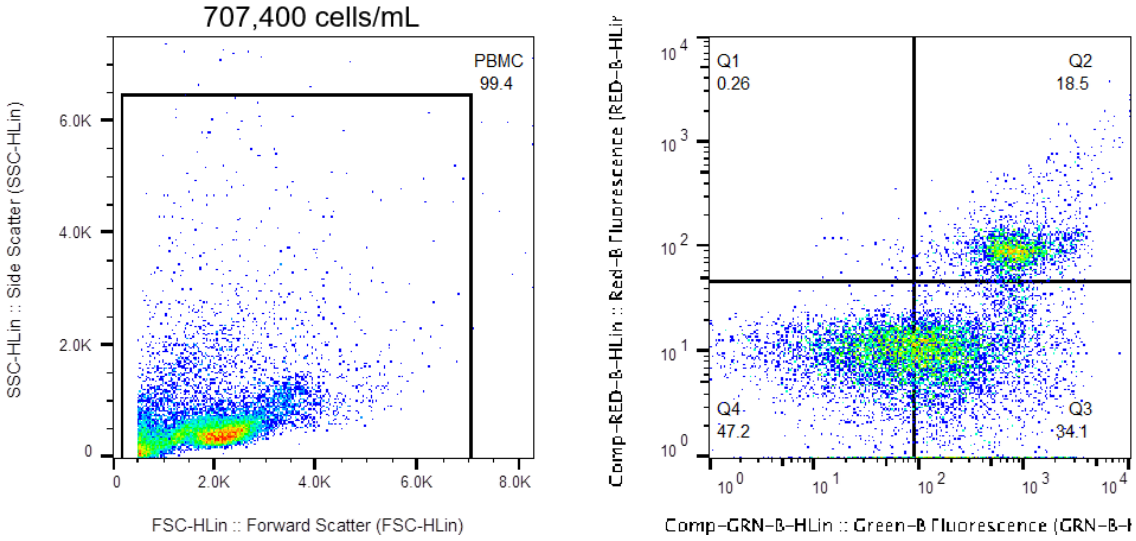
707,400 cells/mL
PBMC
99.4
SSC-HLin :: Side Scatter (SSC-HLin)
FSC-HLin :: Forward Scatter (FSC-HLin)
Q1
0.26
Q2
18.5
Q4
47.2
Q3
34.1
Comp-RED-B-HLin :: Red-B Fluorescence (RED-B-HLin
Comp-GRN-B-HLin :: Green-B Fluorescence (GRN-B-H

(C)

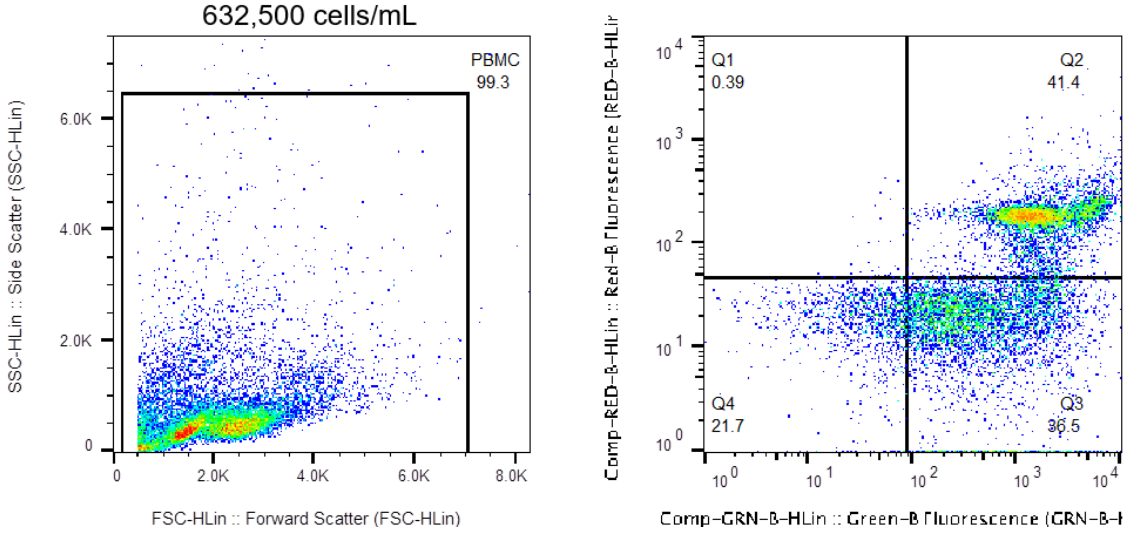
632,500 cells/mL
PBMC
99.3
SSC-HLin :: Side Scatter (SSC-HLin)
FSC-HLin :: Forward Scatter (FSC-HLin)
Q1
0.39
Q2
41.4
Q4
21.7
Q3
36.5
Comp-RED-B-HLin :: Red-B Fluorescence (RED-B-HLin
Comp-GRN-B-HLin :: Green-B Fluorescence (GRN-B-H

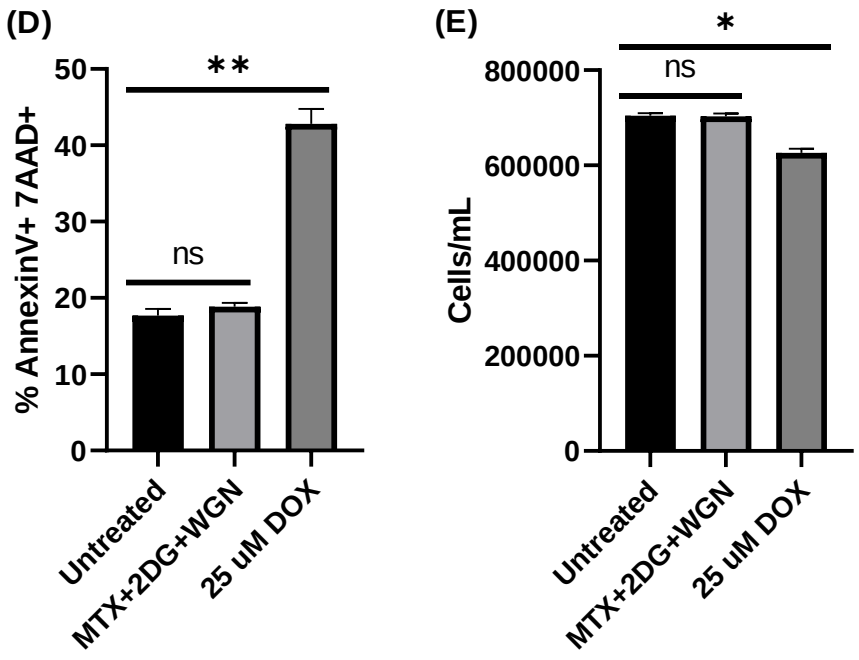


**Figure 40. Our novel combinatorial therapy spares proliferating immune cells whereas doxorubicin induces significant cell death.** PHA-stimulated PBMC's were left untreated **(A)** treated with our novel combinatorial therapy **(B)** or treated with 25 µM doxorubicin **(C)** for 48 h and dot plots of AnnexinV and 7AAD staining were obtained from flow cytometry. The lower right quadrant (Annexin V+/7AAD-) reflects cells at varying stages of apoptosis, while the upper right quadrant (Annexin V+/7AAD+) indicates cells that are dead. The percentage of cell death was significant in the doxorubicin treatment group with respect to untreated control **(D)**. Cell number was significantly reduced by doxorubicin treatment with respect to untreated control **(E)**. Cell counts were determined via trypan blue exclusion. Dot plots are representative of a typical experiment out of two independent ones. Bars represent the average of duplicate experiments ± s.e.m. (ns= not significant, $p>0.05$, *= $p<0.05$, **= $p<0.01$).

After 48 h, untreated PHA-stimulated PBMCs were 18.3% AnnexinV+7AAD+ (Figure 40). After 48 h, quiescent PBMCs treated with our combinatorial therapy were 18.5% AnnexinV+7AAD+. No significant difference was observed between these two groups of cells (ns, $p>0.05$). However, after 48 h, quiescent PBMCs treated with 25 µM doxorubicin were 41.4% AnnexinV+7AAD+. Rapid proliferation of immune cells may have increased their susceptibility to low-dose doxorubicin targeting, causing increased cell death with respect to untreated control ($p<0.01$).

## 3.6 DISCUSSION

Hundreds of thousands of anticancer compounds are screened and analyzed daily across the world. Despite their potential effectiveness against cancer cells, the vast majority fail to progress forward in the drug development process due to marked cytotoxicity towards healthy human cells. This observed cytotoxicity, primarily, is the result of non-specificity. The majority of clinically approved chemotherapeutic agents target replicative pathways. However, normal cells are not spared from this therapeutic targeting, as some have been shown to proliferate faster than cancer cells.

Cachexia commonly associated with chemotherapy is the direct result of toxicity towards healthy cells, at varying degrees. Gastrointestinal cells proliferate rapidly to maintain physiological homeostasis. As a result, they are subject to chemotherapeutic targeting, which triggers nausea and diarrhea in the patient. Termination of chemotherapy is accompanied by reduced nausea and diarrhea shortly after, as GI cells begin to regenerate. However, not all healthy cells recover as quickly from chemotherapy toxicity. Hair follicle cells are subject to chemotherapy toxicity due to their rapid proliferative phenotype, which presents as the loss of hair in cancer patients. Unlike GI cells, the effects of chemo drugs on hair follicle cells is lasting, and hair loss is observed as late as six months post-withdrawal from treatment. Above all, the indirect targeting of white blood cells holds the most detrimental effect. Chemotherapy has been linked to reduced WBC count and immunosuppression, increasing patient risks of infection and communicable disease. The sensitivity to chemotherapy is due large in part to the proliferative profile of bone marrow progenitors, which subjects them to replicative inhibition. Furthermore, bone marrow suppression has been found to persist long after

termination of treatment, and in some cases shown to be irreversible. Immunodeficiency as a result of chemotherapeutic toxicity is a detriment to patient health, in some cases well-beyond the complications of cancer. Thus, evaluating the toxicity of compounds towards leukocytes and lymphocytes above all other cells is of utmost importance.

In the first study, MTX, 2DG and WGN were combined at 0.147 µM, 58 mM, and 60 µM respectively, 3 times greater than their individual $EC_{50}$. Cells were also treated in combination at $EC_{50}$ and 2 times below $EC_{50}$. Treatment of quiescent human PBMCs at this concentration in combination for 48 h showed no evidence of cytotoxicity and no significant decrease in cell viability. In PHA-stimulated cells, an 8% decrease in cell viability was observed post 48 h treatment, which was determined to be statistically insignificant. Using trypan blue exclusion, we were able to demonstrate non-toxicity towards healthy cells at significantly higher concentrations of our combinatorial therapy. Because hypoxic conditions are favorable for glycolytic metabolism and white blood cells have been showed to convert to aerobic glycolysis, the above experiment was repeated under hypoxia.

PHA-stimulated human PBMCs were treated with a combination of 0.147 µM, 58 mM, and 60 µM for 48 h, incubated at 1% $O_2$ and 5% $CO_2$. In the PHA-stimulated cells, viability was decreased by 14% compared to untreated control. We attribute this decrease in viability to the significantly high concentration of 2DG present in the combination. Under hypoxia and stimulated to divide, proliferation of PBMCs subsequently ramps up ATP production via glycolytic pathways, making them susceptible to glycolytic inhibition by 2DG. Most notably, 2DG is not used at this concentration in the clinical setting. Combined at EC50 and 2 times below EC50, 48 h treatment with our novel

combinatorial therapy had no effect on proliferating PBMCs, and absorbance readings were comparable to that of the control. At 25 µM, doxorubicin reduced PBMC viability significantly ($p<0.01$).

To gain insight into the mechanism of cell death and probe deeper into evaluating cytotoxicity, treated cells were analyzed with flow cytometry. Compared to untreated controls, both quiescent and PHA-stimulated PBMCs treated with our combinatorial therapy for 48 h showed no significant difference in cell death (ns, $p>0.05$). Conversely, both quiescent and PHA-stimulated immune cells suffered significant increases in cell death when treated with 25 µM doxorubicin for 48 h. We believe PHA-stimulated cells were more susceptible to doxorubicin due to the replicative targeting of this compound, which is evidenced by a greater degree of cell death in PHA-stimulated cells versus quiescent cells. Additionally, we attribute the ~20% AnnexinV+7AAD+ population of both quiescent and PHA-stimulated untreated PBMCs to the decrease in viability expected from thawed cells after 48 h incubation[133]. Nonetheless, we clearly demonstrate the non-toxicity of our novel combinatorial therapy towards immune cells and highlight the significant toxicity of a standard chemotherapy towards these cells.

In conclusion, our combinatorial therapy at 3 times higher than $EC_{50}$ showed no significant toxicity towards quiescent and PHA-stimulated human peripheral blood mononuclear cells under normoxia. Under hypoxia, PHA-stimulated cells demonstrated a slight decrease in viability, which we attribute to the glycolytic targeting of 2DG present in our combinatorial therapy at significantly high levels. It is important to note that 2DG has not been documented in use at the concentration that we have used in this study. Furthermore, we show that our combinatorial therapy does not induce cell death in

quiescent and proliferating immune cells compared to untreated controls. This discovery is significant, as we anticipate being able to circumvent bone marrow suppression in a clinical setting. The increased cell death caused by a conventional chemotherapy further signifies our work, as we are able to achieve high levels of effectiveness towards cancer cells without jeopardizing healthy immune cells. The substantial increase in concentration and resulting low toxicity gives us confidence in scaling up to achieve a clinically efficacious dose. Additionally, the effectiveness of our combinatorial therapy at such low doses suggests such a high dose will not be necessary to achieve cytotoxicity towards cancer cells *in vivo*. To conclude our preclinical evaluation of this novel combinatorial therapy, we will probe into the mechanism and immunogenicity of elicited cell death, as well as determine the effectiveness of the therapy against tumorspheres.

# CHAPTER 4: A NOVEL LOW-DOSE COMBINATORIAL THERAPY ELICITS IMMUNOGENIC CELL DEATH IN HUMAN AND MOUSE MAMMARY TUMOR CELLS

## 4.1 ABSTRACT

The effectiveness of anticancer therapies is generally understood as the ability to directly kill tumor cells and reduce tumor mass. Recently, however, additional focus has been given to the mechanism of cell death. Whereas apoptosis is immunologically "quiet," cell death via necrosis is accompanied by the release of danger signals that recruit and activate immune cells. In order for cell death to be characterized as immunogenic, three hallmarks must be present: translocation of ER-protein calreticulin to the surface of the plasma membrane, secretion of HMGB-1 from the nucleus to the extracellular environment, and ATP secretion from the dying cells. Neither apoptosis nor necrosis alone fulfill these requirements, therefore immunogenic cell death is classified as a hybrid of both processes. In this study, we gained insight into the mechanism of cell death after treatment with our novel combinatorial therapy, as well as assayed for the presence of key immunogenic cell death markers. Through flow cytometry, we observed varying stages of apoptosis as well as cell death in the 4-T1 and MCF-7 mammary tumor cell lines. Furthermore, through flow cytometry and ELISA, we found significantly increased levels of calreticulin surface expression, as well as secretion of HMGB-1 and ATP from dying tumor cells. We can conclude from these studies that our novel

combinatorial therapy has the potential to induce immunogenic cell death and prime a powerful adaptive immune response in addition to the direct killing of cancer cells.

## 4.2 INTRODUCTION

Eradicating cancer cells and preventing tumor relapse has been the goal of clinicians and researchers for centuries. In less aggressive tumor models, clinical practices have been successful in accomplishing this goal; however, for advanced cancers, a similar feat is much harder to achieve. Primarily due to the substantial growth of the primary tumor and spread of distal metastases, malignant cancers have very poor prognosis, and chemotherapeutic intervention frequently results in tumor relapse[134]. Accompanied by a high degree of abnormality and tissue damage, shouldn't the body innately recognize and remove these cancerous growths? Under normal physiological conditions, it does; by way of the immune system. Immune cells circulate throughout the body, conducting routine "surveillance" to identify and correct for any anomalies. If a cell were to experience DNA damage or irregularities in cell division, prompt corrective action would be taken by the immune system to eliminate the aberrant cells.

Supported by underlying genomic instability and mutation of tumor suppressor genes, cancer cells construct an immune barrier of anti-inflammatory immunosuppressive cells and cytokines, allowing them to circumvent immunosurveillance. The induced immunosuppression blocks cell-mediated responses to the cancer cells. Lack of an adaptive immune response hampers immunological memory, making it easier for a tumor to recur. Thus, a focus of all developing therapies should be to overcome immunosuppression and elicit a powerful, specific antitumor immune response. In the clinic, this is often achieved via immunogenic cell death.

Cell death following chemotherapy generally follows the mechanism of apoptosis or necrosis. In apoptosis, irreparable cellular stress activates the cleavage of caspase proteins that begin this proteolytic process. Often beginning with mitochondrial membrane permeabilization, programmed cell death is followed by autophagy and the formation of apoptotic blebs and debris[77]. Cellular debris is readily phagocytosed by surrounding macrophages and neighboring cells, resulting in absolute clearance of dead cell matter. Although an effective process, and a very important one under normal physiological conditions, the very "neatness" of this mechanism poses an issue in cancer treatment: it is non-immunogenic[135]. The rapid clearance and phagocytosis of apoptotic debris prevents immune cells such as dendritic cells from performing antigen processing and activating the immune system in response. While cell death is a favorable response elicited by anticancer agents, the non-immunogenicity of this mechanism makes them less effective in treating cancer and preventing its recurrence.

Conversely, the toxicity of certain classes of chemotherapy causes significant injury to the cancer cell, resulting in bypass of programmed cell death. The sporadic destruction of the cell is termed necrosis, as it differs from apoptotic pathways and is in fact highly immunogenic[136]. Toxic chemotherapy causes severe membrane instability, which leads to swelling and burst. Necrotic bursts release intracellular components and debris into the extracellular environment. The innate toxicity of this dead matter elicits an inflammatory immune response. While this is perceived as beneficial, it comes at a cost to surrounding tissue due to the build-up of cellular debris and potent immune reactions, causing sepsis and other harmful conditions[137].

Thus, to achieve maximum clinical efficacy, developing therapies should seek to induce a combination of apoptosis and necrosis. Effective clearance of dead cell debris and priming of a specific immune response is hence achieved by immunogenic cell death. Classified as a hybrid of apoptosis and necrosis, ICD is characterized by key molecular expression or secretions that aid in the activation of the immune system[138]. In early apoptosis, dying cells suffer from endoplasmic reticulum stress and dysfunction. This is followed by the translocation of ER-protein calreticulin to the surface of the plasma membrane[139]. Under normal physiological conditions in the ER, calreticulin serves as a regulator of gene transcription and has functions in calcium binding. Translocation to the plasma membrane, however, alters calreticulin function to an "eat me" signal directed towards phagocytic cells of the immune system[140]. Saturated with tumor neoantigens, dead cell phagocytosis by dendritic cells allows for antigen processing and presentation to effector T-cells, generating a specific, powerful cell-mediated response towards tumor cells[141]. Additionally, HMGB-1 secretion is often referred to as a hallmark of ICD[138]. HMGB-1 is found in the nucleus under normal physiological conditions, and functions as a chromatin-binding protein. Necrosis causes nuclear degradation and subsequent release of HMGB-1 into the extracellular space at the site of the tumor. Here, HMGB-1 acts as a powerful immune activator, as it has been shown to bind to Toll-like receptor 4 (TLR-4)[142]. This bond elicits several pro-inflammatory events. First, TLR-4 binding promotes dendritic cell activation and aids in antigen presentation to T-cells[143]. Furthermore, MyD88 gene transcription is upregulated as a result, blocking phagosome-lysosome fusion and promoting tumor antigen processing[142]. Thus, HMGB-1 plays a critical role in immune activation when it is secreted as a result of ICD. The third major indicator of

immunogenic cell death is ATP secretion from the dying cell. A fundamental mechanism of the apoptotic pathways is autophagy, during which cytoplasmic components are broken down along with other cellular organelles. As a result, the formation of the autophagasome-lysosome complex and interaction between lysosomal and plasma membranes facilitates ATP efflux from the cell[144]. Normally functioning as an energy molecule in the cell driving cellular processes, secreted ATP acts as a "find me" signal during ICD[145]. This newly uncovered chemokine function recruits dendritic cells and is often the first and most important step of immunogenic cell death. Once dendritic cell progenitors arrive at the site of cell death, HMGB-1 stimulates their maturity, and surface expression of calreticulin prompts dead cell phagocytosis and neoantigen processing. The result of ICD is a powerful, tumor cell-specific adaptive immune response, that is characterized by cell-mediated and memory mechanisms. Cytotoxic T cells are able to specifically target tumor cells for killing and infiltrate the TME, and antigen processing allows for immunological memory, which facilitates clonal selection and clonal expansion should the cancer recur. Thus, developing therapies should be evaluated for their ability to induce immunogenic cell death as opposed to conventional cell death mechanisms, as the priming of the immune system against cancerous cells has lasting implications in host defense against tumor relapse.

## 4.3 BACKGROUND AND SIGNIFICANCE

An underappreciated facet of effective anticancer therapy is the induction of immunogenic cell death. During the drug development process, compounds are analyzed closely for their cytotoxic effects towards cancer cells and non-toxicity towards healthy cells. Amidst a wide array of pharmacokinetic and pharmacodynamic studies little

attention is given to ICD, despite its profound benefit and implications. To kill the cancer cell and simultaneously invoke a specific adaptive immune response is invaluable to cancer therapy, and hence why our study focuses on its elicitation.

Methotrexate, a component of our novel drug combination, is a folic acid antagonist that inhibits DHFR function and subsequent inhibition of cell death leading to cell death. This pharmacological targeting of nucleotide synthesis causes elevated levels of cellular stress, which triggers intrinsic and extrinsic apoptotic pathway signaling. 2-deoxyglucose, another component of our novel drug combination, is a glycolytic inhibitor that competitively inhibits hexokinase function, impairing glucose metabolism resulting in cell death. Additionally, interference of 2DG with N-glycosylation leads to the unfolded protein response (UPR) in the ER, resulting in cell death[96]. Remarkably, 2DG has been shown to induce both apoptosis and necrosis due to its multi-pathway targeting mechanism of action. Rapid ATP depletion and ER dysfunction as a result of 2DG treatment led to necrotic death of cancer cells *in vitro* and tumor regression *in vivo*, as well as early and late stage apoptosis in multiple cancer cell lines[146,147]. Wogonin, the final component of our novel drug combination, has been shown to increases the expression of *Bax*, a potent pro-apoptotic protein necessary for procaspase activation and induction of apoptotic cell death[128].

In combination, MTX, 2DG, and WGN has demonstrated marked cytotoxicity towards cancer cells with limited toxicity towards normal rapidly proliferating cells of the immune system. The significance of the present study is to determine whether the cytotoxic effects of our novel combinatorial therapy elicits an immunogenic cell death response. Each compound individually induces high levels of cellular stress, and we

anticipate significant release of danger-associated molecular patterns post-treatment. Immunogenic cell death is classified as a hybrid of apoptosis and necrosis and characterized by three major hallmarks: calreticulin surface expression, HMGB-1 secretion, and ATP secretion. The chemoattraction of immune precursors and subsequent activation and phagocytosis promotion facilitated by these ICD markers generates a primed adaptive immune response towards the cancer cells. With great effectiveness against cancer cells and no effect on proliferating immune cells, induction of ICD by our novel combinatorial therapy would solidify it as a leading prospect in developing anticancer therapies.

## 4.4 METHODS

### *4.4.1 Cell culturing and maintenance*

The 4-T1 (Mouse Metastatic Mammary Carcinoma) cell line was kindly donated by Dr. Vijaya Iragavarapu-Charyulu, Department of Biomedical Sciences, Florida Atlantic University. The MCF-7 (Human Metastatic Mammary Tumor) cell line was obtained from Dr. James X. Hartmann, Department of Biological Sciences, Florida Atlantic University. Cells were cultured between $2\times10^5$/mL and $1\times10^6$/mL in 75 $cm^2$ Falcon cell culture flaks containing Gibco RPMI 1640-L-Glutamine medium (Life Technologies-Grand Island, NY, USA) supplemented with 10% fetal bovine serum (Life Technologies-Grand Island, NY, USA) and 100U/mL Gibco Pen Strep (Life Technologies- Grand Island, NY, USA). Cell cultures were incubated at 37 °C under 5% $CO_2$ in a humidified atmosphere.

*4.4.2 Flow cytometry for CLRT-surface expression*

A Guava easyCyte flow cytometer with InCyte software (EMD Millipore, USA), was used to analyze calreticulin surface expression in dying tumor cells. 4-T1 and MCF-7 cells cultured independently ($1\times10^6$ cells/tube) were treated with our novel combinatorial therapy. At 0 h, 1.5 h, and 3 h time points, cells were centrifuged and resuspended in ice-cold PBS, 10% FCS, 1% sodium azide (Abcam, USA). 0.01 μg/mL of conjugated anti-calreticulin antibody was added to the reaction tube. Reaction tubes were gently mixed and incubated for 30 min at RT in the dark. Cells were washed 3 times and finally resuspended in 500 μL of ice-cold PBS, 10% FCS, 1% sodium azide. Samples were then read by flow cytometry and analyzed with FlowJo v9 software. Trypan blue exclusion was performed on all samples to ensure comparable viability to control.

*4.4.3 HMGB-1 ELISA*

The human HMGB1 ELISA kit (Tecan Trading AG, Switzerland) was used to measure the levels of HMGB-1 in treated tumor cell supernatant. 4-T1 and MCF-7 cells were seeded independently in flat-bottom 96 well plates ($1 \times 10^4$ cells/mL) and treated with our novel combinatorial therapy. An additional experimental group of cells was treated with 25 μM of the known ICD-inducer doxorubicin as a positive control. 24 h post-treatment, cells were centrifuged for 20 min at 1000×g and supernatant was harvested. Absorbance readings were taken in an Epoch microplate reader at 450 nm. Computed data was compared to untreated and normalized cells as well as a standard curve.

*4.4.3 ATP Assay*

The ATP Colorimetric/Fluorometric Assay Kit (Sigma-Aldrich, USA) was used to measure the levels of ATP secretion in treated tumor cell supernatant. 4-T1 and MCF-7

cells cultured independently were seeded in flat-bottom 96 well plates ($1 \times 10^4$ cells/mL) and treated with our novel combinatorial therapy. An experimental group of cells was treated with 25 µM of the known ICD-inducer doxorubicin as a positive control. 24 h post-treatment, cells were centrifuged for 20 min at 1000×g and supernatant was harvested. Fluorescence intensity unit readings were taken in a fluorescent microplate reader at λex = 535/λem = 587 nm. Computed data was compared to untreated and normalized cells as well as a standard curve.

*4.4.4 Trypan blue exclusion cell count and viability assay*

After the supernatant was extracted for analysis of the above studies, the resulting cell pellet was resuspended in 100 µL of complete RPMI 1640 cell culture media. 10 µL of 0.4% trypan blue was mixed with 10 µL of cell suspension in a 96-well plate well and incubated for 2 minutes at room temperature. 10 µL of the 0.4% trypan blue/cell suspension mixture was loaded onto a hemacytometer, and stained vs unstained cells were counted. The percentage of viable cells was calculated using the formula:

$$\%\, Viability = \frac{total\ number\ of\ unstained\ cells}{total\ number\ of\ stained\ and\ unstained\ cells}\ x\ 100$$

*4.4.5 Flow cytometry*

A Guava easyCyte flow cytometer with InCyte software (EMD Millipore, USA), was used to determine PBMC viability. Quiescent and PHA-stimulated PBMCs were treated with our novel combinatorial therapy for 48 h. After 48 h, cells were centrifuged and resuspended in 1X Annexin V binding buffer solution (BD Pharmingen, USA). 100 µL of cell suspension was transferred to a 5 mL reaction tube. 5 µL of Annexin V-FITC apoptosis detection dye (BD Pharmingen, USA) was added to the reaction tube. 10 µL of

7-AAD (BD Pharmingen, USA) nucleic acid staining dye was added to the 5 mL reaction tube. Reaction tubes were gently mixed and incubated for 15 min at RT. 400 µL of 1X binding buffer was added after incubation. Samples were then read by flow cytometry and analyzed with FlowJo v9 software. Annexin V+ and 7-AAD+ populations of treated cells were compared to Annexin V+ and 7-AAD + populations of untreated and normalized cells.

*4.4.5 Statistical analysis*

GraphPad Prism v8 software was used for statistical analyses. Data is presented as mean ± s.d. t-test was used to determine statistical significance between groups for normally distributed data. For all tests, *$p<0.05$ was considered significant. Experiments and measurements were performed in triplicate as indicated. Graphed data depicts means of triplicates ± s.e.m. and are representative of three experiments.

## 4.5 RESULTS

### 4.5.1 Low-dose MTX, 2DG, and WGN combinatorial therapy induces apoptosis and cell death in human mammary adenocarcinoma and mouse mammary carcinoma cells.

In the present study, human and mouse mammary tumor cells were treated with our novel combinatorial therapy and analyzed at different time points to gain insight into the mechanism of cell death and study the progression of cell death over time. While the hallmarks of immunogenic cell death are defined as surface expression or secretion of specific molecules, the overall process is characterized as a hybrid of apoptotic and necrotic mechanisms. In this study, we seek to evaluate the degree to which treatment

with our novel combinatorial therapy induces cell death in order to later evaluate the presence of specific ICD makers.

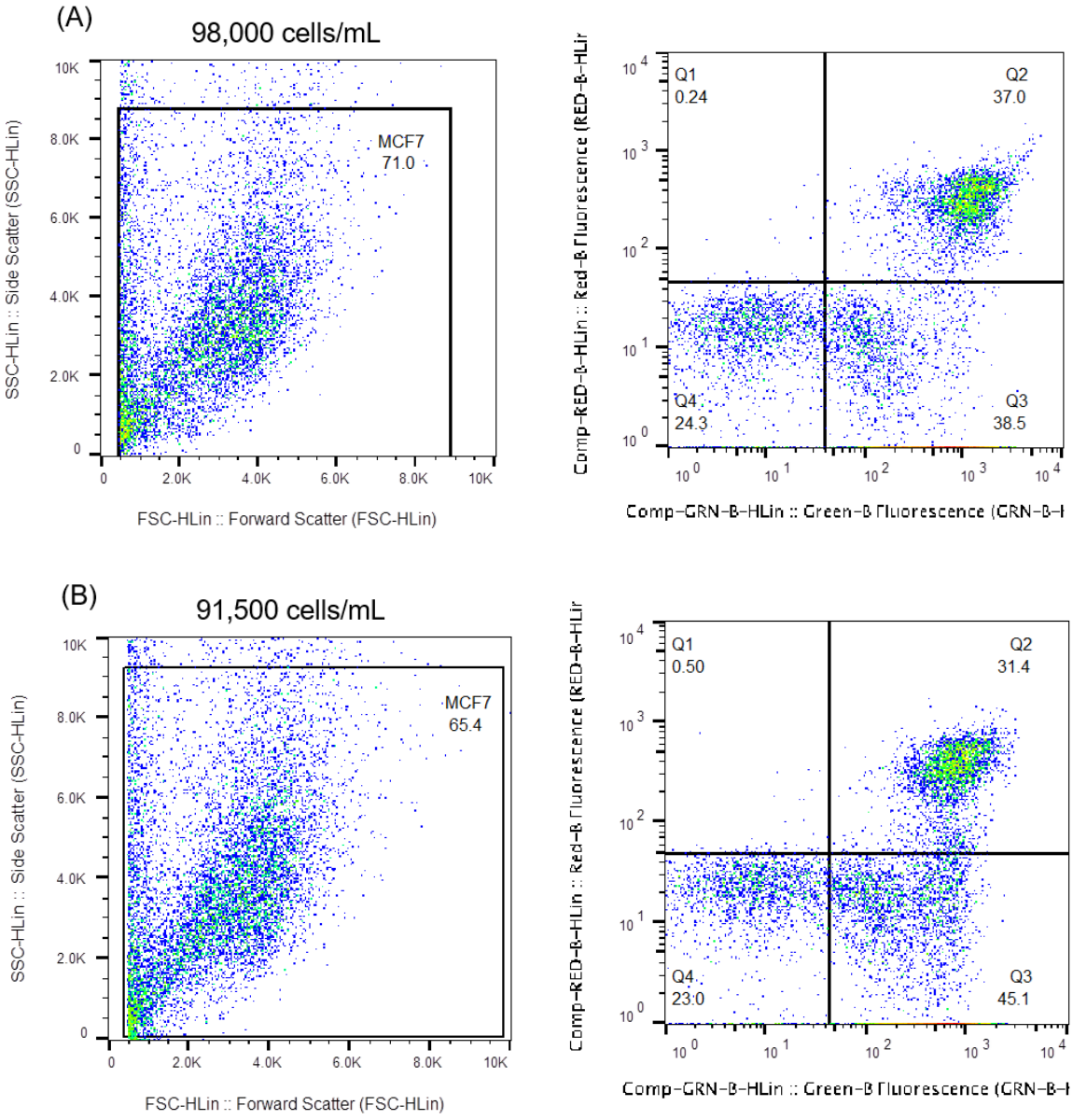

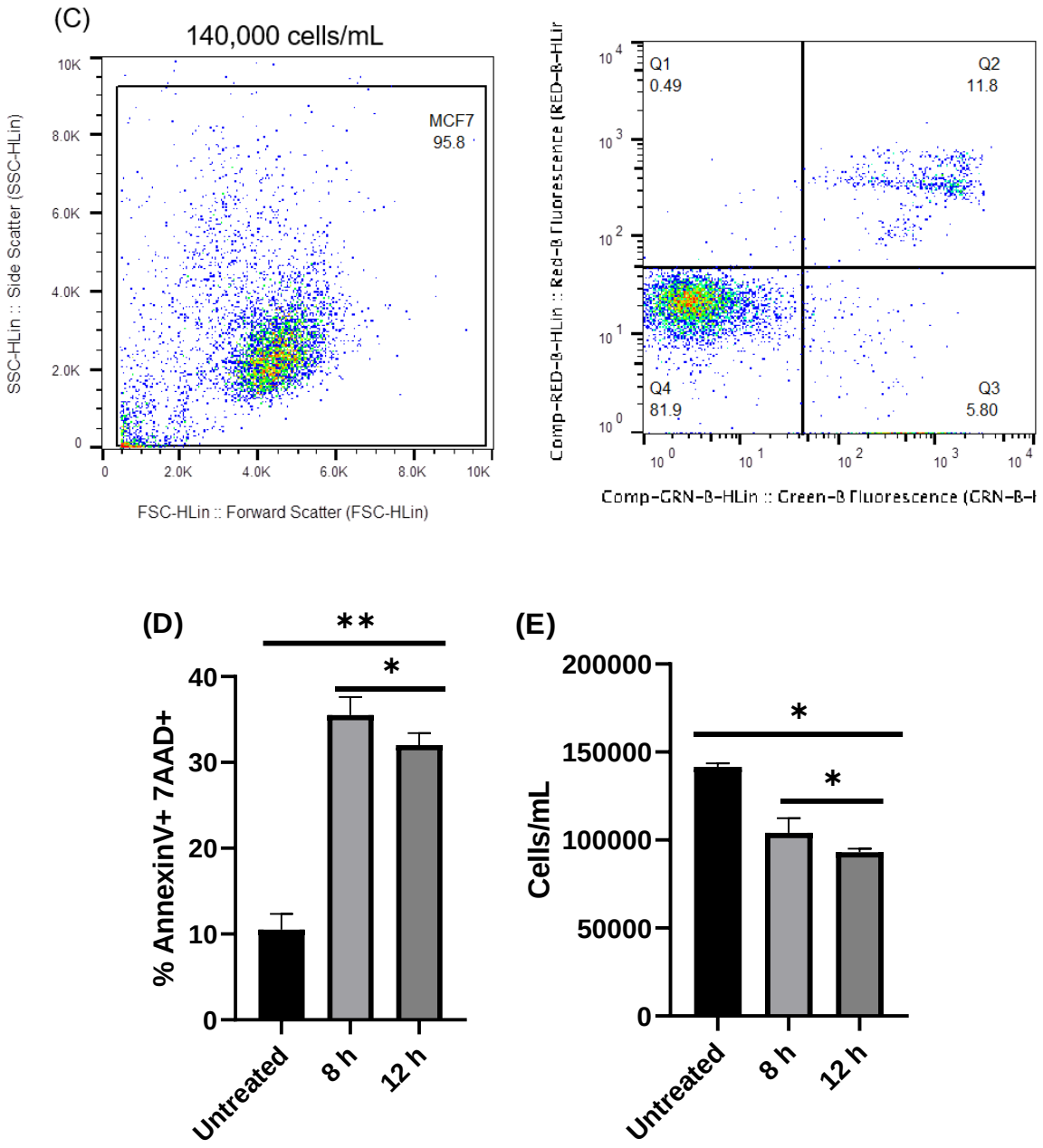


**Figure 41. Our novel combinatorial therapy induces apoptosis and cell death in human mammary adenocarcinoma cells.** MCF-7 cells were treated with our novel combinatorial therapy for 8 h **(A)** 12 h **(B)** or left untreated for 12 h **(C)** and dot plots of AnnexinV and 7AAD staining were obtained from flow cytometry. The lower right quadrant (Annexin V+/7AAD-) reflects cells at varying stages of apoptosis, while the upper right quadrant (Annexin V+/7AAD+) indicates cells that are dead. The percentage of cell death was significant in both the 8 h and 12 treatment groups with respect to untreated control **(D)**. Cell number was significantly reduced after 12 h compared to 8 h with treatment **(E)**. Cell counts were determined via trypan blue exclusion. Dot plots are representative of a typical experiment out of two independent ones. Bars represent the average of duplicate experiments ± s.e.m. (ns= not significant, $p>0.05$, *= $p<0.05$, **= $p<0.01$).

After 8 h of treatment, MCF-7 cells were 37.0% AnnexinV+7AAD+ (Figure 41A). After 12 h of treatment with our combinatorial therapy, MCF-7 cells were 31.4% AnnexinV+7AAD+ (Figure 41B). Importantly, we found a significant decrease in cell number between the 8 h and 12 h treatment groups determined by trypan blue exclusion, which we attribute to the increasing number of dead cells and apoptotic debris. The FSC vs SSC dot plot depicts high levels of apoptotic debris in the population, evidenced by region 1 on the left side of the plot, where low FS values are indicative of apoptotic blebs. Last, untreated cells were 11.8% AnnexinV+7AAD+ after 12 h and 81.9% were AnnexinV-7AAD-, that is alive, after 12 h (Figure 41C).

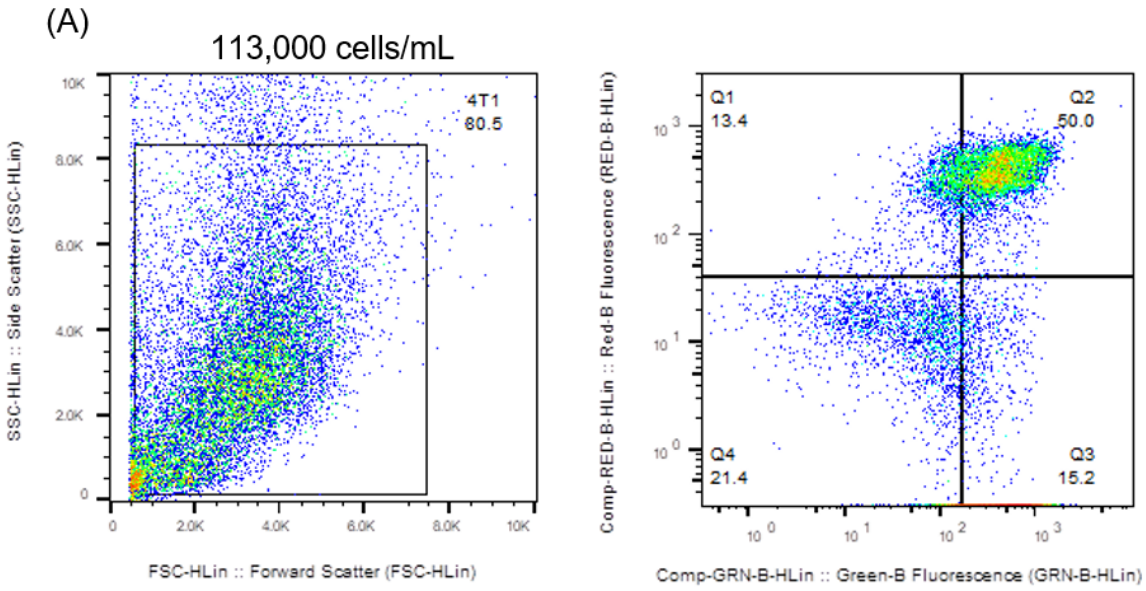

(B)

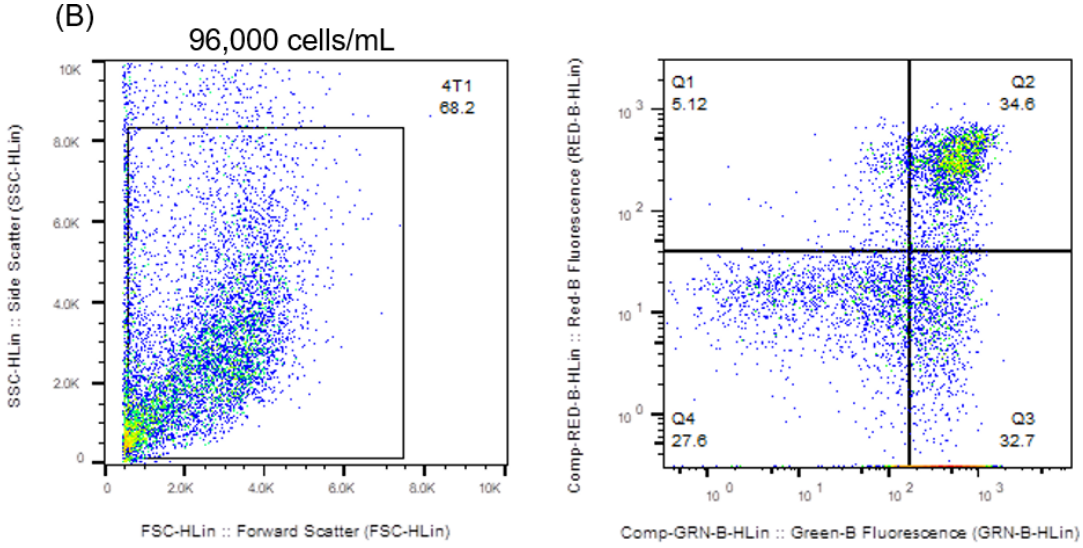
96,000 cells/mL
4T1
68.2
SSC-HLin :: Side Scatter (SSC-HLin)
FSC-HLin :: Forward Scatter (FSC-HLin)
Q1
5.12
Q2
34.6
Q4
27.6
Q3
32.7
Comp-RED-B-HLin :: Red-B Fluorescence (RED-B-HLin)
Comp-GRN-B-HLin :: Green-B Fluorescence (GRN-B-HLin)

(C)

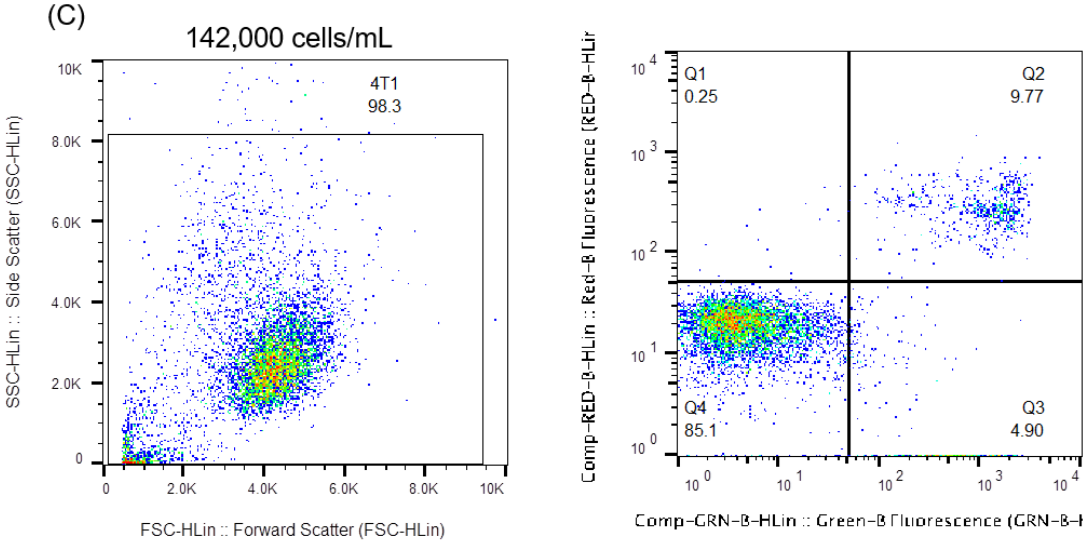
142,000 cells/mL
4T1
98.3
SSC-HLin :: Side Scatter (SSC-HLin)
FSC-HLin :: Forward Scatter (FSC-HLin)
Q1
0.25
Q2
9.77
Q4
85.1
Q3
4.90
Comp-RED-B-HLin :: Red-B Fluorescence (RED-B-HLin)
Comp-GRN-B-HLin :: Green-B Fluorescence (GRN-B-HLin)

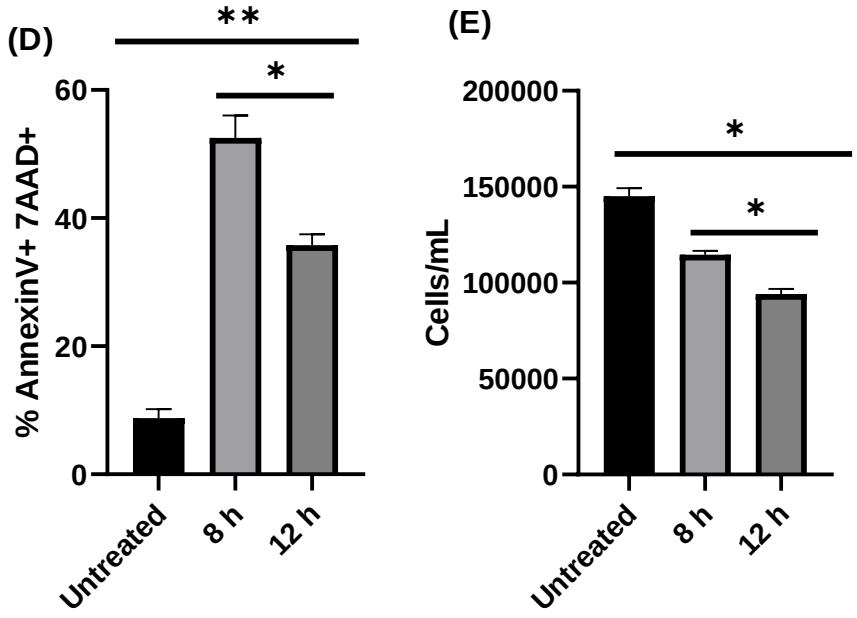


**Figure 42. Our novel combinatorial therapy induces apoptosis and cell death in mouse mammary carcinoma cells.** 4-T1 cells were treated with our novel combinatorial therapy for 8 h **(A)** 12 h **(B)** or left untreated for 12 h **(C)** and dot plots of AnnexinV and 7AAD staining were obtained from flow cytometry. The lower right quadrant (AnnexinV+/7AAD-) reflects cells at varying stages of apoptosis, while the upper right quadrant (AnnexinV+/7AAD+) indicates cells that are dead. The percentage of cell death was significant in both the 8 h and 12 treatment groups with respect to untreated control **(D)**. Cell number was significantly reduced after 12 h compared to 8 h with treatment **(E)**. Cell counts were determined via trypan blue exclusion. Dot plots are representative of a typical experiment out of two independent ones. Bars represent the average of duplicate experiments ± s.e.m. (ns= not significant, $p>0.05$, *= $p<0.05$, **= $p<0.01$).

After 8 h of treatment, 4-T1 cells were 50.0% AnnexinV+7AAD+ (Figure 42A). After 12 h of treatment with our combinatorial therapy, 4-T1 cells were 34.6% AnnexinV+7AAD+ (Figure 42B). We found a significant decrease in cell number between the 8 h and 12 h treatment groups determined by trypan blue exclusion, which we attribute to the increasing number of dead cells and apoptotic debris. The FSC vs SSC dot plot depicts high levels of apoptotic debris in the population, evidenced by region 1 on the left side of the plot, where low FS values are indicative of apoptotic blebs. Last, untreated cells were 9.7% AnnexinV+7AAD+ and 85.1% were AnnexinV-7AAD- after 12 h (Figure 42C).

### 4.5.2 Low-dose MTX, 2DG, and WGN combinatorial therapy induces translocation of ER-protein calreticulin to the plasma membrane in human mammary adenocarcinoma and mouse mammary carcinoma cells.

In the present study, we evaluated the surface expression of a hallmarking immunogenic cell death marker: calreticulin. Under normal physiological conditions, this calcium-binding protein is found in high concentrations in the lumen of the ER[148]. However high levels of cellular stress usually invoked by drug treatment cause a unique phenomenon to occur; the translocation of this ER-protein to the plasma membrane. In the extracellular domain, calreticulin's function drives antigen presentation and immune activation[149]. Surface-expressed calreticulin functions primarily as an "eat me" signal that stimulates surrounding immune cells to phagocytose the pre-apoptotic cells. This process promotes antigen processing and increases antigen presentation to effector cells[140]. The nature of this unique process is pre-apoptotic, thus the current study evaluates calreticulin surface expression at 1.5 h and 3 h post-treatment, only when treated cell viability was comparable to that of untreated control cells. Furthermore, to highlight the significant effects of our novel combinatorial therapy, an additional group of cells were treated with doxorubicin alone. Doxorubicin, an anthracycline, is one of the most commonly used breast cancer chemotherapies and is characterized by researchers as a known-inducer of immunogenic cell death[150]. The literature records high levels of immunogenic cell death in doxorubicin treated cells at a concentration of 25 μM, which we mimicked for the purposes of this study[151]. Here, we evaluate the ability of our novel combinatorial therapy to induce calreticulin translocation to the plasma membrane compared to untreated cells and cells treated with a known immunogenic cell death inducer.

MCF-7 cells were treated with our novel combinatorial therapy or 25 μM doxorubicin for 3 h, and then directly stained with conjugated rabbit monoclonal antibody to calreticulin to evaluate the surface expression of calreticulin. Treated and control cell viability was analyzed at each time point to ensure all groups had similar viability and that cell death was excluded. Untreated MCF-7 cells were analyzed at 0 h to serve as a reference. At 1.5 h, MCF-7 cells treated with our novel combinatorial therapy were 95.3% positive (+) for calreticulin surface expression (Figure 43). Viability of treated cells and control cells were both 93% at 1.5 h (Figure 45A). At 3 h, MCF-7 cells treated with our novel combinatorial therapy were 95.6% positive (+) for calreticulin surface expression. Cells treated with 25 μM doxorubicin were 96.4% positive (+) for calreticulin surface expression after 3 h. Untreated control cells were 4.3% positive (+) for calreticulin surface expression (Figure 44). Viability of treated and control cells was 93% after 3 h (Figure 45B). Treatment with our combinatorial therapy and doxorubicin induced calreticulin translocation to the plasma membrane ($p<0.001$).

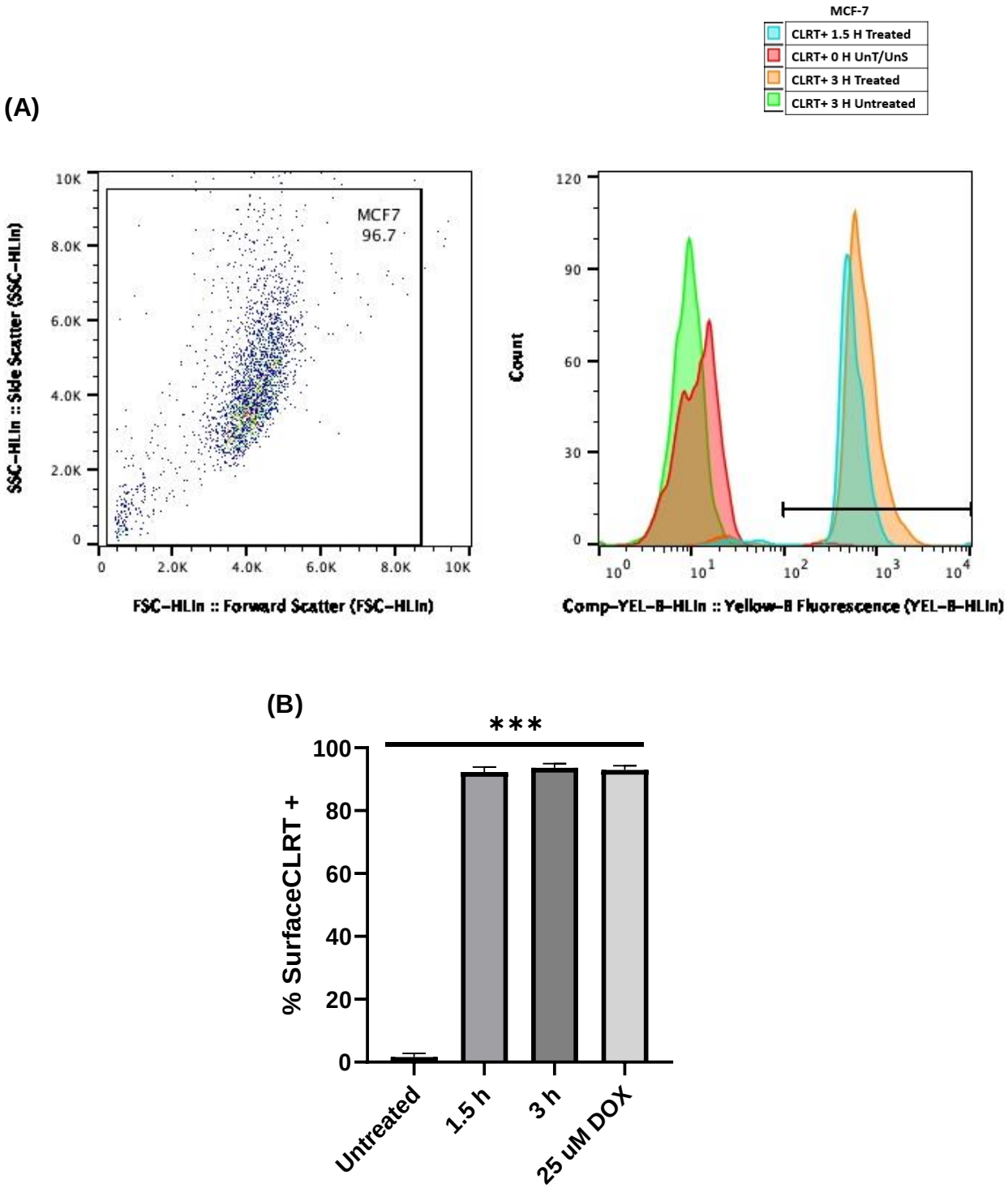


**Figure 43. Our novel combinatorial therapy induces translocation of calreticulin from the ER to the plasma membrane in human mammary adenocarcinoma cells.** Colored peaks show change in CLRT surface expression in MCF-7 cells 0 h, 1.5 h, and 3 h post treatment **(A)**. % Surface CLRT+ cells are shown for 3 h untreated, 1.5 and 3 h combination treatment, and 3 h 25 µM DOX treated **(B)**. Graphs are

representative of a typical experiment out of two independent ones. Bars represent the average of duplicate experiments ± s.e.m. (***= p<0.001).

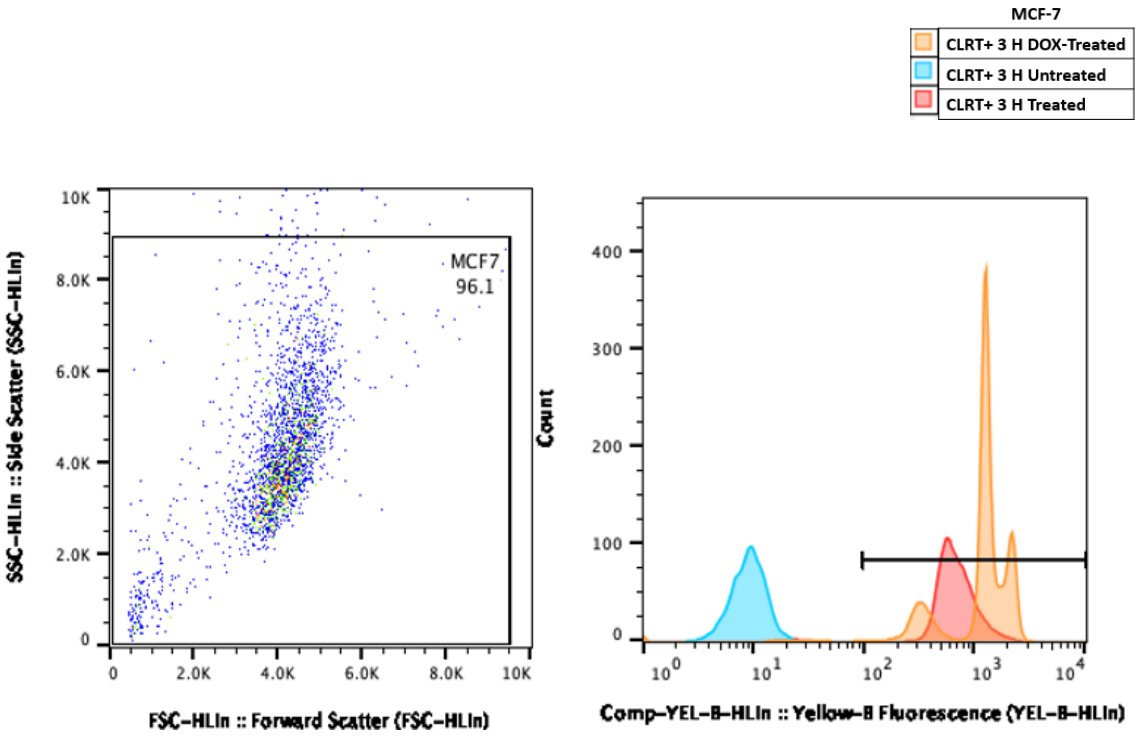


**Figure 44. Our novel combinatorial therapy induces translocation of calreticulin from the ER to the plasma membrane similar to known ICD-inducer doxorubicin in human mammary adenocarcinoma cells.** Colored peaks show difference in CLRT surface expression in untreated, combinatorial therapy treated, and doxorubicin treated MCF-7 cells at 3 h post treatment. Graphs are representative of a typical experiment out of two independent ones.

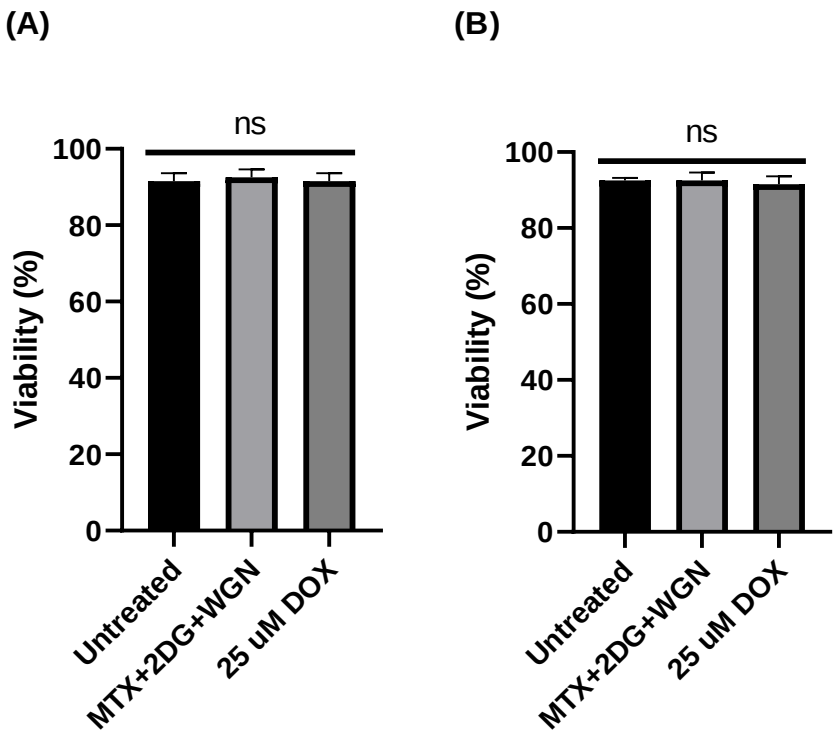


**Figure 45. MCF-7 treated and untreated cell viability at 1.5 h (A) and 3 h (B).** Cell viability was analyzed via trypan blue exclusion at each time point to ensure treated cell and control cell viabilities were comparable. Bars represent the averages of triplicate determinations ± s.e.m. in two separate experiments.

4-T1 cells were treated with our novel combinatorial therapy or 25 µM doxorubicin for 3 h, and then directly stained with conjugated rabbit monoclonal antibody to calreticulin to evaluate the surface expression of calreticulin. Treated and control cell viability was analyzed at each time point to ensure all groups had similar viability and that cell death was excluded. Untreated 4-T1 cells were analyzed at 0 h to serve as a reference. At 1.5 h, 4-T1 cells treated with our novel combinatorial therapy were 84.0% positive (+) for calreticulin surface expression (Figure 46). Viability of treated cells and control cells were both 90% at 1.5 h (Figure 48A). At 3 h, 4-T1 cells treated with our novel combinatorial therapy were 78.3% positive (+) for calreticulin surface expression. Cells treated with 25 µM doxorubicin were 77.6% positive (+) for

calreticulin surface expression after 3 h. Untreated control cells were 2.7% positive (+) for calreticulin surface expression (Figure 47). Viability of treated and control cells was 90% after 3 h (Figure 48B). Treatment with our combinatorial therapy and doxorubicin induced calreticulin translocation to the plasma membrane.

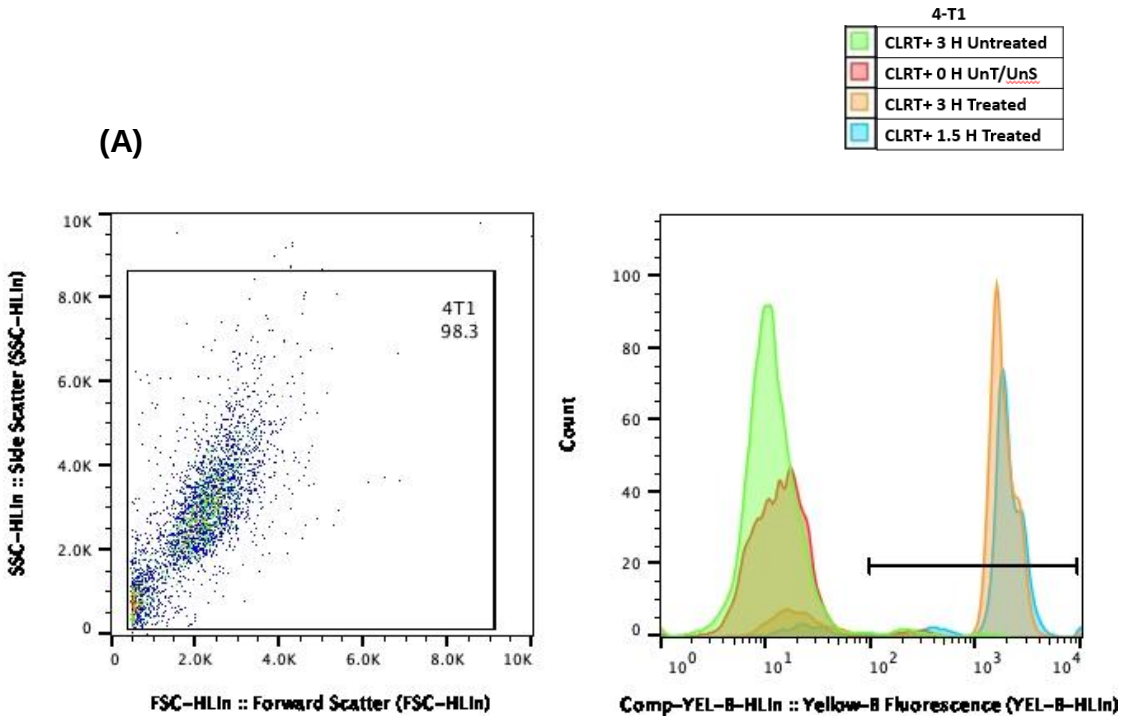

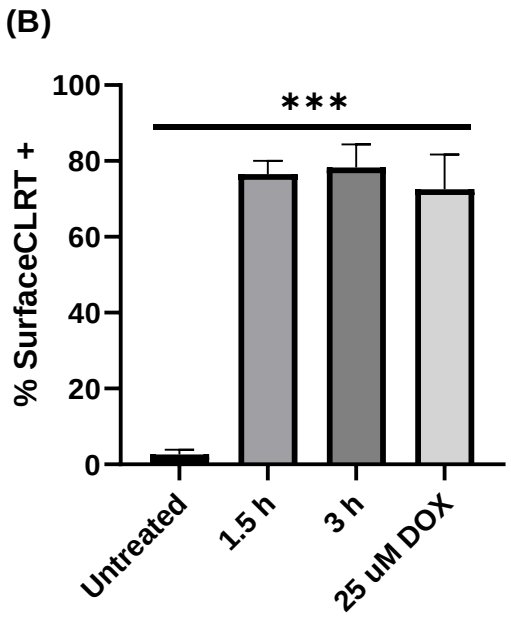


**Figure 46. Our novel combinatorial therapy induces translocation of calreticulin from the ER to the plasma membrane in mouse mammary carcinoma cells.** Colored peaks show change in CLRT surface expression in 4-T1 cells 0 h, 1.5 h, and 3 h post treatment **(A)**. % Surface CLRT+ cells are shown for 3 h untreated, 1.5 and 3 h combination treatment, and 3 h 25 µM DOX treated **(B)**. Graphs are representative of a typical experiment out of two independent ones. Bars represent the average of duplicate experiments ± s.e.m. (***= $p<0.001$).

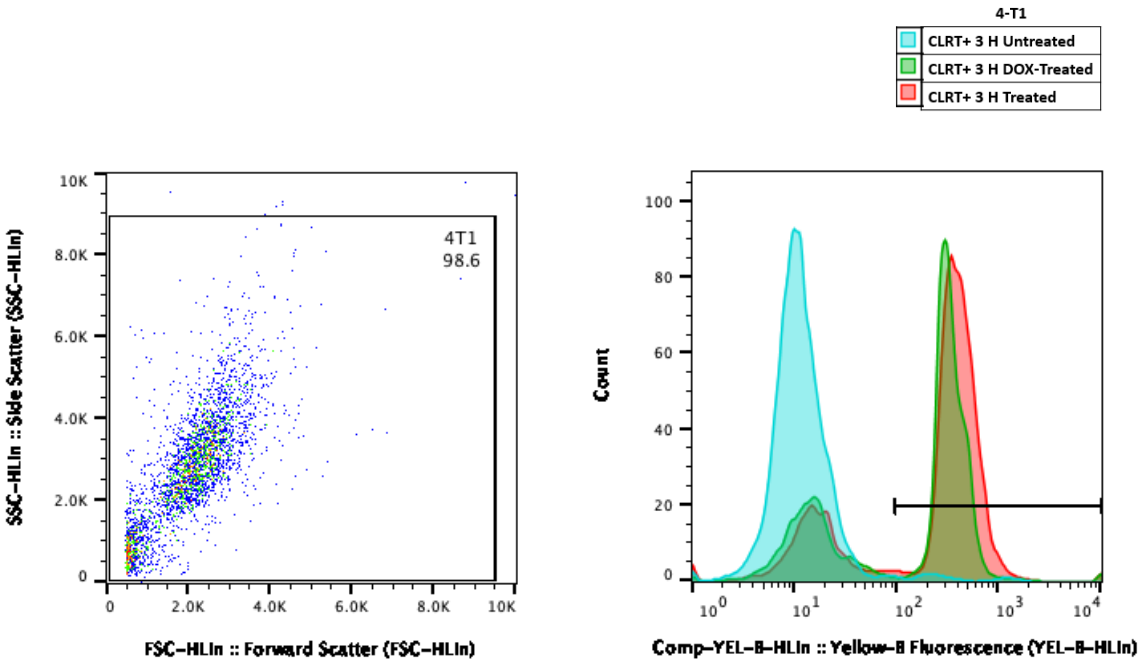


**Figure 47. Our novel combinatorial therapy induces translocation of calreticulin from the ER to the plasma membrane similar to known ICD-inducer doxorubicin in mouse mammary carcinoma cells.** Colored peaks show difference in CLRT surface expression in untreated, combinatorial therapy treated, and doxorubicin treated MCF-7 cells at 3 h post treatment. Graphs are representative of a typical experiment out of two independent ones.

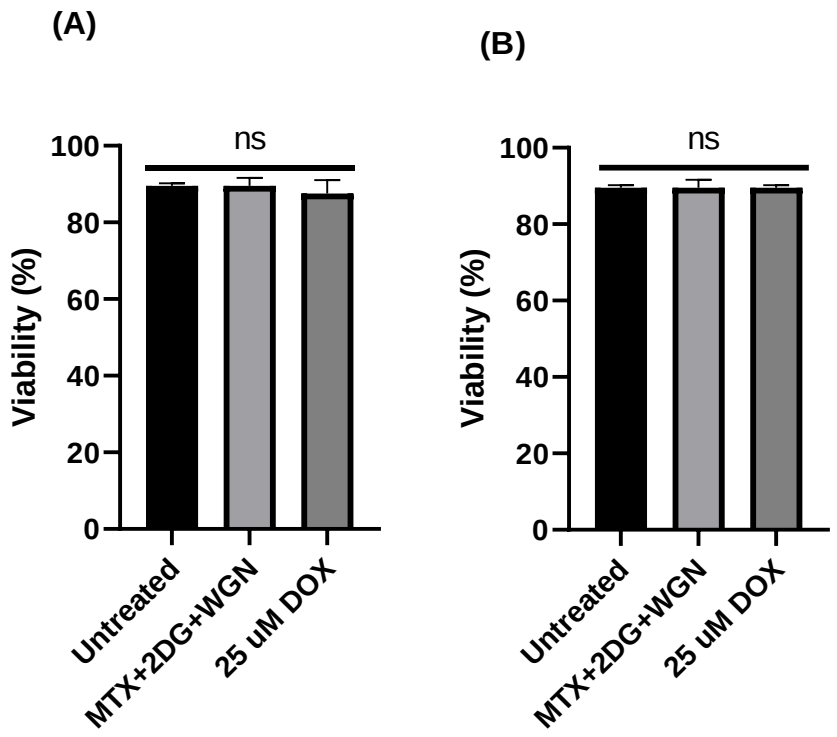


**Figure 48. 4-T1 treated and untreated cell viability at 1.5 h (A) and 3 h (B).** Cell viability was analyzed via trypan blue exclusion at each time point to ensure treated cell and control cell viabilities were comparable. Bars represent the averages of triplicate determinations ± s.e.m. in two separate experiments.

### 4.5.3 Low-dose MTX, 2DG, and WGN combinatorial therapy is more effective than doxorubicin at inducing ATP secretion in human mammary adenocarcinoma and mouse mammary carcinoma cells.

In the present study, secretion of a key immunogenic cell death marker was evaluated after 24 h treatment with our novel combinatorial therapy in two mammary tumor cell lines. ATP is the fuel source of countless cellular processes, however in immunogenic cell death, functions as a potent "find me" signal for circulating antigen-presenting cell progenitors[144]. Under normal physiological conditions, programmed cell death leads to lower levels of intracellular ATP however ATP is not secreted, rather contained in apoptotic blebs[70]. The high degree of cell stress in immunogenic cell death

promotes lysosome-plasma membrane interactions that facilitate the secretion of ATP[144]. Chemoattraction of premature dendritic cells to the site of cell death promotes interactions with DAMPs and subsequent activation of these cells, the primary steps of an active immune response[138]. In this study, we evaluate the ability of our novel combinatorial therapy to induce ATP secretion, as well as compare these levels to those induced by treatment with the standard chemotherapy doxorubicin.

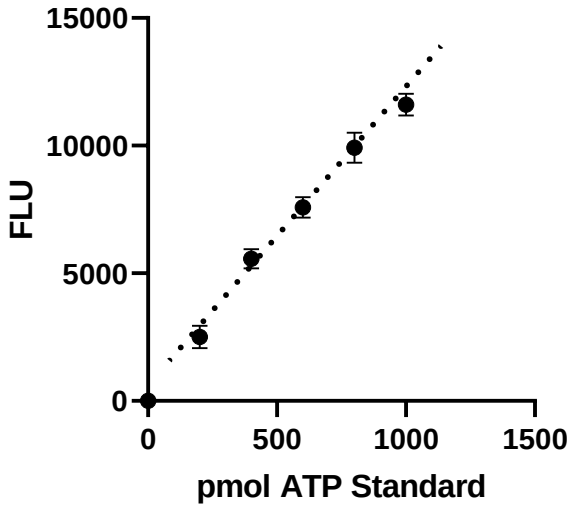


**Figure 49. A standard curve reflecting known concentrations of ATP and corresponding fluorescence intensity units (FLU).** Standard wells containing 1000, 800, 600, 400, 200 and 0 pmol ATP were created to formulate a standard curve and associated FLU value. Plotted points represent the averages of duplicate determinations ± s.e.m. in four separate experiments.

In the human breast carcinoma cell line, MCF-7, cells were treated with our novel combinatorial therapy at 6 times below their respective $EC_{50}$. A second experimental group was also treated with 25 μM doxorubicin, an effective *in vitro* dose that was shown to induce immunogenic cell death and increased levels of extracellular ATP[152]. A standard curve was created using known concentrations of ATP and corresponding these molar concentrations to flourometric intensity unit values (Figure 49). Two blanks, a reaction mixture blank and sample blank, were utilized to correct for any background in the

sample and provide an accurate flourometric reading. After subtracting blanks, the raw experimental data was compared to values of the standard curve to calculate the concentration of extracellular ATP. After 24 h treatment with our novel combinatorial therapy, extracellular ATP was found present at a concentration of 7.2 ng/µl. After 24 h treatment with 25 µM doxorubicin, extracellular ATP was found present at a concentration of 3.1 ng/µl. In untreated controls, extracellular ATP was found present at a concentration of 1.3 ng/µl. Compared to doxorubicin, our novel combinatorial therapy induced significantly higher levels of ATP secretion ($p<0.01$). Furthermore, cells were analyzed for viability using trypan blue exclusion (Figure 50B). After 24 h, cells treated with the combinatorial therapy were 29% viable, significantly lower compared to untreated control cell viability ($p<0.01$). Cells treated with 25 µM doxorubicin for 24 h were 42% viable, significantly lower compared to untreated control cell viability ($p<0.01$). Untreated cells were 89% viable after 24 h.

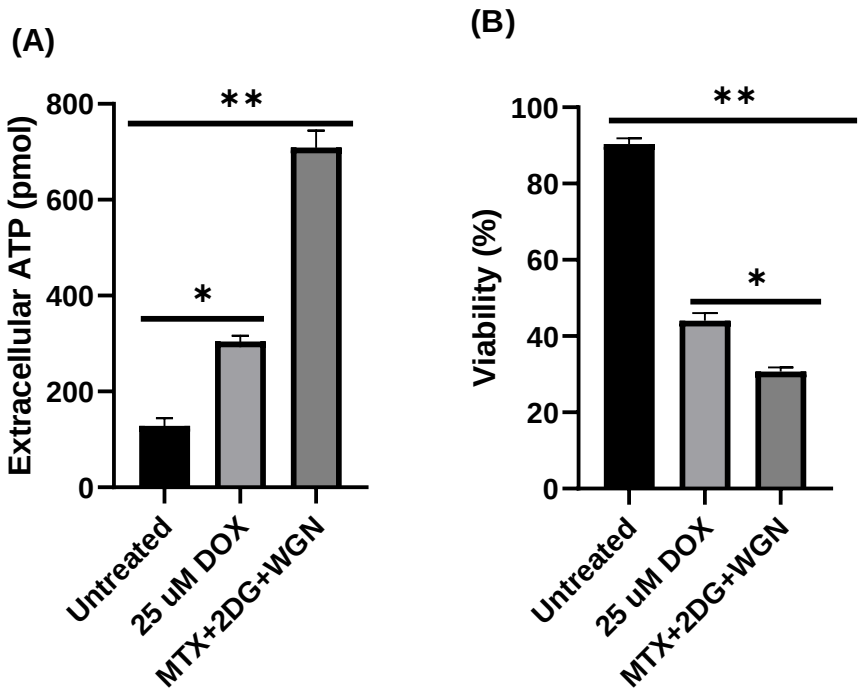


**Figure 50. A combination of three non-mutagenic drugs at combinations 6 times below their $EC_{50}$ is more effective than conventional chemotherapy doxorubicin at inducing ATP release from dying tumor cells.** Treated and untreated cell supernatants were harvested and analyzed with a fluorescent plate reader. Fluorescence intensity unit values were compared to a standard curve to determine extracellular ATP levels. Viability of treated cells was also determined via trypan blue exclusion. Bars represent the average of triplicate experiments ± s.e.m. (*=$p<0.05$, **= $p<0.01$).

In the mouse mammary carcinoma cell line, 4-T1, cells were treated with our novel combinatorial therapy at 6 times below their respective $EC_{50}$. A second experimental group was also treated with 25 µM doxorubicin. Similarly, two blanks, a reaction mixture and sample blank, were utilized to correct for any background in the sample and provide an accurate flourometric reading. After subtracting blanks, the raw experimental data was compared to values of the standard curve to calculate the concentration of extracellular ATP. After 24 h treatment with our novel combinatorial therapy, extracellular ATP was found present at a concentration of 6.5 ng/µl. After 24 h treatment with 25 µM doxorubicin, extracellular ATP was found present at a concentration of 2.8 ng/µl. In untreated controls, extracellular ATP was found present at

a concentration of 1.4 ng/µl. Compared to doxorubicin, our novel combinatorial therapy induced significantly higher levels of ATP secretion ($p<0.01$). Furthermore, cells were analyzed for viability using trypan blue exclusion (Figure 51B). After 24 h, cells treated with the combinatorial therapy were 36% viable, significantly lower compared to untreated control cell viability ($p<0.01$). Cells treated with 25 µM doxorubicin for 24 h were 54% viable, significantly lower compared to untreated control cell viability ($p<0.01$). Untreated cells were 92% viable after 24 h.

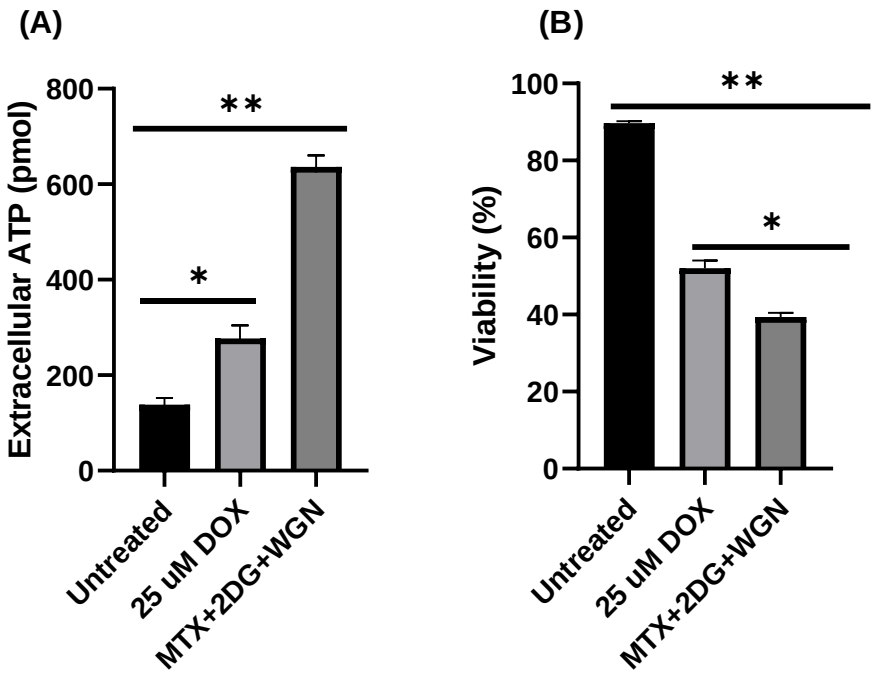


**Figure 51. A combination of three non-mutagenic drugs at combinations 6 times below their $EC_{50}$ is more effective than conventional chemotherapy doxorubicin at inducing ATP release from dying tumor cells.** Treated and untreated cell supernatants were harvested and analyzed with a fluorescent plate reader. Fluorescence intensity unit values were compared to a standard curve to determine extracellular ATP levels. Viability of treated cells was also determined via trypan blue exclusion. Bars represent the average of triplicate experiments ± s.e.m. (*=$p<0.05$, **= $p<0.01$).

### 4.5.4 Low-dose MTX, 2DG, and WGN combinatorial therapy is more effective than doxorubicin at inducing HMGB-1 release in human mammary adenocarcinoma and mouse mammary carcinoma cells.

In the present study, release of a key immunogenic cell death marker was evaluated after 24 h treatment with our novel combinatorial therapy in two mammary tumor cell lines. Endogenous HMGB-1 is a chromatin-binding protein that has profound function in DNA remodeling and in turn transcription[153]. Found in the nucleus, the only avenue for this protein to the extracellular space is through nuclear membrane and plasma membrane disintegration; characteristics of a post-mortem event. Extracellularly, HMGB-1 exhibits a different function: immune activation. Extracellular HMGB-1 has been shown to bind to Toll-like receptor 2, Toll-like receptor 4, and advanced glycosylation end product-specific receptor (RAGE)[154]. These interactions confirm extracellular HMBG-1 acts as a DAMP which activates antigen presenting cells and promotes tumor antigen processing[155]. Furthermore, extracellular HMGB-1 displays marked chemokine function towards APC-progenitors, complexing with CXCL12 and signaling via CXCR4[156]. In this study, we evaluate the ability of our novel combinatorial therapy to induce HMGB-1 release from the nucleus to the extracellular space, as well as compare these levels to those induced by treatment with the standard chemotherapy doxorubicin.

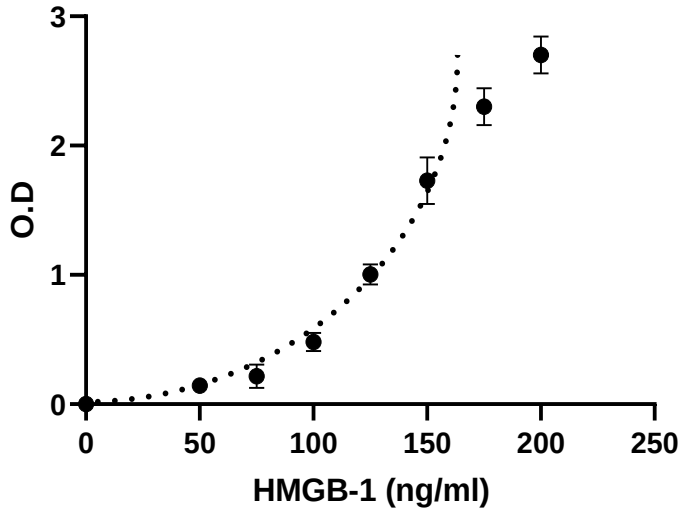


**Figure 52. A standard curve reflecting known concentrations of ATP and corresponding optical density (O.D).** Standard wells containing 200, 175, 150, 125, 100, 75, 50 and 0 ng/ml HMGB-1 were created to formulate a standard curve and associated O.D value. Plotted points represent the averages of duplicate determinations ± s.e.m. in two separate experiments.

In the human breast carcinoma cell line, MCF-7, cells were treated with our novel combinatorial therapy at 6 times below their respective $EC_{50}$. A second experimental group was also treated with 25 μM doxorubicin, an effective *in vitro* dose that was shown to induce immunogenic cell death and increased levels of extracellular HMGB-1[152]. After 24 h, an HMGB-1 ELISA kit (Tecan Trading AG, Switzerland) was used to measure concentrations of extracellular HMGB-1 from treated cell supernatant. A standard curve was created using known concentrations (ng/ml) of HMGB-1 and corresponding these molar concentrations to optical density values (Figure 52). A sample blank was utilized to correct for any background in the sample and provide an accurate absorbance reading. After subtracting the blank, the raw experimental data was compared to values of the standard curve to calculate the concentration of extracellular HMGB-1 (Figure 53A). After 24 h treatment with our novel combinatorial therapy, extracellular HMGB-1 levels were detected at a concentration of 187 ng/ml. After 24 h treatment with 25 μM

doxorubicin, extracellular HMGB-1 levels were detected at a concentration of 87 ng/ml. In untreated controls, no extracellular HMGB-1 was detected by ELISA. Untreated control O.D. values resembled those of the sample blank. Compared to doxorubicin, our novel combinatorial therapy induced significantly higher levels of HMGB-1 secretion ($p<0.01$). Furthermore, cells were analyzed for viability using trypan blue exclusion (Figure 53B). After 24 h, cells treated with the combinatorial therapy were 27% viable, significantly lower compared to untreated control cell viability ($p<0.01$). Cells treated with 25 μM doxorubicin for 24 h were 48% viable, significantly lower compared to untreated control cell viability ($p<0.01$). Untreated cells were 92% viable after 24 h.

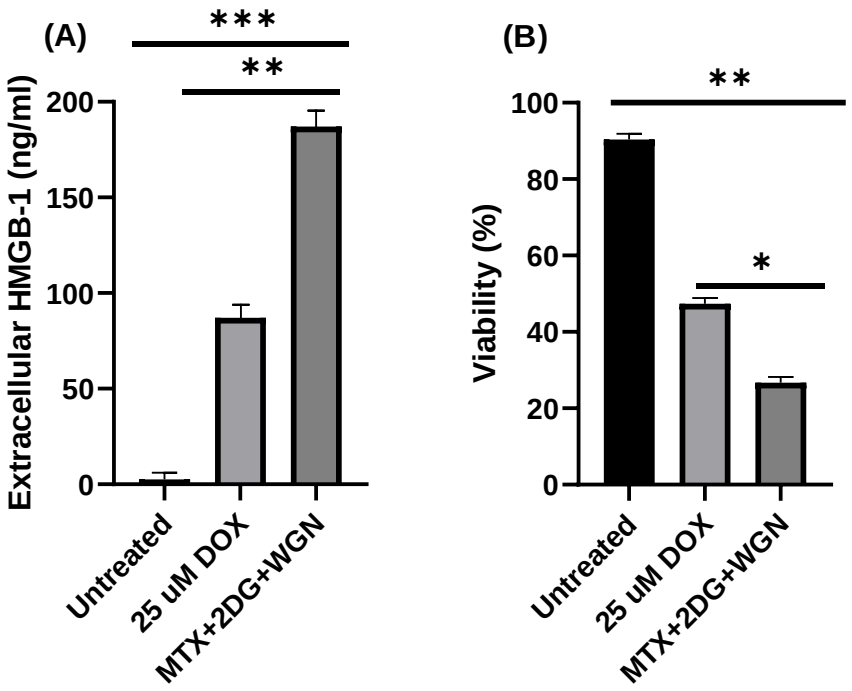


**Figure 53. A combination of three non-mutagenic drugs at combinations 6 times below their $EC_{50}$ is more effective than conventional chemotherapy doxorubicin at inducing HMGB-1 release from dying tumor cells.** Treated and untreated cell supernatants were harvested and analyzed with a spectrophotometer. Absorbance values were compared to a standard curve to determine extracellular

HMGB-1 levels. Viability of treated cells was also determined via trypan blue exclusion. Bars represent the average of triplicate experiments ± s.e.m. (*=$p<0.05$, **= $p<0.01$).

In the mouse mammary carcinoma cell line, 4-T1, cells were treated with our novel combinatorial therapy at 6 times below their respective $EC_{50}$. A second experimental group was also treated with 25 μM doxorubicin. Similarly, a sample blank was utilized to correct for any background in the sample and provide an accurate absorbance reading. After subtracting the blank, the raw experimental data was compared to values of the standard curve to calculate the concentration of extracellular HMGB-1 (Figure 54A). After 24 h treatment with our novel combinatorial therapy, extracellular HMGB-1 levels were detected at a concentration of 167 ng/ml. After 24 h treatment with 25 μM doxorubicin, extracellular HMGB-1 levels were detected at a concentration of 42 ng/ml. In untreated controls, no extracellular HMGB-1 was detected by ELISA. Untreated control O.D. values resembled those of the sample blank. Compared to doxorubicin, our novel combinatorial therapy induced significantly higher levels of HMGB-1 secretion ($p<0.01$). Furthermore, cells were analyzed for viability using trypan blue exclusion (Figure 54B). After 24 h, cells treated with the combinatorial therapy were 30% viable, significantly lower compared to untreated control cell viability ($p<0.01$). Cells treated with 25 μM doxorubicin for 24 h were 62% viable, significantly lower compared to untreated control cell viability ($p<0.01$). Untreated cells were 93% viable after 24 h.

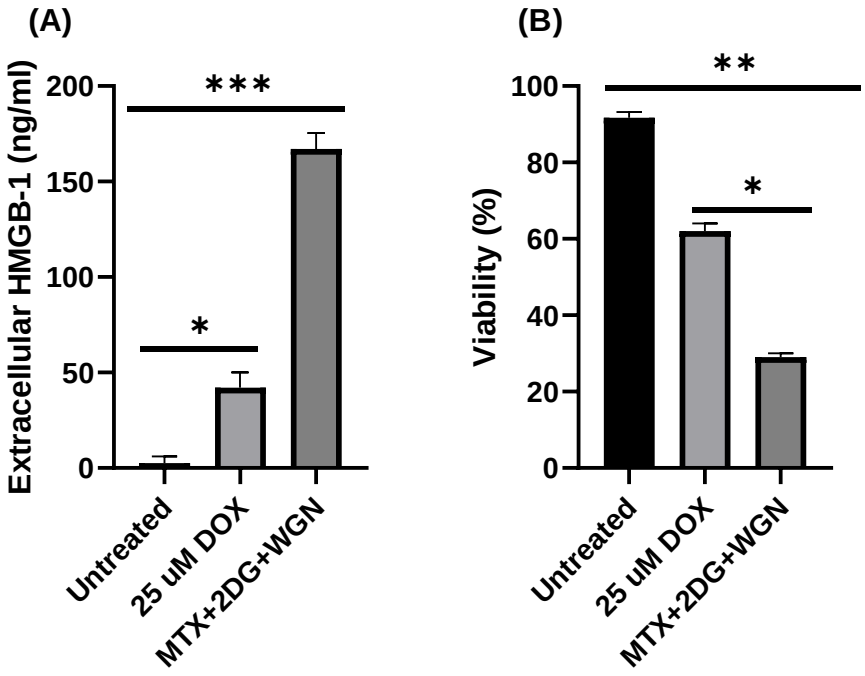


**Figure 54. A combination of three non-mutagenic drugs at combinations 6 times below their $EC_{50}$ is more effective than conventional chemotherapy doxorubicin at inducing ATP release from dying tumor cells.** Treated and untreated cell supernatants were harvested and analyzed with a spectrophotometer. Absorbance values were compared to a standard curve to determine extracellular HMGB-1 levels. Viability of treated cells was also determined via trypan blue exclusion. Bars represent the average of triplicate experiments ± s.e.m. (*=p<0.05, **= p<0.01, ***= p<0.001).

## 4.6 DISCUSSION

The effectiveness of anticancer therapies is often a measure of cytotoxicity towards cancer cells and overall tumor regression post-treatment[157]. Generally, these therapies induce cancer cell death through two pathways: apoptosis or necrosis. Programmed cell death is a relatively "neat" process, in which DNA is cleaved by DNases, dying cells are reduced to apoptotic blebs, and neighboring cells are stimulated to phagocytose debris[70]. The order characterized by this process makes it non-immunogenic, and is in some cases referred to as tolerogenic[77]. Conversely, necrosis is the result of acute cell stress and subsequent cell destructions. Cells that enter the necrotic pathway are characterized by swelling and eventual burst, leaking intracellular

components into the extracellular periphery. This process is viewed as immunogenic as the intracellular components now found in the extracellular domain serve as damage-associated molecular patters that interact with pattern recognition receptors on immune cells to activate an immune response. Notably, cellular debris is not readily cleared in necrosis, which can have lasting implications on patient help if no intervention is sought[137]. What remains to be addressed in this assessment of anticancer therapies is whether the immune system is activated against tumor cells in response to induced cell death and if these treatments can prevent against future tumor recurrence.

Immunogenic cell death has become important in evaluating the effectiveness of developing therapies due to the newly understood importance of activating immune cells to target cancer cells and establishing immunological memory to combat tumor relapse in cancer therapy. ICD has been characterized as a hybrid of apoptotic and necrotic pathways, showing traces of both as it unfolds[138].

Thus, we explored the mechanism by which our novel combinatorial therapy induces cell death in both human and mouse mammary tumor cell lines. After 12 h of treatment, the percentage of AnnexinV-7AAD +/+ cells in both cell lines was significant compared to those of untreated cells ($p<0.05$). After just 12 h of treatment, treatment with our novel combinatorial therapy induces apoptosis and significant cell death in tumor cells. Cell counts were also determined prior to each analysis, and clearly demonstrates a significant decrease in cell number between cells treated for 8 h and 12 h. This account is further evidenced by the high levels of apoptotic and cellular debris depicted in the forward-scatter versus side scatter graphs for each treatment interval.

While the exact mechanism and extent of ICD has yet to be elucidated, three hallmarks of ICD have been identified and are used to characterize this process[158]. In this study, our novel combinatorial therapy has been shown to induce all three, and in some cases provide an even stronger signal than the known anticancer ICD-inducer doxorubicin.

First is the translocation of ER-protein calreticulin to the plasma membrane. Normally functioning as a calcium binding protein in the ER, surface-expressed calreticulin serves as a potent "eat me" signal to antigen presenting cells[149]. The phagocytosis of dying tumor cells promotes tumor neoantigen processing and helps mount a targeted immune response against tumor cells[152]. Notably, calreticulin translocation is characterized as a pre-apoptotic response to increased levels of cell stress[140]. Thus, we monitored the levels of calreticulin surface expression 0 h, 1.5 h, and 3 h after treatment with our novel combinatorial therapies and compared these values to untreated controls as well as cells treated with known ICD inducer doxorubicin. To ensure the findings of these studies were valid, cell viability of each group was analyzed prior to analyzing the surface expression of calreticulin. In all cases, treated cell viability was comparable to that of untreated control cells at each time point, allowing us to directly analyze levels of surface-expressed calreticulin and rule out intracellular levels from obscuring our data. After 3 h, 95.6% of our combinatorial therapy treated cells of the MCF-7 cell line were positive for calreticulin surface expression. MCF-7 cells treated with 25 μM doxorubicin for 3 h were 96.4% positive for calreticulin surface expression. Untreated MCF-7 cells were 4.3% positive for calreticulin surface expression after 3 h. In the 4-T1 cell line, 78.3% of cells treated with our combinatorial therapy for 3 h were

positive for calreticulin surface expression. 77.6% of 4-T1 cells treated with 25 μM doxorubicin for 3 h were positive for calreticulin surface expression. Only 2.7% of untreated 4-T1 cells were positive for calreticulin surface expression. Using measures of viability to exclude the possibility of staining intracellular calreticulin, our findings for each cell line were significant compared to untreated controls ($p<0.001$). Our novel combinatorial therapy is able to induce calreticulin translocation to the plasma membrane similar to a known ICD-inducing agent.

Second comes the secretion of ATP in an autophagy-mediated manner from dying cells[159]. Whereas ATP is generally trapped within vesicles inside apoptotic blebs, lysosomal-plasma membrane interactions during ICD cause it to be secreted into the extracellular space[144]. Here, ATP functions as a potent "find me" signal. This chemokine function attracts immune cells and promotes their interaction with surrounding signals to aid in activation[145]. Thus, cells were treated for 24 h and supernatants were harvested to quantify the levels of extracellular ATP. In the MCF-7 cell line, extracellular ATP was found present at a concentration of 7.2 ng/μl 24 h after treatment with our combinatorial therapy. In MCF-7 cells treated with 25 μM doxorubicin, extracellular ATP was found present at a concentration of 3.1 ng/μl after 24 h. In untreated controls, extracellular ATP was found present at a concentration of 1.29 ng/μl after 24 h. In the 4-T1 cell line, extracellular ATP was found present at a concentration of 6.5 ng/μl 24 h after treatment with our combinatorial therapy. In 4-T1 cells treated with 25 μM doxorubicin, extracellular ATP was found present at a concentration of 2.8 ng/μl after 24 h. In untreated controls, extracellular ATP was found present at a concentration of 1.4 ng/μl after 24 h. Compared to several papers evaluating extracellular ATP levels during ICD,

our combinatorial therapy induces significant ATP exocytosis and provides a stronger signal than that induced by treatment with a known ICD-causing agent[160].

Last, HMGB-1 is released into the extracellular domain at the site of ICD. Under normal physiological conditions, HMGB-1 is contained within the nucleus where it functions as a chromatin-binding protein[161]. During ICD, nuclear and plasma membrane permeabilization cause its release into the extracellular space. Here, extracellular HMGB-1 is a potent danger-associated molecular pattern, and interacts with pattern recognition receptors such as TLR-2, TLR-4, and RAGE on antigen presenting cells to promote activation and subsequent antigen presentation to cytotoxic effector cells[142]. Thus, cells were treated for 24 h and supernatants were harvested to quantify the levels of extracellular HMGB-1. In the MCF-7 cell line, extracellular HMGB-1 was found present at a concentration of 187 ng/ml 24 h after treatment with our combinatorial therapy. In MCF-7 cells treated with 25 μM doxorubicin, extracellular HMGB-1 was found present at a concentration of 87 ng/ml after 24 h. In untreated controls, no extracellular HMGB-1 was detected after 24 h. In the 4-T1 cell line, extracellular HMGB-1 was found present at a concentration of 167 ng/ml 24 h after treatment with our combinatorial therapy. In 4-T1 cells treated with 25 μM doxorubicin, extracellular HMGB-1 was found present at a concentration of 42 ng/ml after 24 h. In untreated controls, no extracellular HMGB-1 was detected after 24 h. Compared to several papers evaluating extracellular HMGB-1 levels during ICD, our combinatorial therapy induces significant HMGB-1 secretion and provides a stronger signal than that induced by treatment with a known ICD-causing agent[150].

In conclusion, treatment with our novel combinatorial therapy induces apoptosis and a high degree of cell death as well as achieves the expression and secretion of the three hallmark signals of immunogenic cell death in both human and mouse mammary tumor cell lines. These findings are significant, as the general consensus on immunogenic cell death states that absence of just one of these markers drastically reduces the immunogenicity of cell death[142,162,163]. The potent elicitation of all three ICD hallmarks by our novel combinatorial therapy solidifies it as an *in vivo* candidate ICD inducer. Numerous studies conducted with similar cell lines expressing similar signals post-treatment have demonstrated great success in priming an adaptive immune response towards cancer cells[164–167]. We are confident in future studies that seek to employ our novel combinatorial therapy in inducing ICD *in vivo* and establishing immunological memory as a result. Future studies in our laboratory will evaluate the effectiveness of our novel combinatorial therapy against 3D tumor models and determine the efficacy of this therapy towards the specific subpopulation of cancer stem cells known to play a significant role in tumor relapse. We anticipate the relationship between the compounds in combination being able to synergize and overcome the strengthened resistance mechanisms displayed by this subpopulation of cells in this tumor model.

# CHAPTER 5: A NOVEL LOW-DOSE COMBINATORIAL THERAPY IS EFFECTIVE AGAINST HUMAN AND MOUSE MAMMARY 3D TUMORSPHERES

## 5.1 ABSTRACT

The foundation of anticancer drug development lies in *in vitro* preclinical studies. Conventional methods analyze drug properties and function against a 2D monolayer of tumor cells. However, challenges are faced with the clinical predictivity and translatability of findings extrapolated from 2D monolayer culture studies. Thus, researchers have turned to tumorspheres, which model in 3D the heterogeneity of a cancer cell population and has shown to be a leading indicator of *in vivo* clinical translatability. Cancer stem cells (CSCs) are the key to meaningful preclinical studies, yet require rigorous isolation processes including fluorescence-activated cell sorting (FCS) and growth factor cultivation. The discovery of tumorspheres, however, allows researchers to specifically study this critical sub-population of tumor cells through selective culture methods. In the present study, we developed mouse and human mammary tumorspheres and evaluated the effectiveness of our novel low-dose combinatorial therapy against this 3D tumor model. 48 h post treatment, we found evidence of significantly decreased cell viability after 3D mammary tumorspheres were homogenized and assayed for viability. Voluminous evidence in the literature supports the translatability of tumorsphere studies to *in vivo* trials, and we anticipate similar drug

effectiveness and success in future animal models with our novel low-dose combinatorial therapy.

## 5.2 INTRODUCTION

Preclinical studies are a gateway to bedside administration of anticancer drugs. *In vitro* analysis of developing drugs is invaluable to understanding their pharmacokinetics and pharmacodynamics. Importantly, clinical trials are planned around the data obtained from these studies. Thus, great attention is given to *in vitro* models to generate the best prediction of clinical outcomes, and forecast any challenges associated with toxicity or therapeutic resistance. However, current models may not accurately represent the conditions observed in the clinic, and as a result, pose challenges in adapting *in vitro* studies to *in vivo* to achieve similar effectiveness.

In anticancer drug development, the effectiveness of developing compounds is studied directly on cancer cells from various species. More specifically, the bulk of *in vitro* studies are performed on 2D monolayers, generated from tissue cell culture[168]. Whereas the findings of these studies are important and guide clinical trials, there are pitfalls associated with 2D monolayer cultures that affect the predictivity of clinical effectiveness. The most common of which is the lack of structural similarity to tumors *in vivo*. The lack of E-cadherin and upregulation of fibronectin promotes aberrant piling and aggregation of tumor cells in tissue which drives critical cell-to cell interactions and forms the underlying tissue architecture[48]. Conversely, adherent cells bind to plastic tissue culture-treated surfaces, limiting the cell-to-environment and cell-to-cell interactions observed in naturally occurring tumor masses and inhibiting the formation of multicellular tissue structures. Second, cell-to-extracellular matrix interactions are

overlooked in conventional culture models. The extracellular matrix is comprised of various proteins, polysaccharides, and glycoproteins. These macromolecules do not only function in tissue structure and support, rather, have been shown to also regulate multiple cell-to-cell signaling pathways and a multitude of other cellular processes[169]. *Wozniak et al.* discovered the influence of increased collagen on integrin signaling, which led to cell proliferation[170]. Furthermore, the stiffness of the ECM has been shown to influence cell differentiation and changes in morphology[171]. In 2D monolayer cultures, however, these interactions do not take place. Cell morphology is altered to enhance attachment to plastic plate or dish[172]. Cell division is altered which limits the heterogeneity of 2D cultures, an important factor in evaluating drug effectiveness. Confluent monolayers of tumor cells are equally exposed to oxygen and nutrients; opposite to the conditions observed in tissue. Progression of a tumor separates cells into sub-populations of externally rapid-growing and internally slow-growing subsets. This characterization is attributed to the lack of access to nutrients and oxygen supply of deeply rooted cells[173]. As a result, cell division is slower at the core, increasing the variance and affecting the functionality between cells of the tumor. Lastly, the above differences between 2D monolayers and tumors in tissue creates variance in drug effectiveness and metabolism[174]. The relative homogeny of cell division and nutrient exposure of cells in monoculture promotes drug efficacy. Cells are equally distributed along a plate or flask, allowing the compounds to interact with each cell in the population. Additionally, cells are generally in the same stage of the cell cycle and exhibit similar division patters, thus are susceptible to the same degree of targeting by these anticancer compounds. The 2D monolayer culture also supports homogenous oxygen exposure across the population, preventing the induction of

hypoxia-induced cell survival mechanisms[175]. In tissue, however, these characteristics are not found. The tumor is an aggregation of cells that develop a surface-to-core gradient of nutrient availability. External cells are sustained and proliferate rapidly, whereas internal cells are viable yet generally quiescent[176]. Therefore, compounds administered usually target cells of the tumor surface, and face challenges with effectiveness against cells of the core due to physiological shielding. Furthermore, varying cell cycle stages between these subsets creates differences in sensitivity to certain compounds, as replicative inhibitors are relatively ineffective towards core cells of the primary tumor[177]. More importantly, the abnormal distribution of cells creates hypoxic regions within the tumor that promote cell survival and drug resistance pathways, ultimately reducing the effectiveness of these compounds *in vivo*[178]. Thus, although widely accepted, 2D monolayer cultures do not accurately model the cell-to-cell and cell-to-ECM interactions that are observed in *in vivo* trials. Therefore, the need for culture models that more accurately portray these features is of utmost importance, and have been found to be exemplified in 3D tumorspheres.

Tumorspheres represent three dimensional culture models of tumor cells. Unlike 2D monolayers, tumorspheres allow researchers to study interactions between the cells and the extracellular matrix. This model mimics the structural and biochemical properties of tumors *in vivo*, allowing for more detailed analysis of drug effectiveness[179]. Primarily, tumorspheres uphold the cell morphology observed *in vivo* and are not subject to changes in morphology as is the case in 2D monolayer cultures[180]. In transitional studies, this characteristic is important. Should a researcher wish to inject tumorsphere cells into an animal, the similar morphology promotes tumorigenesis and allows for comparable

studies. Additionally, gradients of cell proliferation have been identified in tumorspheres; where cell division is higher in the exterior surfaces of the 3D model and lower at central points[181]. This variance plays a key role in drug susceptibility, and is readily assessed by employing this method. Similar gradients are observed in regards to nutrition, pH, and oxygen, with peripheral cells showing heightened levels and increased exposure as opposed to cells closer to the center[181]. In addition to structural and architectural similarities, tumorspheres have been shown to imitate the metabolism, cell signaling, and gene expression of a solid tumor mass[182]. Growth on Matrigel® promotes cell attachment via integrin receptors, which facilitates cell signaling responsible for proliferation, differentiation, and growth[183]. This allows researchers to delve deeper into biochemical and molecular analysis, increasing the translatability to clinical studies. The ability of 3D tumorspheres to model the *in vivo* microenvironment make them invaluable to the transition from *in vitro* to *in vivo* studies. Although data collected from 2D monolayer culture models is widely accepted, developing drugs should be analyzed for their effect on tumorspheres in order to enhance their clinical translatability.

## 5.3 BACKGROUND AND SIGNIFICANCE

Despite the relative heterogeneity of 2D monolayer cell culture populations, this model is unable to capture the breadth of sub-populations identified in solid tumor masses. In part due to the homogenous exposure to nutrients and oxygen, 2D monolayers give rise to a population of tumor cells with varying phenotypes yet similar physiological states[184]. The monolayer cells that are dividing, metabolizing, and respiring at the same rate masks the reality of tumor cells *in vivo*. More importantly, the malignancy and resistance to anticancer drugs exhibited by tumors in tissue are attributed to a

subpopulation of tumor cells known as cancer stem cells (CSCs). Development of effective anticancer therapies should be centered around the targeting of this subset of cells, however the predominant 2D monolayer culture model provides little insight into this population.

CSCs resemble stem cells in their ability to self-renew as well as differentiate into various cell types. This subpopulation of cells has been identified in multiple solid tumors, including breast cancers (BCSCs), lung cancers (LCSCs), pancreatic cancers (PCSCs) and colon cancers (CCSCs)[185]. Through self-renewal, CSCs are able to divide and grow in number while maintaining their undifferentiated state. Under normal physiological conditions, stem cell self-renewal is critical to the regeneration of life-long tissue. However, in the case of CSCs, this promotes proliferation that feeds into the invasive architecture of the tumor mass[186]. Additionally, the heightened self-renewal capabilities of CSCs promote their increased tumorigenecity. In cell culture, CSCs are potent initiators of tumor formation when transplanted into animal models[187]. In tissue, this subset of cells is responsible for the relapse frequently associated with malignant cancer types[188]. CSCs differ from other cells of the population in their gene expression. Studies have shown an upregulation of *Sox2* in cancer stem cells, responsible for their self-renewal properties[189]. Other makers of CSCs include CD44, CD133, and CD24[190]. In addition to their tumorgenicity, CSCs are known to exhibit heightened resistance to drug and radiation treatments. After a primary tumor is established, sustained rapid proliferation is not as crucial to cancer survival. In fact, CSCs have been showed to enter a state of quiescence after tumor development, and only ramp up proliferation pathways when the tumor is pharmacologically targeted[191]. This state of quiescence facilitates CSC

resistance to chemotherapy, as this class of drugs generally targets proliferating cells. In dividing CSCs studies have found increased levels of ATP-binding cassette transporter proteins, which are responsible for multidrug resistance pathway mechanisms and P-glycoprotein pumping of chemo drugs out of the cancer cell[192]. Additionally, anti-apoptotic proteins such as Bcl-2 have been shown to be upregulated in CSCs[193]. Most importantly, this subpopulation of cells possesses powerful DNA repair capabilities[194]. While this may seem counterintuitive to the fundamental genomic instability of cancer cells, the ability to rapidly repair DNA enhances their resistance to chemotherapy and radiation therapy targeting nucleotide synthesis and function. Thus, an effective therapy is one that is results in tumor regression and simultaneously inhibits the proliferation of CSCs. Therefore, it is important that this subpopulation of tumor cells be analyzed in the drug development process.

Tumorsphere models are gaining popularity in preclinical trials due to their clinical predictivity and translatability of drug effectiveness. What makes this culture method even more unique and valuable to researchers is that it mimics the characteristics of CSCs. Tumorspheres and CSCs both possess the ability to initiate tumor formation when transplanted into animal models. In a kidney cancer model, tumorspheres displayed tumorigencity comparable to that of CSCs isolated and reintroduced into the same animal they were derived from[195]. CSCs also display a high degree of tissue invasion facilitated by epithelial-to-mesenchymal transformation (EMT). Tumorspheres grown in Matrigel® showed invasion into the synthetic extracellular matrix as well as increased expression of mesenchymal markers[196]. Additionally, tumorspheres have been shown to mimic the tumor vascularization induced by CSCs. Different from endothelial cell

neovascularization, CSCs form vessel-like channels that supply nutrients and oxygen to surrounding cells[197]. Tumorspheres derived from human breast cancer cells exhibited tumor vascularization properties, evidenced by a $CD31^-/CD144^+$ phenotype[198]. Most importantly, CSCs and tumorspheres share the same drug resistance properties. Multiple studies in various cancer models show the ability of tumorspheres to resist therapy[199,200].

The significance of the present study is to demonstrate effectiveness of our novel combinatorial therapy in tumorsphere models similar to what we have shown in previous *in vitro* studies. This culture method will allow us to evaluate our combination's efficacy against various subsets of the primary tumor population, all of which play a critical role in tumor progression and relapse. Furthermore, this study will allow us to observe the extent to which the components of our combinatorial therapy synergize to overcome resistance mechanisms and elicit a powerful cytotoxic effect against tumor cells. We have previously shown that our novel anticancer therapy is capable of inducing immunogenic cell death in tumor cells while remaining relatively non-toxic towards rapidly proliferating normal cells of the human immune system. We anticipate similar effectiveness against tumorspheres, and in doing so, paving the way for future animal studies with enhanced clinical translatability.

## 5.4 METHODS

### *5.4.1 Cell culturing and maintenance*

The 4-T1 (Mouse Metastatic Mammary Carcinoma) cell line was kindly donated by Dr. Vijaya Iragavarapu-Charyulu, Department of Biomedical Sciences, Florida Atlantic University. The MCF-7 (Human Metastatic Mammary Tumor) cell line was obtained from Dr. James X. Hartmann, Department of Biological Sciences, Florida Atlantic

University. Cells were cultured between $2\times10^5$/mL and $1\times10^6$/mL in 75 $cm^2$ Falcon cell culture flaks containing Gibco RPMI 1640-L-Glutamine medium (Life Technologies-Grand Island, NY, USA) supplemented with 10% fetal bovine serum (Life Technologies-Grand Island, NY, USA) and 100U/mL Gibco Pen Strep (Life Technologies- Grand Island, NY, USA). Cell cultures were incubated at 37 °C under 5% $CO_2$ in a humidified atmosphere.

*5.4.2 3D tumor model culture*

Mammary tumorspheres were grown using Matrigel® Extracellular Matrix Basement Membrane (Corning, USA). 4-T1 and MCF-7 cells were cultured independently and harvested in a single-cell suspension with Gibco RPMI 1640-L-Glutamine medium (Life Technologies- Grand Island, NY, USA) supplemented with 10% fetal bovine serum (Life Technologies- Grand Island, NY, USA) and 100U/mL Gibco Pen Strep (Life Technologies- Grand Island, NY, USA) at a density of $3\times10^5$ cells/mL. Matrigel® Extracellular Basement Membrane (Corning, USA) was used to coat the bottom of ultra-low attachment surface 6-well plates (Corning, USA) and incubated for 30 min at 37 ºC to gel. Cells suspended in complete medium were then carefully seeded on top of the matrix gel and incubated for an additional 30 min at 37 °C under 5% $CO_2$ in a humidified atmosphere. Complete R-10 media supplemented with 10% Matrigel® Extracellular Basement Membrane was then added to each well. Cell cultures were incubated at 37 °C under 5% $CO_2$ in a humidified atmosphere for 8 days. Media was changed every two days.

*5.4.3 Trypan blue exclusion cell viability assay*

After 8 days of culture and 48 h treatment, tumorspheres of roughly 50 cells or more were selected for qualitative analysis. Trypan blue dye was added to all wells and incubated for 10 min at 37 ºC at 5% $CO_2$. After 5 min, tumorspheres were analyzed microscopically. Viable spheroids were characterized as luminescent and unstained. Dead (non-viable) spheroids where characterized as stained and displaying no luminescence.

*5.4.4 MTS cell viability assay*

On the $8^{th}$ day of culture, media from MCF-7 and 4-T1 mammary tumorsphere cultures was changed and cells were then treated with either our novel combinatorial therapy or 25 µM doxorubicin. After 48 h spheres were harvested using a broad-tip pipette and passed through a 40 µm nylon cell strainer (BD Falcon, USA), and seeded into a 96-well plate. 20 µL of CellTiter 96® AQueous One Solution MTS (5 mg/mL) (Promega-Madison, WI, USA) was added to each well and incubated at 5% $CO_2$ at 37°C for an additional 4h. Absorbance readings were taken in an Epoch microplate reader at 490 nm. Computed data was compared to untreated and normalized cells. Cells that were not administered any treatment were considered the control group. Cell viability was calculated by the following formula: Cell viability (%) = (average OD in treated group/average OD in control group) × 100%.

*5.4.5 Statistical analysis*

GraphPad Prism v8 software was used for statistical analyses. Data is presented as mean ± s.d. t-test was used to determine statistical significance between groups for normally distributed data. For all tests, *$p<0.05$ was considered significant. Experiments and

measurements were performed in triplicate. Graphed data depicts means of triplicates ± s.e.m. and are representative of three experiments.

## 5.5 RESULTS

### 5.5.1 Matrigel® promotes the formation of human adenocarcinoma and mouse mammary carcinoma 3D tumorspheres on ultra-low attachment surface well plates.

In the present study, MCF-7 and 4-T1 cells were grown in 10% Matrigel®-supplemented growth medium on ultra-low attachment surface well plates to stimulate the formation of 3D tumorspheres. Tumorspheres allow for better analysis of drug effectiveness, as well as show marked increase in resistance to anticancer therapies[175]. Tumorspheres were identified as spheroids that were composed of roughly ~50 or more cells. Loosely-packed clusters or non-spheroid cell aggregates were disregarded for the purposes of this study. Cells were also grown on ultra-low attachment surface plates in the absence of Matrigel® to signify the importance of the extracellular matrix modeling substance.

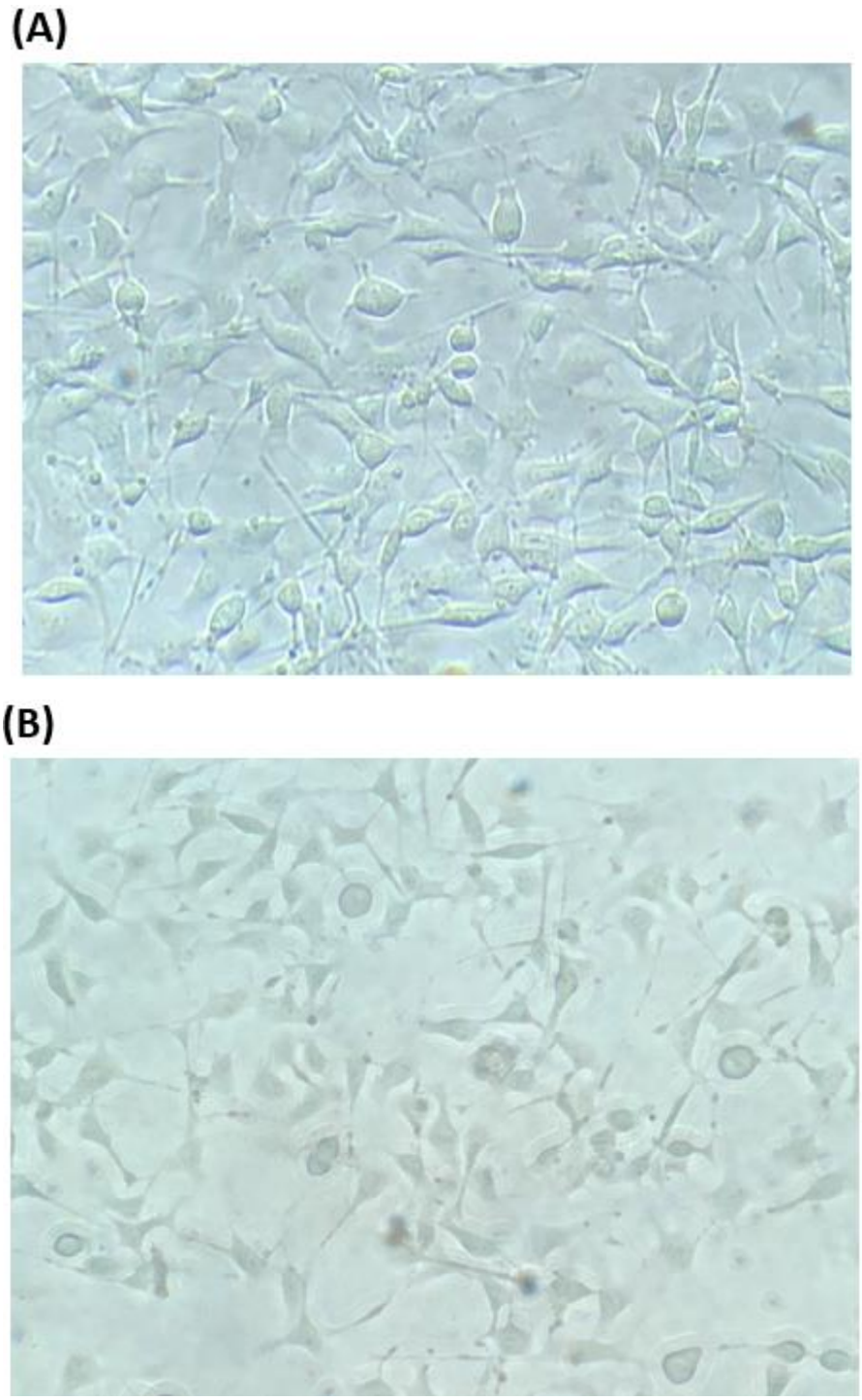


**Figure 55. Absence of Matrigel® inhibits the formation of 3D tumor spheres on ultra-low attachment surface plates.** MCF-7 cells (A) and 4-T1 cells (B) were cultured with complete medium in 6-well ultra-low attachment surface plates. After 48 hours of culture, cells were photographed and analyzed. Photographs are representative of a typical experiment out of three independent ones.

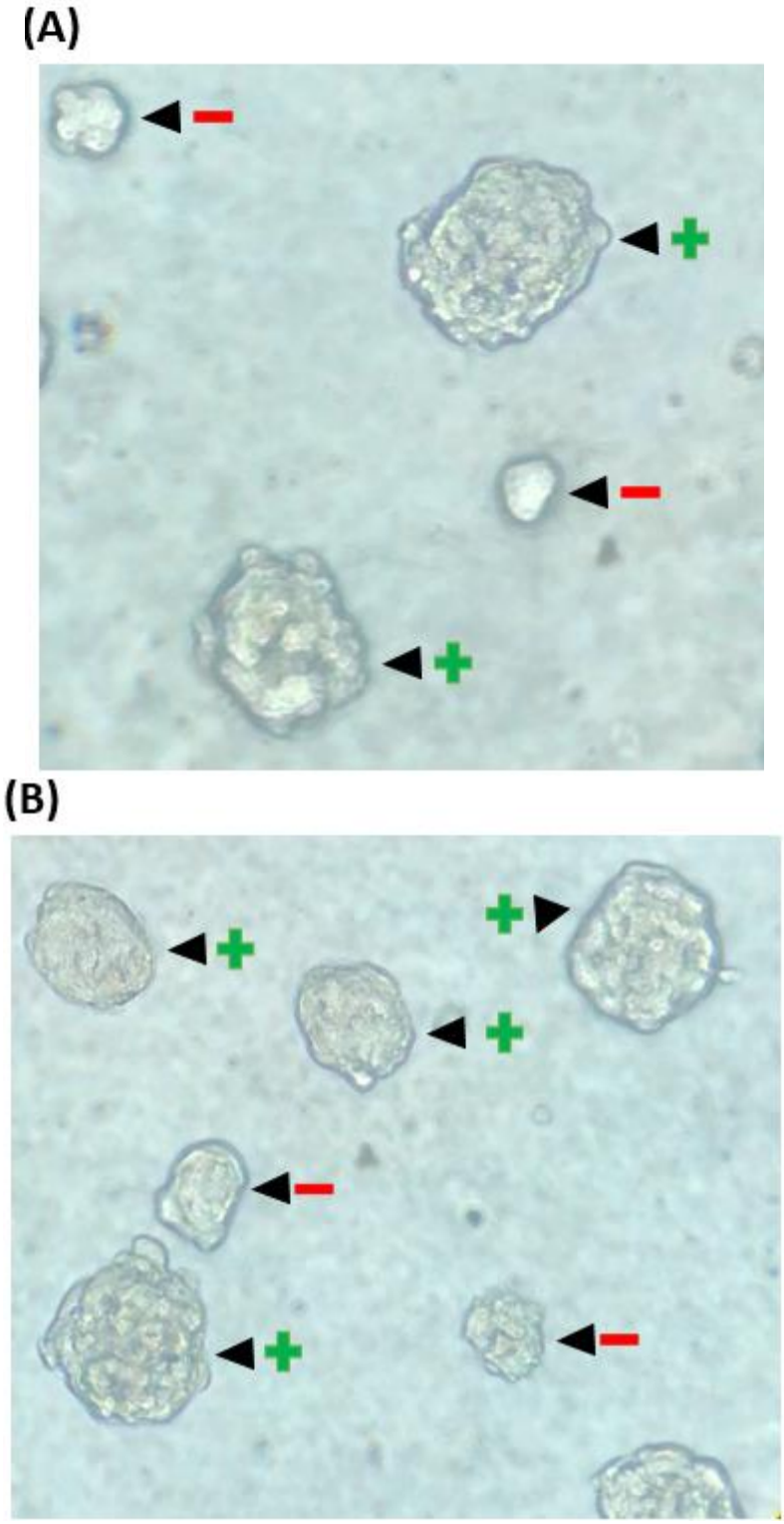


**Figure 56. Matrigel® promotes the formation of mammary 3D tumorspheres on ultra-low attachment surface plates.** MCF-7 cells (A) and 4-T1 cells (B) were cultured with complete medium supplemented with 10% Matrigel® in 6-well ultra-low attachment surface plates. After 48 hours of culture, cells were photographed and analyzed. Photographs are representative of a typical experiment out of three independent ones.

Matrigel® is fundamental to the formation of tumorspheres as it models the extracellular matrix and promotes cell-to-cell interactions observed in tumor cells *in vivo*[172]. Tumorspheres were determined by qualitative analysis, excluding small aggregates or loosely packed clusters. For the purposes of future experiments, we have clearly defined in this study what is considered a tumorsphere and what is not for both the MCF-7 and 4-T1 tumor cell lines (Figure 56). Furthermore, we have shown that cells do not form spheroid structures in the absence of Matrigel® despite being grown on ultra-low attachment surface plates (Figure 55).

### 5.5.2 MTX-2DG-WGN combinatorial therapy is effective against human adenocarcinoma and mouse mammary carcinoma tumorspheres.

In the present study, we evaluated the effectiveness of our novel combinatorial therapy against human adenocarcinoma and mouse mammary carcinoma 3D tumor models. Although we have previously shown the significant effect of our therapy against tumor cells *in vitro*, 3D tumorspheres allow us to further analyze cytotoxicity and provides insight into clinical trials. As a tumorsphere, cells engage in cell-to-cell and cell-to-environment interactions that are not observed in 2D monolayer culture. Furthermore, the formation of a spheroid creates a replicative, nutrient, and oxygen gradient within the structure between cells of the core and cells of the periphery. These processes are shown to have significant influence on cell proliferation, differentiation, and in turn, response to drug treatment[200]. In this study, we determine whether our combinatorial therapy can overcome these heightened resistance mechanisms and cause significant cell death in mammary 3D tumor models.

MCF-7 mammary tumorspheres were cultured for 8 days. After media change, cells were treated with our novel combinatorial therapy for 48 h. Qualitative analysis via trypan blue staining showed significant decrease in treated cell viability compared to untreated tumorspheres (Figure 57). In some cases, tumorspheres began to deteriorate and stained cells can be seen in the near periphery. To quantify these results, tumorsphere cultures were harvested with a broad-tip pipette and carefully transferred to a 96-well plate. Viability was measured using CellTiter 96® AQueous One Solution MTS (Figure 59). After 48 h treatment, MCF-7 tumorspheres were 5% viable relative to untreated control ($p<0.001$).

This study was replicated in the 4-T1 mouse mammary carcinoma cell line. After 8 day culture and 48 h treatment, treated spheroids showed significant decrease in viability when compared to untreated cells stained with trypan blue (Figure 58). Treated cells were visibly darker on the exterior and interior, compared to untreated cells that excluded dye uptake and remained luminescent. Similarly, tumorsphere cultures were harvested with a broad-tip pipette and carefully transferred to a 96-well plate. Viability was measured using CellTiter 96® AQueous One Solution MTS (Figure 60). After 48 h treatment, 4-T1 tumorspheres were 8% viable relative to untreated control ($p<0.001$).

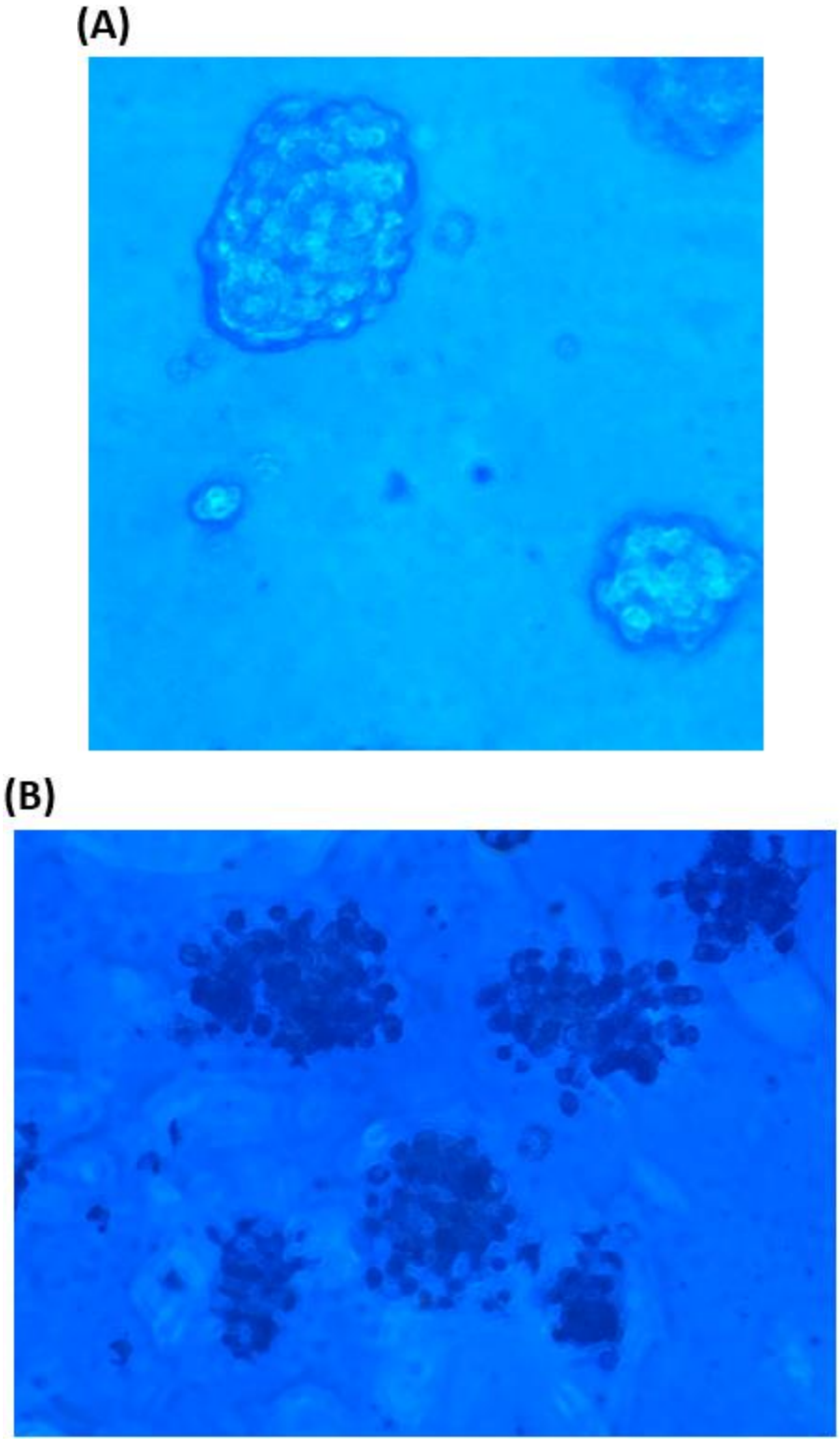


**Figure 57. A novel combinatorial therapy is visibly effective against human mammary adenocarcinoma 3D tumor models.** MCF-7 mammary tumorspheres were left untreated for 48 h (A) or treated with our combinatorial therapy for 48 h (B) and stained with trypan blue. Untreated cells excluded the dye as they were viable and remained luminescent. Treated cells are stained and in some cases

disintegrated from their original spheroid structure as a result of cytotoxic treatment. Photographs are representative of a typical experiment out of three independent ones.

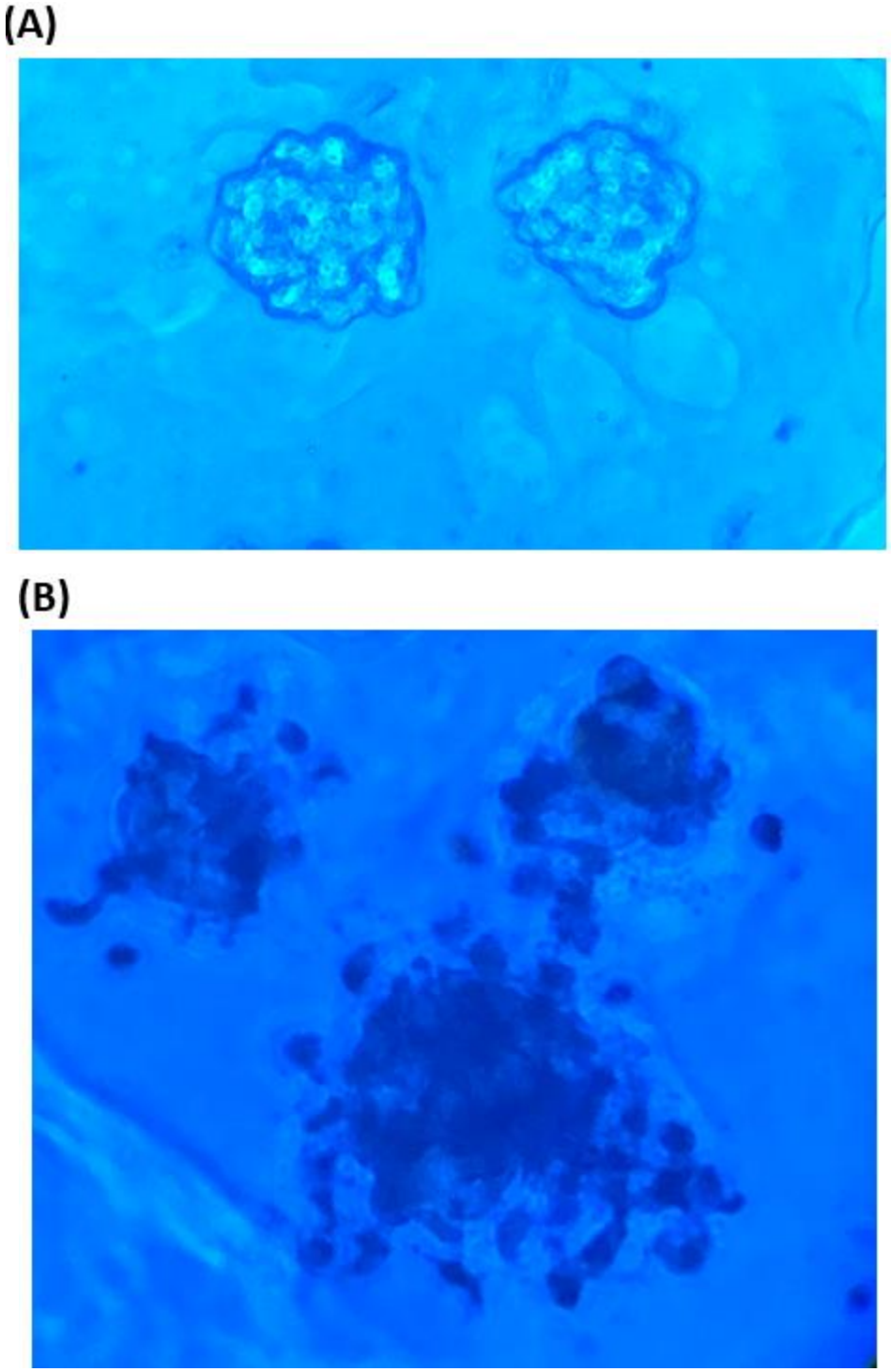


**Figure 58. A novel combinatorial therapy is visibly effective against mouse mammary carcinoma 3D tumor models.** 4-T1 mammary tumorspheres were left untreated for 48 h (A) or treated with our combinatorial therapy for 48 h (B) and stained with trypan blue. Untreated cells excluded the dye as they were viable and remained luminescent. Treated cells are stained and in some cases disintegrated from their

original spheroid structure as a result of cytotoxic treatment. Photographs are representative of a typical experiment out of three independent ones.

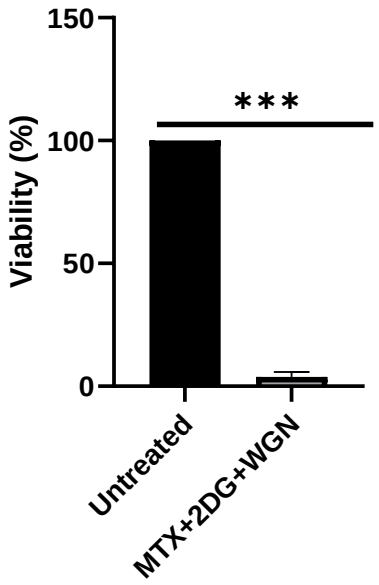


**Figure 59. A novel combinatorial therapy significantly decreases the viability of human mammary adenocarcinoma 3D tumor models.** MCF-7 mammary tumorspheres were treated with our combinatorial therapy for 48 h and analyzed via MTS cell viability assay. Cell viability is expressed as a percentage of the control (100%). Bars represent the average of triplicate experiments ± s.e.m. (***= $p<0.001$).

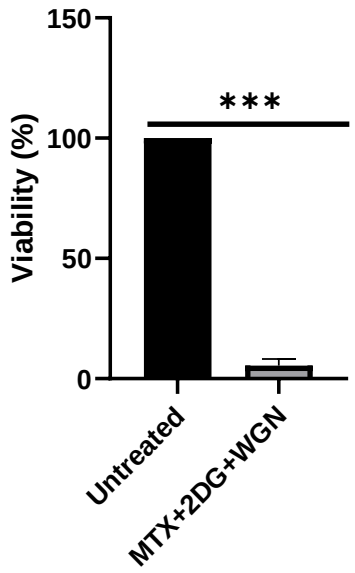


**Figure 60. A novel combinatorial therapy significantly decreases the viability of mouse mammary carcinoma 3D tumor models.** 4-T1 mammary tumorspheres were treated with our combinatorial therapy for 48 h and analyzed via MTS cell viability assay. Cell viability is expressed as a percentage of the control (100%). Bars represent the average of triplicate experiments ± s.e.m. (***= $p<0.001$).

### 5.5.2 Human and mouse mammary tumorspheres are resistant to conventional breast cancer chemotherapy treatment.

In the present study, we evaluated the effectiveness of a conventional breast cancer chemotherapy, doxorubicin, against human and mouse mammary 3D tumor models. Known to be an inducer of immunogenic cell death and widely used in the clinic as an anticancer therapy, the single pathway targeting of doxorubicin makes it increasingly susceptible to cancer cell resistance mechanisms[201]. Additionally, concentration gradients within the tumorsphere promotes hypoxic conditions at the spheroid core. Upregulation of hypoxia-inducible factors increase the function of multidrug resistance pumps and proteins, making 3D tumor models evermore resistant to anticancer targeting. In this study, we determine whether treatment with doxorubicin at a

clinically efficacious dose can overcome the heightened resistance mechanisms displayed by 3D tumor models and cause significant cell death.

MCF-7 mammary tumorspheres were cultured for 8 days. After media change, cells were treated with a clinically relevant dose of doxorubicin (60 µM) for 48 h[132]. Qualitative analysis via trypan blue staining showed no significant difference in treated cell viability compared to untreated tumorspheres. Tumorspheres of both groups remained unstained and luminescent (Figure 61). To quantify these results, treated and control tumorsphere cultures were harvested with a broad-tip pipette and carefully transferred to a 96-well plate. Viability was measured using CellTiter 96® AQueous One Solution MTS (Figure 63). After 48 h treatment, MCF-7 tumorspheres were 98% viable relative to untreated control (ns, $p>0.05$).

This study was replicated in the 4-T1 mouse mammary carcinoma cell line. After 8 day culture and 48 h treatment, doxorubicin treated spheroids showed no significant decrease in viability when compared to untreated cells stained with trypan blue. Treated and untreated spheroids excluded dye uptake and remained luminescent (Figure 62). Similarly, tumorsphere cultures were harvested with a broad-tip pipette and carefully transferred to a 96-well plate. Viability was measured using CellTiter 96® AQueous One Solution MTS (Figure 64). After 48 h treatment, 4-T1 tumorspheres were 99% viable relative to untreated control ($p>0.05$).

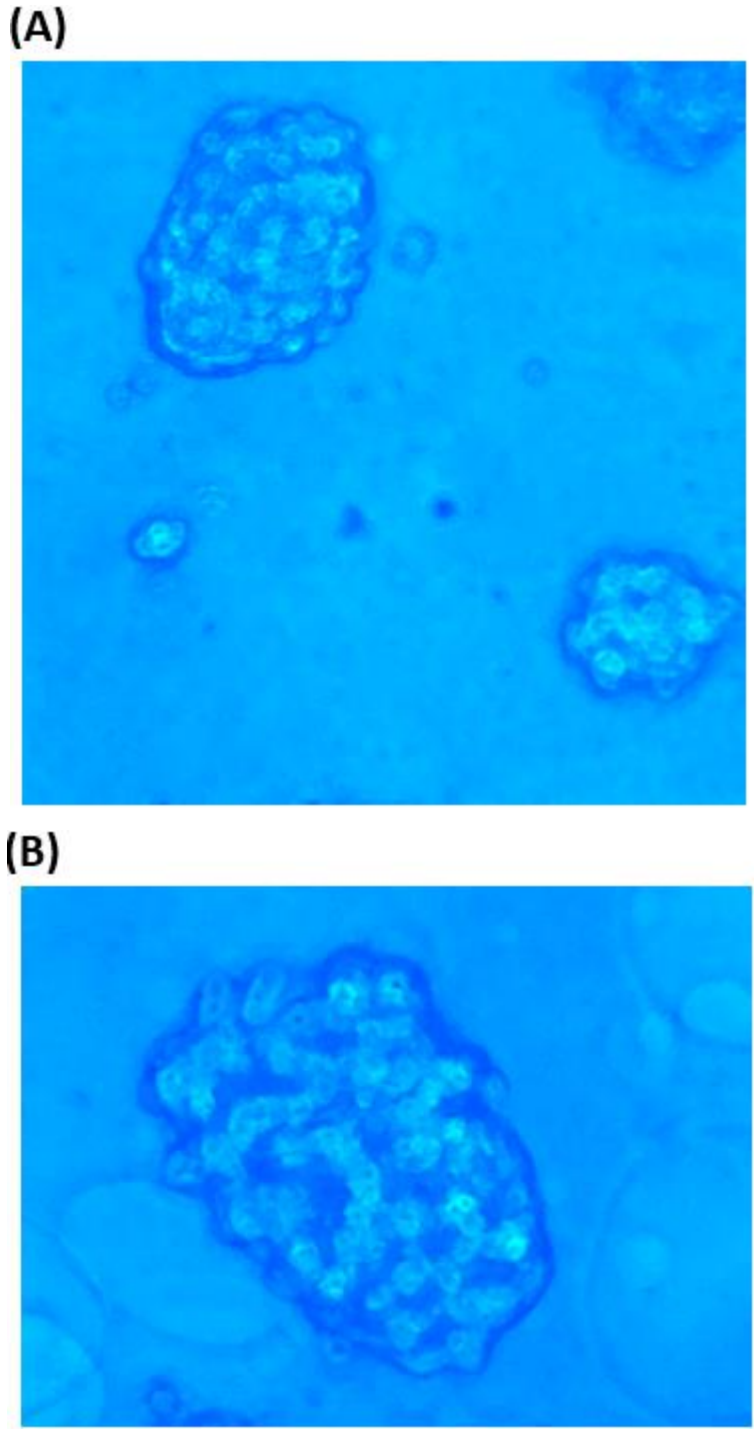


**Figure 61. A conventional chemotherapy is visibly ineffective against human mammary adenocarcinoma 3D tumor models.** MCF-7 mammary tumorspheres were left untreated for 48 h (A) or treated with 60µM doxorubicin for 48 h (B) and stained with trypan blue. Untreated and treated tumorspheres both excluded the dye and remained luminescent. Doxorubicin treatment had no visible effect on tumorsphere viability. Photographs are representative of a typical experiment out of three independent ones.

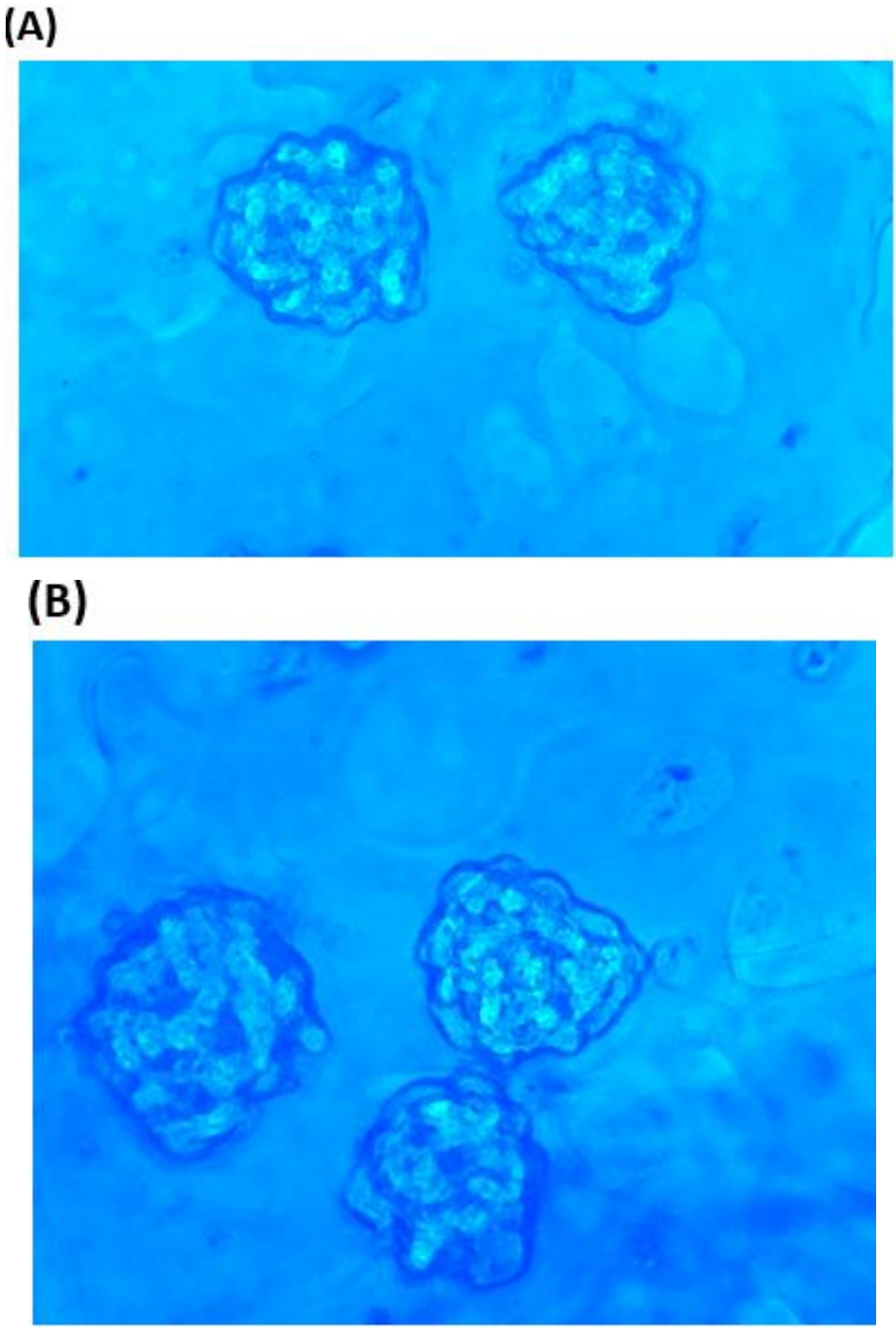


**Figure 62. A conventional chemotherapy is visibly ineffective against mouse mammary carcinoma 3D tumor models.** 4-T1 mammary tumorspheres were left untreated for 48 h (A) or treated 60 µM doxorubicin for 48 h (B) and stained with trypan blue. Untreated and treated tumorspheres both excluded the dye and remained luminescent. Doxorubicin treatment had no visible effect on tumorsphere viability. Photographs are representative of a typical experiment out of three independent ones.

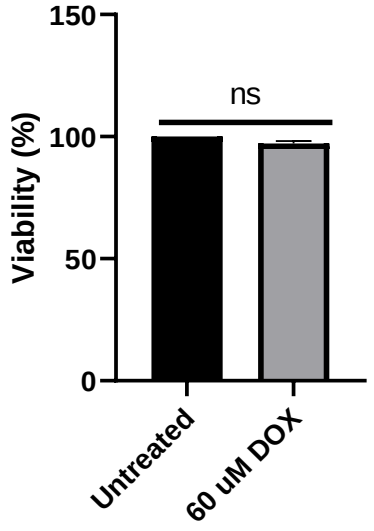


**Figure 63. Clinically-effective dose of doxorubicin has no effect on human mammary adenocarcinoma 3D tumor viability.** MCF-7 mammary tumorspheres were treated with 60 µM doxorubicin for 48 h and analyzed via MTS cell viability assay. Cell viability is expressed as a percentage of the control (100%). Bars represent the average of triplicate experiments ± s.e.m. (ns= p>0.05).

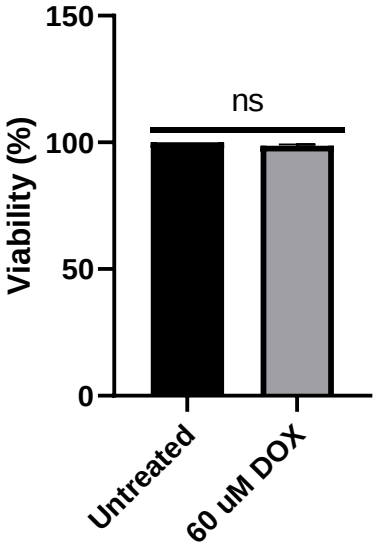


**Figure 64. Clinically-effective dose of doxorubicin has no effect on mouse mammary carcinoma 3D tumor viability.** 4-T1 mammary tumorspheres were treated with 60 µM doxorubicin for 48 h and analyzed via MTS cell viability assay. Cell viability is expressed as a percentage of the control (100%). Bars represent the average of triplicate experiments ± s.e.m. (ns= p>0.05).

## 5.6 DISCUSSION

All modern-day clinical therapies stem from preclinical trials. In the case of developing cancer therapies, *in vitro* models are invaluable to researchers in understanding drug mechanisms, effectiveness, and targeting. Currently, the conventional *in vitro* model is the 2D tumor monolayer[168]. Cells of various cancer lines are grown in flasks and tested for the above drug properties. Unlike tumors found in tissue, 2D monolayer cultures experience equal exposure to nutrients and oxygen and display a near homogenous replicative profile. Additionally, this culture model inhibits cell-to-cell and cell-to-environment interactions, which play a key role in cell proliferation and differentiation. More importantly, cells of the tumor monolayer are equally exposed to drug during treatment, which obscures the resistance mechanisms employed by cells of the tumor core in tissue. The pitfalls in this *in vitro* model has caused a recent shift to evaluating anticancer therapy effectiveness in 3D tumor models.

In this study, we have shown the ability to grow human and mouse mammary 3D tumorspheres from the MCF-7 and 4-T1 tumor cell lines. Cells were grown on ultra-low attachment surface 6-well plates in complete medium supplemented with 10% Matrigel®. Qualitative analysis was used to identify tumorspheres. Only structures of a tightly-packed spheroid were considered tumorspheres. Loose clusters or small aggregates of cells were disregarded (Figure 32). Furthermore, we have shown the significance of Matrigel® in culturing tumorspheres, as the absence of this extracellular matrix model inhibited the formation of tumorspheres in cells seeded on ultra-low attachment 96-well plates. These designations were normalized and used to accurately conduct qualitative analysis of treated cells in future experiments.

Tumorspheres exhibit extracellular matrix interactions and model the tissue architecture observed in primary tumors. Furthermore, tumorspheres are comprised by a subpopulation of cancer stem cells that display a high replicative phenotype and are the leading cause of tumor relapse[193]. The uncontrolled proliferation of these cells *in vitro* forms a spheroid tumor structure that exhibits a concentration gradient of nutrients, oxygen, drug susceptibility, and replicative state[186]. Exterior cells have increased access to oxygen and nutrients which drives their replicative profile, and also are the first cells exposed to drug treatments. Conversely, cells of the core are hypoxic and slow growing due to inadequate nutrient supply, and benefit from physiological shielding from anticancer compounds that fail to penetrate to the core of the tumor. These hypoxic conditions drive tumor drug resistance and survival pathways[193].

Despite heightened resistance mechanisms, treatment with our novel combinatorial therapy for 48 h induced significant cell death in both MCF-7 and 4-T1 tumorspheres. Qualitatively, treated cells stained with trypan blue showed no degree of luminescence and were completely stained with the dye. Furthermore, treated spheroids of both cell lines appeared to disintegrate into individual cells around the periphery, with the core remaining loosely intact. Conversely, untreated spheroids excluded the dye and were luminescent, showing no degree of decreasing viability. Untreated spheroids maintained a compact composition and displayed no evidence of disintegration. However, a conventional chemotherapy was unable to overcome the profound resistance mechanisms displayed by tumorspheres. Treatment with 60 µM doxorubicin, a clinically relevant dose, had no visible effect on both MCF-7 and 4-T1 tumorspheres after 48 h. Dox-treated tumorspheres resembled that of untreated spheroids; no dye uptake and

luminescent. The structural integrity of dox-treated tumorspheres was also maintained after 48 h treatment, with no signs of disintegration.

To quantify these findings, tumorspheres were harvested and an MTS cell viability assay was performed. MCF-7 tumorspheres were 5% viable compared to untreated controls and 4-T1 tumorspheres were 8% viable compared to untreated controls. Dox-treated tumorspheres of the MCF-7 and 4-T1 cell line were 98% and 99% viable, respectively, compared to untreated controls. *Lovitt et al.* demonstrated heightened resistance to doxorubicin in the same *in vitro* model mediated by cell-to-ECM interactions not observed in monolayer cultures[201]. Upregulation of survival proteins such as Bcl-2 were found to drastically decrease tumorsphere sensitivity to doxorubicin[202]. Although recognized as the most commonly used chemotherapeutic for breast cancer, doxorubicin's use in single drug regimens make it a substrate of anticancer compound resistance mechanisms, which was further confirmed by our findings[203]. Thus, we attribute the marked effectiveness of our combinatorial therapy towards tumorspheres to its multi-pathway targeting properties, attacking both the highly replicative cells of the exterior and the slow growing cells of the interior.

In conclusion, we have shown that our novel combinatorial therapy is able to overcome powerful tumorsphere resistance mechanisms and significantly decrease viability in two 3D tumor models, whereas a conventional chemotherapy had no significant effect. Tumorspheres are the center of recent praise due to their clinical translatability and how well they model tumor conditions and processes found in tissue. As a defined liaison between *in vitro* and *in vivo* studies, we are confident in the clinical predictivity observed from the above studies. The ability to circumvent drug resistance

and induce a strong cytotoxic effect in these tumor models holds great promise for our novel drug combination as a developing therapy.

# APPENDIX

## Appendix A: Permission to Reproduce Copyrighted Material

Permission to use Figure 1. License Number: 4926720197730

Permission to use Figure 2. License Number: 4926720709509

Permission to use Figure 4. License Number: 4926730230504

Permission to use Figure 5. License Number: 4926730358613

Permission to use Figure 7. License Number: 4926730624135

Permission to use Figure 10. License Number: 4926731182573

Permission to use Figure 12. License Number: 4926731503107

Permission to use Figure 13. License Number: 4926740127005

## REFERENCES


1. Barnes JL, Zubair M, John K, Poirier MC, Martin FL. Carcinogens and DNA damage. *Biochem Soc Trans*. 2018. doi:10.1042/BST20180519

2. Kucab JE, Zou X, Morganella S, et al. A Compendium of Mutational Signatures of Environmental Agents. *Cell*. 2019. doi:10.1016/j.cell.2019.03.001

3. Coussens LM, Werb Z. Inflammation and cancer. *Nature*. 2002. doi:10.1038/nature01322

4. Cavallo F, De Giovanni C, Nanni P, Forni G, Lollini PL. 2011: The immune hallmarks of cancer. In: *Cancer Immunology, Immunotherapy*. ; 2011. doi:10.1007/s00262-010-0968-0

5. Broustas CG, Lieberman HB. DNA Damage Response Genes and the Development of Cancer Metastasis. *Radiat Res*. 2014;181(2):111-130. doi:10.1667/RR13515.1

6. Boyd NF, Martin LJ, Bronskill M, Yaffe MJ, Duric N, Minkin S. Breast tissue composition and susceptibility to breast cancer. *J Natl Cancer Inst*. 2010. doi:10.1093/jnci/djq239

7. Ataollahi MR, Sharifi J, Paknahad MR, Paknahad A. Breast cancer and associated factors: a review. *J Med Life*. 2015.

8. Petrucelli N, Daly MB, Pal T. *BRCA1- and BRCA2-Associated Hereditary Breast and Ovarian Cancer*.; 1993.

9. Boulton SJ. Cellular functions of the BRCA tumour-suppressor proteins. *Biochem Soc Trans*. 2006. doi:10.1042/BST0340633

10. O'Donovan PJ, Livingston DM. BRCA1 and BRCA2: Breast/ovarian cancer susceptibility gene products and participants in DNA double-strand break repair. *Carcinogenesis*. 2010. doi:10.1093/carcin/bgq069

11. Dall GV, Britt KL. Estrogen effects on the mammary gland in early and late life and breast cancer risk. *Front Oncol*. 2017. doi:10.3389/fonc.2017.00110

12. Wang K, Li F, Chen L, Lai YM, Zhang X, Li HY. Change in risk of breast cancer after receiving hormone replacement therapy by considering effect-modifiers: A systematic review and dose-response meta-analysis of prospective studies. *Oncotarget*. 2017. doi:10.18632/oncotarget.20154

13. Yue W, Wang JP, Li Y, et al. Effects of estrogen on breast cancer development: Role of estrogen receptor independent mechanisms. *Int J Cancer*. 2010.

doi:10.1002/ijc.25207

14. Hanahan D, Weinberg RA. Hallmarks of cancer: The next generation. *Cell*. 2011. doi:10.1016/j.cell.2011.02.013

15. Fitzmaurice C, Dicker D, Pain A, et al. The Global Burden of Cancer 2013. *JAMA Oncol*. 2015. doi:10.1001/jamaoncol.2015.0735

16. Heasley LE. Autocrine and paracrine signaling through neuropeptide receptors in human cancer. *Oncogene*. 2001. doi:10.1038/sj.onc.1204183

17. Sporn MB, Roberts AB. Autocrine growth factors and cancer. *Nature*. 1985. doi:10.1038/313745a0

18. Jakowlew SB. Transforming growth factor-β in cancer and metastasis. *Cancer Metastasis Rev*. 2006. doi:10.1007/s10555-006-9006-2

19. Walsh JH, Karnes WE, Cuttitta F, Walker A. Autocrine growth factors and solid tumor malignancy. *West J Med*. 1991.

20. Sever R, Brugge JS. Signal transduction in cancer. *Cold Spring Harb Perspect Med*. 2015. doi:10.1101/cshperspect.a006098

21. Fresno Vara JÁ, Casado E, de Castro J, Cejas P, Belda-Iniesta C, González-Barón M. P13K/Akt signalling pathway and cancer. *Cancer Treat Rev*. 2004. doi:10.1016/j.ctrv.2003.07.007

22. Inoue K, Fry EA. Haploinsufficient tumor suppressor genes. In: *Advances in Medicine and Biology*. ; 2017.

23. Chinnam M, Goodrich DW. *RB1, Development, and Cancer*.; 2011. doi:10.1016/B978-0-12-380916-2.00005-X

24. Toufektchan E, Toledo F. The guardian of the genome revisited: P53 downregulates genes required for telomere maintenance, DNA repair, and centromere structure. *Cancers (Basel)*. 2018. doi:10.3390/cancers10050135

25. Gartel AL, Tyner AL. The role of the cyclin-dependent kinase inhibitor p21 in apoptosis. *Mol Cancer Ther*. 2002.

26. Zhao J, Zhang Z, Liao Y, Du W. Mutation of the retinoblastoma tumor suppressor gene sensitizes cancers to mitotic inhibitor induced cell death. *Am J Cancer Res*. 2014.

27. Petrilli AM, Fernández-Valle C. Role of Merlin/NF2 inactivation in tumor biology. *Oncogene*. 2016. doi:10.1038/onc.2015.125

28. Hahn WC. Role of telomeres and telomerase in the pathogenesis of human cancer. *J Clin Oncol*. 2003. doi:10.1200/JCO.2003.06.018

29. Shay JW. Role of telomeres and telomerase in aging and cancer. *Cancer Discov*. 2016. doi:10.1158/2159-8290.CD-16-0062

30. Jafri MA, Ansari SA, Alqahtani MH, Shay JW. Roles of telomeres and telomerase

in cancer, and advances in telomerase-targeted therapies. *Genome Med*. 2016. doi:10.1186/s13073-016-0324-x

31. Vinagre J, Almeida A, Pópulo H, et al. Frequency of TERT promoter mutations in human cancers. *Nat Commun*. 2013. doi:10.1038/ncomms3185

32. Reynolds LP, Grazul-Bilska AT, Redmer DA. Angiogenesis in the female reproductive organs: Pathological implications. *Int J Exp Pathol*. 2002. doi:10.1046/j.1365-2613.2002.00277.x

33. Bergers G, Benjamin LE. Tumorigenesis and the angiogenic switch. *Nat Rev Cancer*. 2003. doi:10.1038/nrc1093

34. Walia A, Yang JF, Huang YH, Rosenblatt MI, Chang JH, Azar DT. Endostatin's emerging roles in angiogenesis, lymphangiogenesis, disease, and clinical applications. *Biochim Biophys Acta - Gen Subj*. 2015. doi:10.1016/j.bbagen.2015.09.007

35. Ramchandran R, Karumanchi SA, Hanai J ichi, Alper SL, Sukhatme VP. Cellular actions and signaling by endostatin. *Crit Rev Eukaryot Gene Expr*. 2002. doi:10.1615/CritRevEukaryotGeneExpr.v12.i3.20

36. Sherwood LM, Parris EE, Folkman J. Tumor Angiogenesis: Therapeutic Implications. *N Engl J Med*. 1971. doi:10.1056/NEJM197111182852108

37. Chen C, Parangi S, Tolentino MJ, et al. A Strategy to Discover Circulating Angiogenesis Inhibitors Generated by Human Tumors. *Cancer Res*. 1995.

38. Nishida N, Yano H, Nishida T, Kamura T, Kojiro M. Angiogenesis in cancer. *Vasc Health Risk Manag*. 2006;2(3):213-219. doi:10.2147/vhrm.2006.2.3.213

39. Carmeliet P, Jain RK. Molecular mechanisms and clinical applications of angiogenesis. *Nature*. 2011. doi:10.1038/nature10144

40. Tong RT, Boucher Y, Kozin S V., Winkler F, Hicklin DJ, Jain RK. Vascular normalization by vascular endothelial growth factor receptor 2 blockade induces a pressure gradient across the vasculature and improves drug penetration in tumors. *Cancer Res*. 2004. doi:10.1158/0008-5472.CAN-04-0074

41. McDonald DM, Baluk P. Significance of blood vessel leakiness in cancer. *Cancer Res*. 2002.

42. Yuan F, Chen Y, Dellian M, Safabakhsh N, Ferrara N, Jain RK. Time-dependent vascular regression and permeability changes in established human tumor xenografts induced by an anti-vascular endothelial growth factor/vascular permeability factor antibody. *Proc Natl Acad Sci U S A*. 1996. doi:10.1073/pnas.93.25.14765

43. Chiang SPH, Cabrera RM, Segall JE. Tumor cell intravasation. *Am J Physiol - Cell Physiol*. 2016. doi:10.1152/ajpcell.00238.2015

44. Caplan AI. Mesenchymal stem cells. *J Orthop Res*. 1991.

doi:10.1002/jor.1100090504

45. Van Zijl F, Krupitza G, Mikulits W. Initial steps of metastasis: Cell invasion and endothelial transmigration. *Mutat Res - Rev Mutat Res*. 2011. doi:10.1016/j.mrrev.2011.05.002

46. Lamouille S, Xu J, Derynck R. Molecular mechanisms of epithelial-mesenchymal transition. *Nat Rev Mol Cell Biol*. 2014. doi:10.1038/nrm3758

47. Friedl P, Gilmour D. Collective cell migration in morphogenesis, regeneration and cancer. *Nat Rev Mol Cell Biol*. 2009. doi:10.1038/nrm2720

48. Friedl P, Hegerfeldt Y, Tusch M. Collective cell migration in morphogenesis and cancer. *Int J Dev Biol*. 2004. doi:10.1387/ijdb.041821pf

49. Condeelis J, Segall JE. Intravital imaging of cell movement in tumours. *Nat Rev Cancer*. 2003. doi:10.1038/nrc1231

50. Sporn MB. The war on cancer. *Lancet*. 1996. doi:10.1016/S0140-6736(96)91015-6

51. Houghton AN, Guevara-Patiño JA. Immune recognition of self in immunity against cancer. *J Clin Invest*. 2004;114(4):468-471. doi:10.1172/JCI200422685

52. Garrido F, Ruiz-Cabello F, Cabrera T, et al. Implications for immunosurveillance of altered HLA class I phenotypes in human tumours. *Immunol Today*. 1997. doi:10.1016/S0167-5699(96)10075-X

53. Beatty GL, Gladney WL. Immune escape mechanisms as a guide for cancer immunotherapy. *Clin Cancer Res*. 2015. doi:10.1158/1078-0432.CCR-14-1860

54. Brightwell RM, Grzankowski KS, Lele S, et al. The CD47 “don’t eat me signal” is highly expressed in human ovarian cancer. *Gynecol Oncol*. 2016. doi:10.1016/j.ygyno.2016.08.325

55. Pardoll DM. The blockade of immune checkpoints in cancer immunotherapy. *Nat Rev Cancer*. 2012. doi:10.1038/nrc3239

56. Dong H, Strome SE, Salomao DR, et al. Tumor-associated B7-H1 promotes T-cell apoptosis: A potential mechanism of immune evasion. *Nat Med*. 2002. doi:10.1038/nm730

57. Principe DR, Mangan RJ, Grippo PJ. Transforming Growth Factor β. In: *Cancer Therapeutic Targets*. ; 2017. doi:10.1007/978-1-4419-0717-2_137

58. Gabrilovich DI, Chen HL, Girgis KR, et al. Production of vascular endothelial growth factor by human tumors inhibits the functional maturation of dendritic cells. *Nat Med*. 1996. doi:10.1038/nm1096-1096

59. Rabinovich GA, Gabrilovich D, Sotomayor EM. Immunosuppressive Strategies that are Mediated by Tumor Cells. *Annu Rev Immunol*. 2007;25(1):267-296. doi:10.1146/annurev.immunol.25.022106.141609

60. Denko NC, Fontana LA, Hudson KM, et al. Investigating hypoxic tumor

physiology through gene expression patterns. *Oncogene*. 2003. doi:10.1038/sj.onc.1206703

61. Dvorak HF. Tumors: wounds that do not heal. Similarities between tumor stroma generation and wound healing. *N Engl J Med*. 1986. doi:10.1056/NEJM198612253152606

62. Chaudhary B, Elkord E. Regulatory T Cells in the Tumor Microenvironment and Cancer Progression: Role and Therapeutic Targeting. *Vaccines*. 2016;4(3):28. doi:10.3390/vaccines4030028

63. Umansky V, Blattner C, Gebhardt C, Utikal J. The Role of Myeloid-Derived Suppressor Cells (MDSC) in Cancer Progression. *Vaccines*. 2016;4(4):36. doi:10.3390/vaccines4040036

64. Mantovani A, Schioppa T, Porta C, Allavena P, Sica A. Role of tumor-associated macrophages in tumor progression and invasion. *Cancer Metastasis Rev*. 2006;25(3):315-322. doi:10.1007/s10555-006-9001-7

65. Dang C V., Gao P, Kim J. Warburg Effect. In: *Encyclopedia of Cancer*. ; 2017. doi:10.1007/978-3-662-46875-3_6229

66. Heiden MGV, Cantley LC, Thompson CB. Understanding the warburg effect: The metabolic requirements of cell proliferation. *Science (80- )*. 2009. doi:10.1126/science.1160809

67. Jones RG, Thompson CB. Tumor suppressors and cell metabolism: A recipe for cancer growth. *Genes Dev*. 2009. doi:10.1101/gad.1756509

68. Semenza GL. Defining the role of hypoxia-inducible factor 1 in cancer biology and therapeutics. *Oncogene*. 2010. doi:10.1038/onc.2009.441

69. Kroemer G, Pouyssegur J. Tumor Cell Metabolism: Cancer's Achilles' Heel. *Cancer Cell*. 2008. doi:10.1016/j.ccr.2008.05.005

70. Elmore S. Apoptosis: A Review of Programmed Cell Death. *Toxicol Pathol*. 2007. doi:10.1080/01926230701320337

71. Green DR, Kroemer G. The pathophysiology of mitochondrial cell death. *Science (80- )*. 2004. doi:10.1126/science.1099320

72. Walczak H, Krammer PH. The CD95 (APO-1/Fas) and the TRAIL (APO-2L) apoptosis systems. *Exp Cell Res*. 2000. doi:10.1006/excr.2000.4840

73. Fulda S, Debatin KM. Extrinsic versus intrinsic apoptosis pathways in anticancer chemotherapy. *Oncogene*. 2006. doi:10.1038/sj.onc.1209608

74. Wood W, Turmaine M, Weber R, et al. Mesenchymal cells engulf and clear apoptotic footplate cells in macrophageless PU.1 null mouse embryos. *Development*. 2000.

75. Junttila MR, Evan GI. P53 a Jack of all trades but master of none. *Nat Rev Cancer*. 2009. doi:10.1038/nrc2728

76. Lowe SW, Cepero E, Evan G. Intrinsic tumour suppression. *Nature*. 2004. doi:10.1038/nature03098

77. Choi AMK, Wang X. Apoptosis. In: *Encyclopedia of Respiratory Medicine, Four-Volume Set*. ; 2006. doi:10.1016/B0-12-370879-6/00030-2

78. Wu Y, Zhao D, Zhuang J, Zhang F, Xu C. Caspase-8 and Caspase-9 functioned differently at different stages of the cyclic stretch-induced apoptosis in human periodontal ligament cells. *PLoS One*. 2016. doi:10.1371/journal.pone.0168268

79. Adams JM, Cory S. The Bcl-2 apoptotic switch in cancer development and therapy. *Oncogene*. 2007. doi:10.1038/sj.onc.1210220

80. LeRoith D, Roberts CT. The insulin-like growth factor system and cancer. *Cancer Lett*. 2003. doi:10.1016/S0304-3835(03)00159-9

81. Mahmood Z, Shukla Y. Death receptors: Targets for cancer therapy. *Exp Cell Res*. 2010. doi:10.1016/j.yexcr.2009.12.011

82. Frenzel A, Grespi F, Chmelewskij W, Villunger A. Bcl2 family proteins in carcinogenesis and the treatment of cancer. *Apoptosis*. 2009. doi:10.1007/s10495-008-0300-z

83. DeVita VT, Chu E. A history of cancer chemotherapy. *Cancer Res*. 2008. doi:10.1158/0008-5472.CAN-07-6611

84. Szikriszt B, Póti Á, Pipek O, et al. A comprehensive survey of the mutagenic impact of common cancer cytotoxics. *Genome Biol*. 2016;17:99. doi:10.1186/s13059-016-0963-7

85. Du XL, Chan W, Giordano S, et al. Variation in modes of chemotherapy administration for breast carcinoma and association with hospitalization for chemotherapy-related toxicity. *Cancer*. 2005. doi:10.1002/cncr.21271

86. Liu B, Ezeogu L, Zellmer L, Yu B, Xu N, Joshua Liao D. Protecting the normal in order to better kill the cancer. *Cancer Med*. 2015. doi:10.1002/cam4.488

87. Zhang J, Lou X, Zellmer L, Liu S, Xu N, Liao DJ. Just like the rest of evolution in Mother Nature, the evolution of cancers may be driven by natural selection, and not by haphazard mutations. *Oncoscience*. 2014. doi:10.18632/oncoscience.83

88. Galluzzi L, Vacchelli E, Bravo-San Pedro JM, et al. Classification of current anticancer immunotherapies. *Oncotarget*. 2014. doi:10.18632/oncotarget.2998

89. Morrissey K, Yuraszeck T, Li CC, Zhang Y, Kasichayanula S. Immunotherapy and Novel Combinations in Oncology: Current Landscape, Challenges, and Opportunities. *Clin Transl Sci*. 2016. doi:10.1111/cts.12391

90. Fares CM, Van Allen EM, Drake CG, Allison JP, Hu-Lieskovan S. Mechanisms of Resistance to Immune Checkpoint Blockade: Why Does Checkpoint Inhibitor Immunotherapy Not Work for All Patients? *Am Soc Clin Oncol Educ B*. 2019. doi:10.1200/edbk_240837

91. Guttà C, Rahman A, Aura C, et al. Low expression of pro-apoptotic proteins Bax, Bak and Smac indicates prolonged progression-free survival in chemotherapy-treated metastatic melanoma. *Cell Death Dis*. 2020. doi:10.1038/s41419-020-2309-3

92. Huang S. Tumor progression: Chance and necessity in Darwinian and Lamarckian somatic (mutationless) evolution. *Prog Biophys Mol Biol*. 2012. doi:10.1016/j.pbiomolbio.2012.05.001

93. Ganapathy-Kanniappan S. Taming tumor glycolysis and potential implications for immunotherapy. *Front Oncol*. 2017. doi:10.3389/fonc.2017.00036

94. WICK AN, DRURY DR, NAKADA HI, WOLFE JB. Localization of the primary metabolic block produced by 2-deoxyglucose. *J Biol Chem*. 1957;224(2):963-969. doi:10.1126/science.1321497

95. Kurtoglu M, Gao N, Shang J, et al. Under normoxia, 2-deoxy-D-glucose elicits cell death in select tumor types not by inhibition of glycolysis but by interfering with N-linked glycosylation. *Mol Cancer Ther*. 2007;6(11):3049-3058. doi:10.1158/1535-7163.MCT-07-0310

96. Merchan JR, Kovács K, Railsback JW, et al. Antiangiogenic activity of 2-deoxy-D-glucose. *PLoS One*. 2010;5(10). doi:10.1371/journal.pone.0013699

97. Rajagopalan PTR, Zhang Z, McCourt L, Dwyer M, Benkovic SJ, Hammes GG. Interaction of dihydrofolate reductase with methotrexate: ensemble and single-molecule kinetics. *Proc Natl Acad Sci U S A*. 2002;99(21):13481-13486. doi:10.1073/pnas.172501499

98. Goodsell DS. The molecular perspective: Methotrexate. *Stem Cells*. 1999;17(5):314-315. doi:10.1002/stem.170314

99. Tian H, Cronstein BN. Understanding the mechanisms of action of methotrexate: Implications for the treatment of rheumatoid arthritis. *Bull NYU Hosp Jt Dis*. 2007;65(3):168-173.

100. Landreneau JP, Shurin MR, Agassandian M V., Keskinov AA, Ma Y, Shurin G V. Immunological Mechanisms of Low and Ultra-Low Dose Cancer Chemotherapy. *Cancer Microenviron*. 2015;8(2):57-64. doi:10.1007/s12307-013-0141-3

101. Tai MC, Tsang SY, Chang LYF, Xue H. Therapeutic Potential of Wogonin: A Naturally Occurring Flavonoid. *CNS Drug Rev*. 2006;11(2):141-150. doi:10.1111/j.1527-3458.2005.tb00266.x

102. Wu X, Zhang H, Salmani JMM, Fu R, Chen B. Advances of wogonin, an extract from Scutellaria baicalensis, for the treatment of multiple tumors. *Onco Targets Ther*. 2016;9:2935-2943. doi:10.2147/OTT.S105586

103. Xiao W, Yin M, Wu K, et al. High-dose wogonin exacerbates DSS-induced colitis by up-regulating effector T cell function and inhibiting Treg cell. *J Cell Mol Med*. 2017;21(2):286-298. doi:10.1111/jcmm.12964

104. Maher JC, Wangpaichitr M, Savaraj N, Kurtoglu M, Lampidis TJ. Hypoxia-inducible factor-1 confers resistance to the glycolytic inhibitor 2-deoxy-D-glucose. *Mol Cancer Ther*. 2007;6(2):732-741. doi:10.1158/1535-7163.MCT-06-0407

105. Dean M, Hamon Y, Chimini G. The human ATP-binding cassette (ABC) transporter superfamily. *J Lipid Res*. 2001. doi:10.1101/gr.184901

106. Paulusma CC, Kool M, Bosma PJ, et al. A mutation in the human canalicular multispecific organic anion transporter gene causes the Dubin-Johnson syndrome. *Hepatology*. 1997. doi:10.1002/hep.510250635

107. Masuda M, I'izuka Y, Yamazaki M, et al. Methotrexate is excreted into the bile by canalicular multispecific organic anion transporter in rats. *Cancer Res*. 1997.

108. Kool M, Van Der Linden M, De Haas M, et al. MRP3, an organic anion transporter able to transport anti-cancer drugs. *Proc Natl Acad Sci U S A*. 1999. doi:10.1073/pnas.96.12.6914

109. Yu CP, Hsieh YC, Shia CS, et al. Increased Systemic Exposure of Methotrexate by a Polyphenol-Rich Herb via Modulation on Efflux Transporters Multidrug Resistance-Associated Protein 2 and Breast Cancer Resistance Protein. *J Pharm Sci*. 2016;105(1):343-349. doi:10.1016/j.xphs.2015.11.031

110. Chorawala M, Oza P, Shah G. Mechanisms of anticancer drugs resistance: an overview. *Int J Pharm Sci Drug Res*. 2012.

111. Anderson KG, Stromnes IM, Greenberg PD. Obstacles Posed by the Tumor Microenvironment to T cell Activity: A Case for Synergistic Therapies. *Cancer Cell*. 2017. doi:10.1016/j.ccell.2017.02.008

112. Chen S hong, Lahav G. Two is better than one; toward a rational design of combinatorial therapy. *Curr Opin Struct Biol*. 2016. doi:10.1016/j.sbi.2016.07.020

113. Lord CJ, Tutt ANJ, Ashworth A. Synthetic lethality and cancer therapy: Lessons learned from the development of PARP inhibitors. *Annu Rev Med*. 2015. doi:10.1146/annurev-med-050913-022545

114. Bosch A, Li Z, Bergamaschi A, et al. PI3K inhibition results in enhanced estrogen receptor function and dependence in hormone receptor-positive breast cancer. *Sci Transl Med*. 2015. doi:10.1126/scitranslmed.aaa4442

115. Song X, Yao J, Wang F, et al. Wogonin inhibits tumor angiogenesis via degradation of HIF-1α protein. *Toxicol Appl Pharmacol*. 2013;271(2):144-155. doi:10.1016/j.taap.2013.04.031

116. Zhong H, De Marzo AM, Laughner E, et al. Overexpression of hypoxia-inducible factor 1α in common human cancers and their metastases. *Cancer Res*. 1999.

117. Eales KL, Hollinshead KER, Tennant DA. Hypoxia and metabolic adaptation of cancer cells. *Oncogenesis*. 2016. doi:10.1038/oncsis.2015.50

118. Szymański P, Markowicz M, Mikiciuk-Olasik E. Adaptation of high-throughput

screening in drug discovery-toxicological screening tests. *Int J Mol Sci*. 2012. doi:10.3390/ijms13010427

119. Friberg S, Nystrom A. Cancer Metastases: Early Dissemination and Late Recurrences. *Cancer Growth Metastasis*. 2015. doi:10.4137/cgm.s31244

120. Lou X, Zhang J, Liu S, Lou X, Liao DJ. The other side of the coin: The tumor-suppressive aspect of oncogenes and the oncogenic aspect of tumor-suppressive genes, such as those along the CCND–CDK4/6–RB axis. *Cell Cycle*. 2014. doi:10.4161/cc.29082

121. Kanti V, Nuwayhid R, Lindner J, et al. Analysis of quantitative changes in hair growth during treatment with chemotherapy or tamoxifen in patients with breast cancer: A cohort study. *Br J Dermatol*. 2014. doi:10.1111/bjd.12716

122. Wang Y, Probin V, Zhou D. Cancer Therapy-Induced Residual Bone Marrow Injury: Mechanisms of Induction and Implication for Therapy. *Curr Cancer Ther Rev*. 2006. doi:10.2174/157339406777934717

123. Pauley JL, Panetta JC, Crews KR, et al. Between-course targeting of methotrexate exposure using pharmacokinetically guided dosage adjustments. *Cancer Chemother Pharmacol*. 2013. doi:10.1007/s00280-013-2206-x

124. Campbell JM, Bateman E, Stephenson MD, Bowen JM, Keefe DM, Peters MDJ. Methotrexate-induced toxicity pharmacogenetics: an umbrella review of systematic reviews and meta-analyses. *Cancer Chemother Pharmacol*. 2016. doi:10.1007/s00280-016-3043-5

125. Kornberg MD. The immunologic Warburg effect: Evidence and therapeutic opportunities in autoimmunity. *Wiley Interdiscip Rev Syst Biol Med*. 2020. doi:10.1002/wsbm.1486

126. Kornberg MD, Bhargava P, Kim PM, et al. Dimethyl fumarate targets GAPDH and aerobic glycolysis to modulate immunity. *Science (80- )*. 2018. doi:10.1126/science.aan4665

127. Huang HC, Hsieh LM, Chen HW, Lin YS, Chen JS. Effects of baicalein and esculetin on transduction signals and growth factors expression in T-lymphoid leukemia cells. *Eur J Pharmacol Mol Pharmacol*. 1994. doi:10.1016/0922-4106(94)90121-X

128. Chen YC, Shen SC, Lee WR, et al. Wogonin and fisetin induction of apoptosis through activation of caspase 3 cascade and alternative expression of p21 protein in hepatocellular carcinoma cells SK-HEP-1. *Arch Toxicol*. 2002. doi:10.1007/s00204-002-0346-6

129. Lin CM, Chang H, Chen YH, Wu IH, Chiu JH. Wogonin inhibits IL-6-induced angiogenesis via down-regulation of VEGF and VEGFR-1, not VEGFR-2. *Planta Med*. 2006. doi:10.1055/s-2006-951692

130. Hui KM, Huen MSY, Wang HY, et al. Anxiolytic effect of wogonin, a benzodiazepine receptor ligand isolated from Scutellaria baicalensis Georgi.

*Biochem Pharmacol*. 2002. doi:10.1016/S0006-2952(02)01347-3

131. Taylor CT, Colgan SP. Regulation of immunity and inflammation by hypoxia in immunological niches. *Nat Rev Immunol*. 2017. doi:10.1038/nri.2017.103

132. Liston DR, Davis M. Clinically relevant concentrations of anticancer drugs: A guide for nonclinical studies. *Clin Cancer Res*. 2017. doi:10.1158/1078-0432.CCR-16-3083

133. Perdomo-Celis F, Salgado DM, Castañeda DM, Narváez CF. Viability and functionality of cryopreserved peripheral blood mononuclear cells in pediatric dengue. *Clin Vaccine Immunol*. 2016. doi:10.1128/CVI.00038-16

134. Lafourcade A, His M, Baglietto L, Boutron-Ruault MC, Dossus L, Rondeau V. Factors associated with breast cancer recurrences or mortality and dynamic prediction of death using history of cancer recurrences: The French E3N cohort. *BMC Cancer*. 2018. doi:10.1186/s12885-018-4076-4

135. Singh R, Letai A, Sarosiek K. Regulation of apoptosis in health and disease: the balancing act of BCL-2 family proteins. *Nat Rev Mol Cell Biol*. 2019. doi:10.1038/s41580-018-0089-8

136. Yatim N, Jusforgues-Saklani H, Orozco S, et al. RIPK1 and NF-kB signaling in dying cells determines cross-priming of CD8+ T cells. *Science (80- )*. 2015. doi:10.1126/science.aad0395

137. Stearns-Kurosawa DJ, Osuchowski MF, Valentine C, Kurosawa S, Remick DG. The pathogenesis of sepsis. *Annu Rev Pathol Mech Dis*. 2011. doi:10.1146/annurev-pathol-011110-130327

138. Zhou J, Wang G, Chen Y, Wang H, Hua Y, Cai Z. Immunogenic cell death in cancer therapy: Present and emerging inducers. *J Cell Mol Med*. 2019. doi:10.1111/jcmm.14356

139. Menger L, Vacchelli E, Adjemian S, et al. Cardiac glycosides exert anticancer effects by inducing immunogenic cell death. *Sci Transl Med*. 2012. doi:10.1126/scitranslmed.3003807

140. Lu YC, Weng WC, Lee H. Functional roles of calreticulin in cancer biology. *Biomed Res Int*. 2015. doi:10.1155/2015/526524

141. Tuettenberg A, Schmitt E, Knop J, Jonuleit H. Dendritic Cell-Based Immunotherapy of Malignant Melanoma: Success and Limitations. *JDDG*. 2007. doi:10.1111/j.1610-0387.2007.06179.x

142. Apetoh L, Ghiringhelli F, Tesniere A, et al. Toll-like receptor 4-dependent contribution of the immune system to anticancer chemotherapy and radiotherapy. *Nat Med*. 2007;13(9):1050-1059. doi:10.1038/nm1622

143. Shiratsuchi A, Watanabe I, Takeuchi O, Akira S, Nakanishi Y. Inhibitory Effect of Toll-Like Receptor 4 on Fusion between Phagosomes and Endosomes/Lysosomes in Macrophages. *J Immunol*. 2004. doi:10.4049/jimmunol.172.4.2039

144. Zhang Z, Chen G, Zhou W, et al. Regulated ATP release from astrocytes through lysosome exocytosis. *Nat Cell Biol*. 2007. doi:10.1038/ncb1620

145. Michaud M, Martins I, Sukkurwala AQ, et al. Autophagy-dependent anticancer immune responses induced by chemotherapeutic agents in mice. *Science (80- ).* 2011;334(6062):1573-1577. doi:10.1126/science.1208347

146. Spurlock CF, Aune ZT, Tossberg JT, et al. Increased sensitivity to apoptosis induced by methotrexate is mediated by JNK. *Arthritis Rheum*. 2011. doi:10.1002/art.30457

147. Kosic M, Arsikin-Csordas K, Paunovic V, et al. Synergistic anticancer action of lysosomal membrane permeabilization and glycolysis inhibition. *J Biol Chem*. 2016. doi:10.1074/jbc.M116.752113

148. Afshar N, Black BE, Paschal BM. Retrotranslocation of the Chaperone Calreticulin from the Endoplasmic Reticulum Lumen to the Cytosol. *Mol Cell Biol*. 2005. doi:10.1128/mcb.25.20.8844-8853.2005

149. Panaretakis T, Joza N, Modjtahedi N, et al. The co-translocation of ERp57 and calreticulin determines the immunogenicity of cell death. *Cell Death Differ*. 2008;15(9):1499-1509. doi:10.1038/cdd.2008.67

150. Fucikova J, Kralikova P, Fialova A, et al. Human tumor cells killed by anthracyclines induce a tumor-specific immune response. *Cancer Res*. 2011;71(14):4821-4833. doi:10.1158/0008-5472.CAN-11-0950

151. Wang YJ, Fletcher R, Yu J, Zhang L. Immunogenic effects of chemotherapy-induced tumor cell death. *Genes Dis*. 2018. doi:10.1016/j.gendis.2018.05.003

152. Obeid M, Tesniere A, Ghiringhelli F, et al. Calreticulin exposure dictates the immunogenicity of cancer cell death. *Nat Med*. 2007;13(1):54-61. doi:10.1038/nm1523

153. Klune JR, Dhupar R, Cardinal J, Billiar TR, Tsung A. HMGB1: Endogenous danger signaling. *Mol Med*. 2008. doi:10.2119/2008-00034.Klune

154. Scaffidi P, Misteli T, Bianchi ME. Release of chromatin protein HMGB1 by necrotic cells triggers inflammation. *Nature*. 2002. doi:10.1038/nature00858

155. Apetoh L, Ghiringhelli F, Tesniere A, et al. Toll-like receptor 4-dependent contribution of the immune system to anticancer chemotherapy and radiotherapy. *Nat Med*. 2007. doi:10.1038/nm1622

156. Schiraldi M, Raucci A, Muñoz LM, et al. HMGB1 promotes recruitment of inflammatory cells to damaged tissues by forming a complex with CXCL12 and signaling via CXCR4. *J Exp Med*. 2012. doi:10.1084/jem.20111739

157. Florento L, Matias R, Tuaño E, Santiago K, Cruz F Dela, Tuazon A. Comparison of cytotoxic activity of anticancer drugs against various human tumor cell lines using in vitro cell-based approach. *Int J Biomed Sci*. 2012.

158. Galluzzi L, Buqué A, Kepp O, Zitvogel L, Kroemer G. Immunogenic cell death in cancer and infectious disease. *Nat Rev Immunol*. 2016;17(2):97-111. doi:10.1038/nri.2016.107

159. Michaud M, Martins I, Sukkurwala AQ, et al. Autophagy-dependent anticancer immune responses induced by chemotherapeutic agents in mice. *Science (80- ).* 2011. doi:10.1126/science.1208347

160. Martins I, Wang Y, Michaud M, et al. Molecular mechanisms of ATP secretion during immunogenic cell death. *Cell Death Differ*. 2014. doi:10.1038/cdd.2013.75

161. Lotze MT, Tracey KJ. High-mobility group box 1 protein (HMGB1): Nuclear weapon in the immune arsenal. *Nat Rev Immunol*. 2005. doi:10.1038/nri1594

162. Ghiringhelli F, Apetoh L, Tesniere A, et al. Activation of the NLRP3 inflammasome in dendritic cells induces IL-1B-dependent adaptive immunity against tumors. *Nat Med*. 2009. doi:10.1038/nm.2028

163. Vacchelli E, Galluzzi L, Fridman WH, et al. Trial watch: Chemotherapy with immunogenic cell death inducers. *Oncoimmunology*. 2012. doi:10.4161/onci.1.2.19026

164. Zarandi PK, Mirakabadi AZ, Sotoodehnejadnematalahi F. Cytotoxic and anticancer effects of ICD-85 (Venom derived peptides) in human breast adenocarcinoma and normal human dermal fibroblasts. *Iran J Pharm Res*. 2019. doi:10.22037/ijpr.2019.2341

165. Di Somma S, Amato J, Iaccarino N, et al. G-quadruplex binders induce immunogenic cell death markers in aggressive breast cancer cells. *Cancers (Basel)*. 2019. doi:10.3390/cancers11111797

166. Yin SY, Efferth T, Jian FY, et al. Immunogenicity of mammary tumor cells can be induced by shikonin via direct binding-interference with hnRNPA1. *Oncotarget*. 2016. doi:10.18632/oncotarget.9660

167. Gao J, Deng F, Jia W. Inhibition of indoleamine 2,3-dioxygenase enhances the therapeutic efficacy of immunogenic chemotherapeutics in breast cancer. *J Breast Cancer*. 2019. doi:10.4048/jbc.2019.22.e23

168. Breslin S, O'Driscoll L. Three-dimensional cell culture: The missing link in drug discovery. *Drug Discov Today*. 2013. doi:10.1016/j.drudis.2012.10.003

169. Baker BM, Chen CS. Deconstructing the third dimension-how 3D culture microenvironments alter cellular cues. *J Cell Sci*. 2012. doi:10.1242/jcs.079509

170. Wozniak MA, Desai R, Solski PA, Der CJ, Keely PJ. ROCK-generated contractility regulates breast epithelial cell differentiation in response to the physical properties of a three-dimensional collagen matrix. *J Cell Biol*. 2003. doi:10.1083/jcb.200305010

171. Engler AJ, Sen S, Sweeney HL, Discher DE. Matrix Elasticity Directs Stem Cell Lineage Specification. *Cell*. 2006. doi:10.1016/j.cell.2006.06.044

172. Ivascu A, Kubbies M. Rapid generation of single-tumor spheroids for high-throughput cell function and toxicity analysis. *J Biomol Screen*. 2006. doi:10.1177/1087057106292763

173. Lin RZ, Chang HY. Recent advances in three-dimensional multicellular spheroid culture for biomedical research. *Biotechnol J*. 2008. doi:10.1002/biot.200700228

174. Wang C, Tang Z, Zhao Y, Yao R, Li L, Sun W. Three-dimensional in vitro cancer models: A short review. *Biofabrication*. 2014. doi:10.1088/1758-5082/6/2/022001

175. Pampaloni F, Reynaud EG, Stelzer EHK. The third dimension bridges the gap between cell culture and live tissue. *Nat Rev Mol Cell Biol*. 2007. doi:10.1038/nrm2236

176. Jong BK. Three-dimensional tissue culture models in cancer biology. *Semin Cancer Biol*. 2005. doi:10.1016/j.semcancer.2005.05.002

177. Trédan O, Galmarini CM, Patel K, Tannock IF. Drug resistance and the solid tumor microenvironment. *J Natl Cancer Inst*. 2007. doi:10.1093/jnci/djm135

178. Speight PM, Farthing PM. The pathology of oral cancer. *Br Dent J*. 2018. doi:10.1038/sj.bdj.2018.926

179. Fuchs E, Tumbar T, Guasch G. Socializing with the neighbors: Stem cells and their niche. *Cell*. 2004. doi:10.1016/S0092-8674(04)00255-7

180. Petersen OW, Ronnov-Jessen L, Howlett AR, Bissell MJ. Interaction with basement membrane serves to rapidly distinguish growth and differentiation pattern of normal and malignant human breast epithelial cells. *Proc Natl Acad Sci U S A*. 1992. doi:10.1073/pnas.89.19.9064

181. Griffith LG, Swartz MA. Capturing complex 3D tissue physiology in vitro. *Nat Rev Mol Cell Biol*. 2006. doi:10.1038/nrm1858

182. Hamill OP, Martinac B. Molecular basis of mechanotransduction in living cells. *Physiol Rev*. 2001. doi:10.1152/physrev.2001.81.2.685

183. Holzwarth JM, Ma PX. Biomimetic nanofibrous scaffolds for bone tissue engineering. *Biomaterials*. 2011. doi:10.1016/j.biomaterials.2011.09.009

184. Li Q, Chen C, Kapadia A, et al. 3D models of epithelial-mesenchymal transition in breast cancer metastasis: High-throughput screening assay development, validation, and pilot screen. *J Biomol Screen*. 2011. doi:10.1177/1087057110392995

185. Buczacki S. Cancer Stem Cells. In: *Encyclopedia of Cell Biology*. ; 2016. doi:10.1016/B978-0-12-394447-4.30119-5

186. Lawson JC, Blatch GL, Edkins AL. Cancer stem cells in breast cancer and metastasis. *Breast Cancer Res Treat*. 2009. doi:10.1007/s10549-009-0524-9

187. Al-Hajj M, Wicha MS, Benito-Hernandez A, Morrison SJ, Clarke MF. Prospective identification of tumorigenic breast cancer cells. *Proc Natl Acad Sci U S A*. 2003.

doi:10.1073/pnas.0530291100

188. Das T, Nair RR, Green R, et al. Actinomycin D down-regulates SOX2 expression and induces death in breast cancer stem cells. *Anticancer Res*. 2017. doi:10.21873/anticanres.11496

189. Leis O, Eguiara A, Lopez-Arribillaga E, et al. Sox2 expression in breast tumours and activation in breast cancer stem cells. *Oncogene*. 2012. doi:10.1038/onc.2011.338

190. Hayashi T, Ding Q, Kuwahata T, et al. Interferon-alpha modulates the chemosensitivity of CD133-expressing pancreatic cancer cells to gemcitabine. *Cancer Sci*. 2012. doi:10.1111/j.1349-7006.2012.02235.x

191. Pastrana E, Silva-Vargas V, Doetsch F. Eyes wide open: A critical review of sphere-formation as an assay for stem cells. *Cell Stem Cell*. 2011. doi:10.1016/j.stem.2011.04.007

192. Begicevic RR, Falasca M. ABC transporters in cancer stem cells: Beyond chemoresistance. *Int J Mol Sci*. 2017. doi:10.3390/ijms18112362

193. Safa AR. Resistance to cell death and its modulation in cancer stem cells. *Crit Rev Oncog*. 2016. doi:10.1615/CritRevOncog.2016016976

194. Steinbichler TB, Dudás J, Skvortsov S, Ganswindt U, Riechelmann H, Skvortsova II. Therapy resistance mediated by cancer stem cells. *Semin Cancer Biol*. 2018. doi:10.1016/j.semcancer.2018.11.006

195. Dieter SM, Ball CR, Hoffmann CM, et al. Distinct types of tumor-initiating cells form human colon cancer tumors and metastases. *Cell Stem Cell*. 2011. doi:10.1016/j.stem.2011.08.010

196. Lichner Z, Saleh C, Subramaniam V, Seivwright A, Prud'homme GJ, Yousef GM. miR-17 inhibition enhances the formation of kidney cancer spheres with stem cell/tumor initiating cell properties. *Oncotarget*. 2015. doi:10.18632/oncotarget.1901

197. Zhang S, Zhang D, Sun B. Vasculogenic mimicry: Current status and future prospects. *Cancer Lett*. 2007. doi:10.1016/j.canlet.2006.12.036

198. Larson AR, Lee CW, Lezcano C, et al. Melanoma spheroid formation involves laminin-associated vasculogenic mimicry. *Am J Pathol*. 2014. doi:10.1016/j.ajpath.2013.09.020

199. Ryoo IG, Choi BH, Kwak MK. Activation of NRF2 by p62 and proteasome reduction in sphere-forming breast carcinoma cells. *Oncotarget*. 2015. doi:10.18632/oncotarget.3047

200. Hashimoto N, Tsunedomi R, Yoshimura K, Watanabe Y, Hazama S, Oka M. Cancer stem-like sphere cells induced from de-differentiated hepatocellular carcinoma-derived cell lines possess the resistance to anti-cancer drugs. *BMC Cancer*. 2014. doi:10.1186/1471-2407-14-722

201. Lovitt CJ, Shelper TB, Avery VM. Doxorubicin resistance in breast cancer cells is mediated by extracellular matrix proteins. *BMC Cancer*. 2018. doi:10.1186/s12885-017-3953-6

202. Holle AW, Young JL, Spatz JP. In vitro cancer cell-ECM interactions inform in vivo cancer treatment. *Adv Drug Deliv Rev*. 2016. doi:10.1016/j.addr.2015.10.007

203. Rebucci M, Michiels C. Molecular aspects of cancer cell resistance to chemotherapy. *Biochem Pharmacol*. 2013. doi:10.1016/j.bcp.2013.02.017